Intrinsic Developmental Mechanisms Promoting Interneuron Identity in the Drosophila Embryo

by

Heather Christine Pollington

A dissertation accepted and approved in partial fulfillment of the

requirements for the degree of

Doctor of Philosophy

in Biology

Dissertation Committee:

Dr. Tory Herman, Chair

Dr. Chris Doe, Advisor

Dr. Judith Eisen, Core Member

Dr. Dan Grimes, Core Member

Dr. Adam Miller, Core Member

Dr. Matt Smear, Institutional Representative

University of Oregon

Spring 2025

DISSERTATION ABSTRACT

Heather Christine Pollington

Doctor of Philosophy in Biology

Title: Intrinsic Developmental Mechanisms Promoting Interneuron Identity in the Drosophila Embryo

The generation of complex behaviors is dependent on proper neural circuit assembly to connect sensory input and motor output. Interneurons in the central nervous system (CNS) are essential for integrating sensory-motor information and increase neural circuit complexity to enable for highly precise and complex behavioral responses to environment stimuli. However, little is known about how CNS neural circuits are assembled. During development, a small pool of neural progenitor cells generates a highly diverse population of interneurons. The generation of unique interneurons facilitates proper connectivity and circuit assembly. Individual interneuron identity is defined by the integration of multiple neuronal aspects, including molecular identity (combinatory transcription factor expression), morphology, pre- and post-synapse connectivity, neurotransmitter expression, and electrophysiology. Yet, the developmental mechanism that promote these aspects remains unknown.

In *Drosophila*, neural progenitors (neuroblasts; NBs) sequentially express a cascade of temporal transcription factors (TTFs): Hunchback (Hb) > Krüppel (Kr) > Pdm > Castor (Cas) > Grainyhead (Grh). During each expression window, NBs divide to generate a ganglion mother cell (GMC) that generates two sibling neurons with transiently maintained TTF expression and differential Notch signaling ($Notch^{ON}$ and $Notch^{OFF}$). This generates early-born $Notch^{ON/OFF}$ Hb+ and late-born $Notch^{ON/OFF}$ Cas+ sibling interneurons. However, very few studies have thoroughly defined the role of TTFs and Notch signaling in specifying specific aspects of interneuron identity.

In this dissertation, I address this question by investigating the role of Hunchback, Castor, and Notch signaling in promoting specific aspects of interneuron identity. Using the model system, *Drosophila melanogaster*, we found that (i) the early TTF, Hb, specifies early-born interneuron molecular identity, morphology, and presynapse targeting in the NB5-2 lineage, (ii) NB5-2 misexpression of the late TTF, Castor, disrupts late-born interneuron proprioceptive

circuit behavior, and (iii) Notch signaling is necessary and sufficient for dorsal neurite targeting. These results display the importance of intrinsic mechanisms in promoting aspects of interneuron identity, and thus, proper circuit establishment during the development of the CNS.

This dissertation contains previously published and co-authored material.

CURRICULUM VITAE

NAME OF AUTHOR: Heather Christine Pollington

GRADUATE AND UNDERGRADUATE SCHOOLS ATTENDED:

University of Oregon, Eugene OR
University of Puget Sound, Tacoma WA
Montana State University, Bozeman MT

DEGREES AWARDED:

Doctor of Philosophy, Biology, 2025, University of Oregon
Bachelor of Science, Cell and Molecular Biology, 2018, University of Puget Sound

AREAS OF SPECIAL INTEREST:

Cellular and Developmental Neuroscience
Developmental Biology

PROFESSIONAL EXPERIENCE:

Graduate Researcher, University of Oregon, 2019-2025
Laboratory of Dr. Chris Q. Doe

Graduate Teaching Assistant, University of Oregon, 2019-2020

Undergraduate Research Assistant, University of Puget Sound, 2016-2018
Laboratory of Alyce DeMarais

Sherman Fairchild Summer Research Scholar, University of Puget sound, 2017

GRANTS, AWARDS, AND HONORS:

National Institute of Health Genetics Training Program Grant, Determining the role of Hunchback in specifying interneuron identity, University of Oregon, 2020 - 2021

ARCS Foundation Scholar, University of Oregon, 2019-2021

Beverly Pierson Research Engagement Award, University of Puget sound, 2018

Phi Kappa Phi Honor Society, University of Puget Sound, 2018

Sherman Fairchild Scholar Award, Undergraduate Summer Research Program, University of Puget Sound, 2017

Phi Sigma Biological Honor Society, University of Puget Sound, 2016-2018

PUBLICATIONS:

Mark, B., Lai, S., Zarin, A.A., Manning, L., Pollington, H.Q., Litwin-Kumar, A., Cardona, A., Truman, J.W., Doe, C.Q., (2021) A developmental framework linking neurogenesis and circuit formation in the *Drosophila* CNS. *eLife.* 2021 May. doi.org/10.7554/eLife.67510

Pollington, H.Q., Seroka, A.Q., Doe, C.Q., (2023) From temporal patterning to neuronal connectivity in *Drosophila* type I neuroblast lineages. *Seminars in Cell & Developmental Biology*. 2022 May. doi.org/10.1016/j.semcdb.2022.05.022

Pollington H.Q., Doe C.Q., (2025) The Hunchback transcription factor determines interneuron molecular identity, morphology, and presynapse targeting in the *Drosophila* NB5-2 lineage. *PLOS Biology* 23(3): e3002881. doi.org/10.1371/journal.pbio.3002881

ACKNOWLEDGMENTS

I, like many scientists, have taken a winding path to finally discover my passion. I thank my first research mentor Dr. Alyce DeMarais, for her continuous patience and guidance during my time at the University of Puget Sound. She encouraged my curiosity and fostered my love of scientific research as an undergraduate. I cannot thank her enough for her mentorship and guidance as a budding new scientist, and for instilling the belief that I am capable of becoming a successive researcher.

I give a heartfelt thank you to Dr. Chris Q. Doe for his mentorship and continuous guidance as I further my understanding and passion of developmental biology in his lab. Throughout my Ph.D. he has shown me that I am capable of more than believed, supported my creativity, and strengthened my confidence in my ability to pursue difficult biological questions. I also thank the Doe Lab members (Nathan Anderson, Elena Barth, Ben Brissette, Arnaldo Carreira-Rosario, Noah Dillon, Kasey Drake, Derek Epiney, Katie Fisher, Josmarie Graciani, Janet Hanawalt, Emily Heckman, Keiko Hirono, Sen-Lin Lai, Kristen Lee, Laurina Manning, Gonzalo Morales Chaya, Jordan Munroe, Peter Newstein, Megan Radler, Tyler Ramos, Natalie Rico Carvajal, Rishi Sastry, Austin Seroka, Alanna Sowles, and Chundi Xu) for the many insightful and collaborative conversations. Your feedback is always invaluable in helping me improve as a scientist. I also thank my dissertation advisory committee, Dr. Tory Herman, Dr. Judith Eisen, Dr. Dan Grimes, Dr. Adam Miller, and Dr. Matt Smear for their guidance and advice as I have developed my dissertation.

For the work in Chapter II, I thank fellow lab member Noah Dillon for constructive comments on the manuscript. I also thank Tory Herman (Oregon) for comments on the manuscript. I thank lab members Sen-Lin Lai and Chundi Xu for reagents and the construction of fly genetics. I thank Stefan Thor, Richard Mann, Jim Skeath, and Claude Desplan for antibody reagents. I thank lab member Peter Newstein for writing the custom Python code and assistance in data analysis of presynapses shown in Figure 8H-K. I thank lab member Kristen Lee for training and feedback on behavior experiments.

For the work in Chapter III, I thank Sen-Lin Lai and Ward Odenwald for fly reagents and the construction of fly genetics. I thank Stefan Thor for antibody reagents. I thank my co-authors

currently working on this project, Keiko Hirono (Figure 3.1) and Kristen M. Lee (Figure 3.2), for your hard work and dedication as we continue this investigation.

For the work in Chapter IV, I thank fellow lab member, Laurina Manning, for generating samples presented in Figure 4.1. I thank Alex Kolodkin for antibody reagents.

I would also like to show my gratitude for the many resources that have elevated my scientific research: FlyBase (http://flybase.org/) for the breadth of *Drosophila* genetic information provided. Antibodies obtained from the Developmental Studies Hybridoma Bank, created by the NICHD of the NIH and maintained at the University of Iowa, Department of Biology, Iowa City, IA were used in this study. Stocks obtained from the Bloomington Drosophila Stock Center (NIH P40OD018537) and Vienna Drosophila Resource Center were used in this study. Funding was provided by HHMI and NIH HD27056 (CQD) and T32 HD07348 (HQP). The funders had no role in study design, data collection and analysis, decision to publish, or preparation of the manuscript.

DEDICATION

For my Family. For my husband, Nick, who has given me unwavering support, unconditional love, patience, and continuous reassurance. You have truly been my rock and I will never be able to thank you enough for the support you have given me throughout this process. For my son, Auden, who brings me so much joy, laughter, and love every day. For my dad and brother, Geoff and Jaysen, for always giving me your love and support and being unimaginable examples of strength and resilience. For my amazing in-laws, Margaret, Ken, and Amy, who have provided me with extraordinary love and support and given me a listening ear when I needed it most.

Most importantly, for those I have lost during my PhD journey. For my grandmother, Bammie, who gave every person she met unconditional love and compassion and was one of the most courageous and creative people I know. And for my mom, Dawna, who was a born leader and an amazing example of unwavering determination, grit, and perseverance in the face of adversity. I will carry these qualities from you both with me, always.

You have all played a major part in making me the person I am today, and I profoundly thank you.

TABLE OF CONTENTS

LIST OF FIGURES

LIST OF TABLES

CHAPTER I

FROM TEMPORAL PATTERNING TO NEURAL CONNECTIVITY IN *DROSOPHILA* TYPE I NEUROBLAST LINEAGES

Pollington, H. Q., Seroka, A. Q., Doe, C. Q. (2022). From Temporal Patterning to Neural Connectivity in *Drosophila* Type I Neuroblast Lineages. Seminars in Cell & Developmental Biology, 142, 4-12. https://doi.org/10.1016/j.semcdb.2022.05.022

Author contributions

Conceptualization: C.Q.D., H.Q.P., A.Q.S; Literature compilation: C.Q.D., H.Q.P., A.Q.S; Writing – original draft: C.Q.D., H.Q.P., A.Q.S; Writing – review & editing: C.Q.D., H.Q.P., A.Q.S; Supervision: C.Q.D.; Project administration: C.Q.D.; Funding acquisition: C.Q.D.

Introduction

During *Drosophila* neurogenesis, a small pool of neural progenitor cells generates a diverse population of neurons. Initially, embryonic neural progenitors (or neuroblasts; NBs) are diversified by spatially restricted expression of early transcription factors (reviewed in (Skeath & Thor, 2003). *Drosophila* NBs undergo type I or type II lineages. In type I lineages, the NB generates a series of ganglion mother cells (GMCs) that each produce a pair of sibling neurons; in type II NB lineages, the NB generates a series of intermediate neural progenitors (INPs) which each divide asymmetrically to generate 4-6 GMCs and their subsequent sibling neurons. In this review we focus on temporal patterning in type I NBs; type II lineages will be covered by another review in this issue.

Diversity within type I clonally related neurons is achieved through temporal patterning, in which each NB undergoes a series of asymmetric divisions, sequentially expressing a cascade of key temporal transcription factors (TTFs) (Isshiki et al., 2001). Recent work in the ventral nerve cord (VNC) and central complex (CX) has demonstrated the ability of TTFs to regulate high-order features of neuronal identity in post-mitotic neurons, including molecular identity, morphology, and axon and dendrite targeting (Mark et al., 2021; Meng et al., 2019, 2020; A. Seroka et al., 2020; A. Q. Seroka & Doe, 2019; Sullivan et al., 2019). These results define

temporal patterning as a powerful mechanism for generating neuronal diversity and determining terminal features. While this phenomenon has been well characterized in the VNC, temporal patterning is employed in other key brain regions as well, including the central brain and visual processing centers (optic lobes). Here we review the recent advances in understanding the role of temporal patterning and TTFs in circuit assembly and neural function in the *Drosophila* CNS.

Type I neuroblasts in the ventral nerve cord

Neuroblasts in the *Drosophila* VNC sequentially express the TTFs Hunchback (Hb), Krüppel (Kr), Pdm1/2 (Pdm), and Castor (Cas) (Figure 1.1). As they progress through the TTF cascade, they undergo asymmetric cell division to generate a series of GMCs; each GMC inherits the TTF expressed at the time of its birth. Next, GMC division generates two siblings, one with a "Notch^{ON}" identity and one with a "Notch^{OFF}" identity (Doe, 2017). Together, these processes generate a highly diverse population of neurons within the VNC.

The best known embryonic lineage is that of NB7-1, which sequentially generates the U1, U2, U3, VO, U4 and U5 Notch^{ON} motor neurons (MNs; Figure 1.1) (Averbukh et al., 2018; Grosskortenhaus et al., 2006; Isshiki et al., 2001; Kohwi et al., 2013; Pearson & Doe, 2003; A. Seroka et al., 2020). Named after their U-shaped morphology, the U MNs each target individual dorsal or lateral larval muscles. The first TTF, Hunchback, specifies the earliest temporal identity in most NB lineages, including U1/U2 in the NB7-1 lineage. Misexpression studies show that prolonged expression of Hb produces an increased number of Hb+ early-born cells, largely at the expense of late-born U3-U5 cells in the NB7-1 lineage (Isshiki et al., 2001; Novotny et al., 2002). Krüppel expression follows Hb, to specify an early-intermediate temporal identity; U3 in the NB7-1 lineage. Misexpression of Kr generates ectopic Kr+ U3 neurons without interfering with Hb+ neuronal identity. *Kr* mutants fail to produce the expected Kr+ U3 neurons (Isshiki et al., 2001). The overlapping combination of Kr/Pdm specifies VO MN identity (see below for more details), while Pdm specifies U4 identity, and the Pdm/Cas combination specifies U5 MN identity (Grosskortenhaus et al., 2006). Additionally, Pdm and Cas have been shown to close the second and third temporal identity windows in NB3-1, regulating the transition from Kr>Pdm and Pdm>Cas (Grosskortenhaus et al., 2006; Tran & Doe, 2008). Note that the Notch^{OFF} interneurons in the NB7-1 and NB3-1 lineages have yet to be characterized. Similarly, Cas has been shown to specify temporal identity of abdominal leucokinin+ (ABLK) neurons, involved in

osmotic balance, from the NB5-5 lineage (Benito-Sipos, Estacio-Gomez, et al., 2010). These studies highlight how a single TTF or combinatorial TTFs promotes the identity of a single neuron.

Lineages that generate two Hb+ GMCs have been reported to have different levels of Hb protein (Kanai et al., 2005; Mettler et al., 2006; Moris-Sanz, Estacio-Gomez, et al., 2014; Urban & Mettler, 2006). Further analysis will elucidate whether TTF concentration is important in specifying temporal identity or if a particular concentration threshold is sufficient. These examples clearly show the role of TTFs in specifying unique neuronal identity. While our understanding of the combinatorial potential of temporal identity deepens, recent work has also begun to extend temporal identity fate determination in promoting circuit assembly.

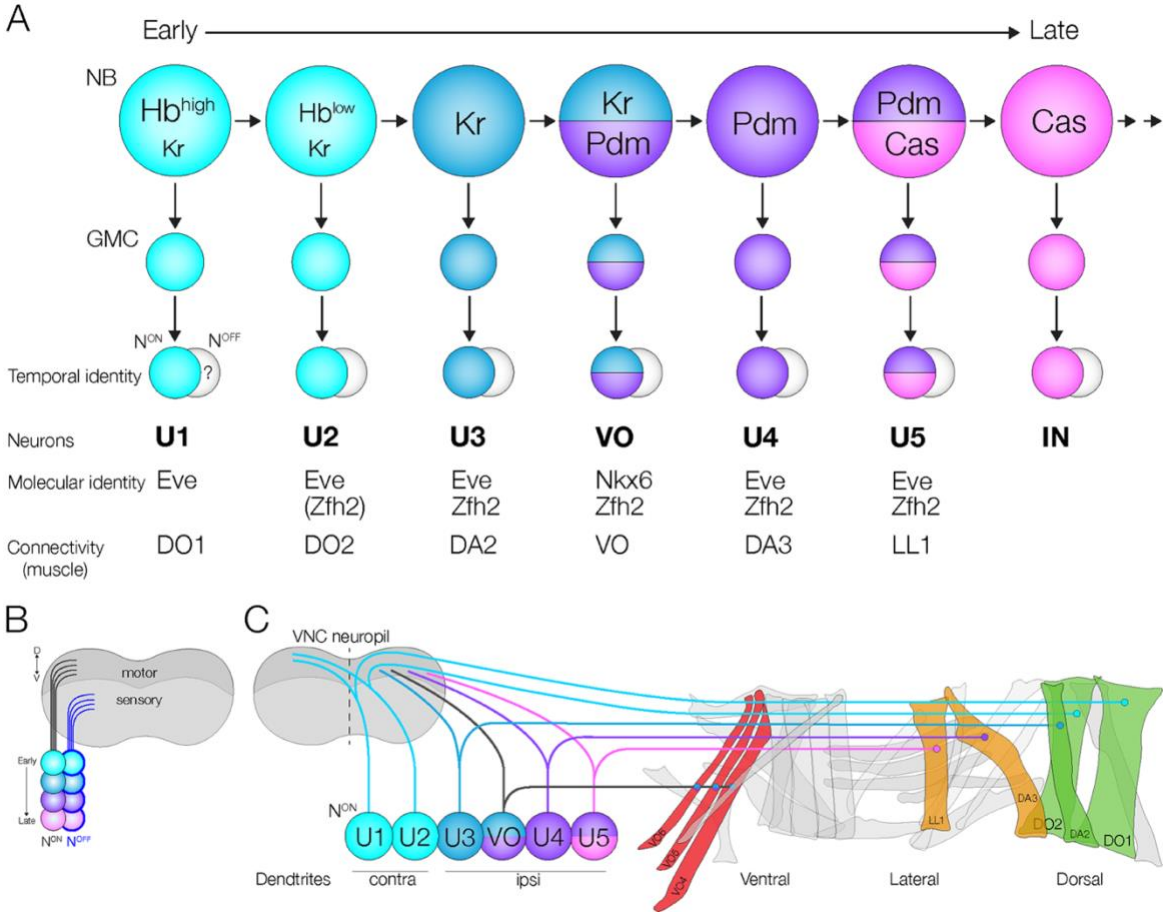

Figure 1.1. The TTF cascade in type I VNC NBs.
(A) Most VNC NBs sequentially express Hunchback (Hb), Kruppel (Kr), Pdm1/Nubbin and Pdm2 (Pdm), and Castor (Cas). Notch^{ON} neurons are shown on top of Notch^{OFF} neurons.
(B) Hemilineages formed by Notch^{ON} or Notch^{OFF} at the time of GMC division.
(C) Motor neuron axon and dendrite projections in the NB7-1 lineage. See text for details.

Temporal cohorts and circuit membership of interneurons

During *Drosophila* neurogenesis, NB divisions displace cells towards the interior of the CNS, thereby positioning early-born Hb+ cells deep in the VNC cortex and later-born Cas+ cells more superficially (Brody & Odenwald, 2000; Isshiki et al., 2001; Kambadur et al., 1998; Mark et al., 2021). In this way, neurons can be placed into temporal cohorts, or birth-order categories, based on their radial position alone. Each cohort, divided into approximately four birth-order categories (i.e. early, early-intermediate, late-intermediate, and late), consist of different cell types and various cell numbers per NB lineage. For example, the neurons located the deepest (near the neuropil) are an early temporal cohort and likely to be Hb+, although the relationship between temporal cohorts and TTF expression windows is only approximate. Thus, categorizing neurons into temporal cohorts serves as a proxy for their position in the TTF cascade.

Recent work reveals a strong correlation between temporal cohort identity and circuit assembly. NB3-3 gives rise to a population of interneurons identified by Even-skipped (Eve) expression and lateral cell body positioning ("Eve Lateral" or EL neurons) (Bossing et al., 1996; Schmid et al., 1999; Schmidt et al., 1997). The EL interneuron population is subdivided into early and late temporal cohorts based on expression of the *R11F02-Gal4* line; the deep positioned early-born temporal cohort lacks *R11F02-Gal4* expression, while the superficial positioned late-born temporal cohort expresses *R11F02-Gal4*, allowing each temporal cohort to be studied separately (Wreden et al., 2017). Optogenetic stimulation of the early-born ELs alone, using *EL-Gal4* (expressed in both temporal cohorts) and *R11F02-Gal80* (to prevent expression in the late temporal cohort) induces a larval escape rolling behavior. In contrast, specific stimulation of the late temporal cohort, using *R11F02-Gal4*, results in left/right uncoordinated movements (Wreden et al., 2017). Supporting these behavioral results, analysis of the EL partner neurons in a Transmission Electron Microscopy (TEM) reconstruction of the larval CNS showed that early-born EL neurons receive direct synaptic inputs from mechanosensory chordotonal neurons (neuron that can induce rolling) whereas the late-born EL neurons received direct input from proprioceptive neurons (Heckscher et al., 2015; Wreden et al., 2017). Thus, the early temporal cohort is in a mechanosensitive circuit whereas the late temporal cohort is in a proprioceptive circuit, supporting a model in which different temporal cohorts have distinct circuit membership.

Shared connectivity of temporal cohorts has also been demonstrated in the analysis of seven bilateral NB lineages mapped in the TEM volume (Mark et al., 2021). Each of these lineages produces a Notch^{ON} and Notch^{OFF} hemilineage; with Notch^{ON} hemilineages projecting to the dorsal (motor) neuropil and Notch^{OFF} hemilineages projecting to a more ventral domain (Figure 1.1B) (Mark et al., 2021). Within each NB hemilineage there are four temporal cohorts, and thus each lineage consists of eight "hemilineage/temporal" cohorts e.g. a Notch^{ON} early temporal cohort or a Notch^{OFF} late temporal cohort. Analysis of synapse localization within hemilineage/temporal cohorts revealed that each temporal cohort within a Notch^{ON} hemilineage localizes presynapses to a shared region of the neuropil, while each ventral hemilineage-temporal cohort localized postsynapses to a distinct region in the ventral sensory neuropil (Mark et al., 2021). Thus, hemilineage/temporal cohorts share a common synapse localization domain in the neuropil; the authors hypothesize this may allow each temporal cohort to receive distinct sensory input and generate distinct motor output, consistent with participation in distinct circuits (Mark et al., 2021).

The shared synapse localization, connectivity, and circuit membership of temporal cohorts in multiple NB lineages in the VNC generates a clear and testable hypothesis that temporal cohort membership (a proxy for temporal identity) plays a crucial role in determining synapse targeting, connectivity and circuit membership throughout the VNC. Functional studies will be needed to test this hypothesis.

Temporal cohorts and circuit membership of motor neurons

In addition to the link between TTFs and circuit membership of NB3-3 interneurons (described above), TTFs have been shown to be functionally important for MN synapse targeting and connectivity in the NB7-1 lineage. NB7-1 divides every 30 min to generate the U1-U5 and the single VO MN (Figure 1.1); the identity of the sibling neurons is unknown. The morphology and connectivity of each MN is unique: U1 and U2 project axons ipsilaterally to the dorsal oblique muscles (DO1 and DO2, respectively), whereas U3-U5 form neuromuscular junctions with lateral muscles (DA2, DA3, and LL1), and the VO motor neuron projects to the ventral-most muscles (ventral oblique; VO) (Figure 1.1C) (Meng et al., 2020; A. Seroka et al., 2020).

U1-U5 axons grow into the muscle field sequentially, in order of their birth. They also have distinct temporal identity. Two independent studies asked whether U MNs target their

muscle based on birth timing ("first come, first served") or molecular temporal identity (Meng et al., 2019; A. Q. Seroka & Doe, 2019). To break the correlation between birth timing and temporal identity, each lab misexpressed Hb throughout the NB7-1 lineage to generate ectopic U1 MNs that had the same temporal identity but had different birth dates. If all ectopic U1 neurons target the dorsal muscles, then temporal identity regulates targeting; if ectopic U1 neurons progressively target dorsal, lateral, and ventral muscles, then birth timing is most important for neuromuscular connectivity. Both labs observed the former result: muscle targeting correlated with temporal identity not birth timing (Meng et al., 2019; A. Seroka et al., 2020; A. Q. Seroka & Doe, 2019). These experiments strongly indicate that at least one TTF, Hb, encodes the information necessary for proper MN-muscle connectivity. The relevant downstream cell recognition molecules await discovery.

The Heckscher lab extended these experiments to determine if MN-muscle targeting was stable over larval development, and whether the connectivity was functional (Meng et al., 2019). Interestingly, third instar larvae following Hb misexpression show significantly more synaptic connections to muscle DO2 (normal U2 target) than muscle DO1 (normal U1 target). They propose this may be due to the increased occupancy of muscle DO1, in which the muscle is physically over crowed with ectopic U1 MNs, driving later-born ectopic U1s to form connections with the closest alternative, DO2. Ectopic synapses were observed to make functional connections based on localization of pre-synaptic markers for synaptic vesicles (Synapsin; Syn) and active zones (Bruchpilot; Brp), as well as the postsynaptic markers for muscle post-synaptic density (Discs large; Dlg) and the neurotransmitter glutamate receptor, GluRIIA (Meng et al., 2019). Post-synaptic responses from spontaneous synaptic vesicle release were also observed in every synaptic branch in both controls and Hb misexpressed larvae, indicating functional synapses.

In addition to a role in MN axon target choice, TTFs are also implicated in MN dendrite targeting (Meng et al., 2019; A. Q. Seroka & Doe, 2019). U1 and U2 dendrites project to both the ipsilateral and contralateral dorsal neuropil, whereas U3-U5 dendrites project to the same domain but remain ipsilateral. Hb misexpression generated ectopic U1 neurons based on molecular identity, and many of them projected to the contralateral dorsal neuropil as do endogenous U1 neurons. The ectopic U1 neurons did not, however, perfectly replicate endogenous U1 neuron dendrite targeting. Ectopic neurons projected contralaterally in a dorsal

region whereas endogenous U1 neurons cross the midline ventrally. Nevertheless, despite the new routing, ectopic U1 neurons projected contralaterally to the U1 dendrite domain, showing that temporal identity plays an important role in motor dendrite targeting in addition to its role in axon targeting and circuit formation (Meng et al., 2019; A. Q. Seroka & Doe, 2019). It remains an open question whether the ectopic U1 neurons have the same premotor inputs as endogenous U1 neurons.

In all experiments where Hb is misexpressed throughout the NB7-1 lineage, it loses its ability to induce U1 neurons over time. There are several possible explanations. First, Hb alone is not sufficient to promote U1 MN identity (Meng et al., 2019). The authors propose a context dependent model, in which Hb promotes neuronal identity in combination with additional temporally regulated gene programs. Second, failure of Hb to transform all neurons in the lineage may be due to loss of NB competency to respond to Hb (Kohwi et al., 2013; A. Q. Seroka & Doe, 2019). Third, expression of the *NB7-1-Gal4* driver line declines over time (A. Q. Seroka & Doe, 2019), such that there may be insufficient Hb levels late in the lineage. Anyone, or all, of these mechanisms may be occurring.

Hb also specifies early-born MN connectivity in the NB3-1 lineage. NB3-1 produces four "Raw Prawn" (RP) MNs in the sequence of RP1, RP4, RP3, and RP5 (Tran & Doe, 2008); these neurons connect with ventral muscles VL1-4 (Landgraf et al., 1997). Similar to NB7-1, prolonged expression of Hb in NB3-1 resulted in an increase in RP1/4 early-born Hb+ MNs with functional synaptic connections to muscles VL1 and VL2 (Meng et al., 2020). However, electrophysiology did not show an increased response in muscle stimulation. Upon further observation, animals with ectopic RP1/4 neurons appeared to release more synaptic vesicles compared to controls, but showed a decrease in postsynaptic receptor sensitivity, measured by miniature-EPSP (mEPSP) amplitude (Meng et al., 2020). This result provides a clear example of how homeostatic compensation during development allows for near-normal muscle responses to generate wild-type behavior.

Hb is not the only TTF to specify neuronal identity in embryonic type I NB lineages. Misexpression of Pdm alone in NB7-1 results in an extended Pdm/Cas window and the corresponding increase in U5 neurons (Grosskortenhaus et al., 2006; Meng et al., 2020). Surprisingly, there were regional differences in the response to Pdm misexpression: in segments A1-A3 there were an increased number of U5 neurons only, whereas in segments A4-A7 there

was a lack of the U3 Kr+ neuron. It is tempting to propose that ectopic Pdm created a Kr/Pdm window that generated a VO neuron rather than a U3 neuron (see below for more details). Interestingly, segments with increased U5 MNs showed a significant increase in synaptic branching to muscle LL1, but all other muscles showed no change in synapse branching number. Synapses of muscle LL1 were also shown to be functionally connected, visualized by post-synaptic responses to spontaneous synaptic vesicle release in MNs. In addition, hemisegments lacking U3 had a significant decrease in the number of synapses to muscle DA2 (Meng et al., 2020). These results are evidence that, similar to the function of Hb, Pdm temporal identity promotes neuromuscular specificity, directing LL1 muscle targeting to form functional connections and may generate ectopic VO MNs at the expense of U3 Kr+ neurons.

Individual embryonic TTFs have been assayed by both loss- and gain-of-function experiments, yet there are additional examples where the overlap of two TTFs creates a unique neuronal identity. First, the combination of Pdm/Cas in the NB7-1 gives rise to the U5 neuron (Grosskortenhaus et al., 2006). Misexpression of Pdm on top of the endogenous Cas window creates an extended Pdm/Cas window of NB expression that leads to additional U5 neurons (Grosskortenhaus et al., 2006). More recently, the identification of a Kr/Pdm+ GMC in the NB7-1 lineage has led to the discovery of a previously undiscovered Kr/Pdm+ neuron, termed the VO neuron (Averbukh et al., 2018; A. Seroka et al., 2020). Unlike U1-5 neurons, the VO MN has an Eve- Nkx6+ Zfh1+ molecular identity (A. Seroka et al., 2020). VO dendrites remain ipsilaterally and axonal projections travel the intersegmental nerve d branch (ISNd) and target ventral oblique muscles, VO4-6. Interestingly, VO does not share similar dendrite projections or postsynaptic localization with U3 or U4 within the neuropil. This discovery shows that NB7-1 produces both Eve+ MNs projecting to dorsal/lateral muscles and a Nkx6+ ventral projecting neuron. To determine if Kr/Pdm combinatorial temporal identity promotes VO muscle targeting, Kr/Pdm were co-misexpressed in the NB7-1 lineage. Co-misexpression resulted in the generation of U1/U2 Hb+ and U3 Kr+ neurons, as expected, plus an increase of 2-3 Nkx6+ Zfh1+ VO neurons at the expense of later-born U4/U5 neurons. Using multi-color flip out (MCFO) (Nern et al., 2015), two individually labeled HA and V5 tagged neurons were shown to target the ventral oblique muscles through the ISNd, proving that the ectopic VO neurons were not just molecularly transformed but also morphologically transformed (A. Seroka et al., 2020). The functional properties of the ectopic VO neurons await investigation. This is a strong example of

how combinatorial expression of the TTFs, Kr and Pdm, function to define temporal identity and promote neuromuscular targeting.

Downstream effectors of temporal transcription factors

Temporal transcription factors are expressed transiently, leading to a model in which TTFs drive expression of downstream TFs that consolidate and maintain neuronal identity. However, until recently, scant evidence in the *Drosophila* VNC supported this model. Recent work has provided support for this model in the specification of the VO motor neuron. The neuron develops from the Kr/Pdm double positive temporal window, and this TTF combination is necessary and sufficient for the expression of the homeodomain TF Nkx6 (Flybase: HGTX). Interestingly, similar to Kr/Pdm misexpression, misexpression of Nkx6 in NB7-1 resulted in production of ectopic VO MNs at the expense of U3-U5 neurons (A. Q. Seroka & Doe, 2019). Complementing these findings, Nkx6 RNAi knockdown resulted in a loss of VO neurons and an additional Eve+ neuron. Nkx6 knockdown also showed a complete loss of neuron projections through the ISNd to the ventral oblique muscle (A. Seroka et al., 2020). These findings, together with Kr/Pdm manipulations discussed above, provide strong support for the model whereby transient TTFs drive expression of homeodomain TFs that establish and maintain neuronal identity. It is likely that Eve and Nkx6 function similarly: the former acting with co-factors to establish unique U1-U5 neuron identity, while the latter acting alone to specify the single VO motor neuron identity (A. Seroka et al., 2020). In each case there is accumulating evidence that the TTF/homeodomain TFs function to not only specify molecular identity but also higher order properties such as neuronal projections, synapse localization, and connectivity. These conclusions are based on the role of TTF/TFs in motor neurons; it remains to be seen if a similar mechanism is used to drive higher order properties of interneurons.

Type I neuroblasts in the optic lobe

Neurogenesis and identification of TTF cascade in the optic lobe

In addition to the VNC, the *Drosophila* optic lobe (OL) provides a powerful model for understanding the contribution of developmental specification programs to the morphological and connectivity features of mature post-mitotic neurons. The OL is comprised of four distinct regions: the lamina, medulla, lobula and lobula plate (Egger et al., 2007; X. Li et al., 2013;

Yasugi et al., 2008). These structures are derived from two primary regions of the OL: the superficially located outer proliferation center (OPC) which gives rise to the neurons of the lamina and medulla, and the inner proliferation center (IPC) which generates the lobula and lobula plate neurons (Apitz & Salecker, 2014; Hofbauer & Campos-Ortega, 1990). Additionally, a specialized region at the tips of the OPC (tOPC) uses Notch-dependent mechanisms to contribute a subset of neurons to the medulla, lobula and lobula plate (Bertet et al., 2014).

Each medulla NB generates a set of postmitotic neurons which are arranged by birth-order in a linear and radial orientation. Investigation of the developmental determinants producing this arrangement initially revealed six candidate TTFs sequentially expressed: Homothorax (Hth) > Klumpfuss (Klu) > Eyeless (Ey) > Sloppy paired 1/2 (Slp) > Dichaete (D) > Tailless (Tll). These TTFs determine the downstream expression of previously characterized TFs in concentric rings of mature OL neurons (X. Li et al., 2013; Suzuki et al., 2013)(Figure 1.2A). More recently, Konstantinides et al. and Zhu et al. performed single-cell sequencing of OL cells to determine the TTF cascade in these lineages with higher resolution. They demonstrate that most TTFs are expressed in overlapping windows to create combinatorial codes, which could specify neuronal identity. They uncovered 12 putative TTF windows that, when combined with five spatial patterning domains and Notch-dependent hemilineage diversification, would be sufficient to generate the roughly 120 cell types in the medulla (Konstantinides et al., 2021; Zhu et al., 2022). As seen in the VNC, the OL also uses a Notch$^{ON/OFF}$ mechanism to further diversify each lineage into hemilineages with unique features: for example, about half of the neurons born during the Ey window maintain Ey expression, while the other half are Ey-/Apterous+ (Ap). In mutants for *Suppressor of Hairless* (*SuH*), the transcriptional effector of Notch signaling, all the neuronal progeny of the Ey window are converted to an Ey+ identity, with complete loss of Ap expression. Overall, the combined action of the spatial, TTF cascade, and Notch-dependent signaling generate remarkable diversity in the OL, in parallel to the function of these mechanisms in the VNC (X. Li et al., 2013; Mark et al., 2021; Suzuki et al., 2013).

Neuronal progeny arising from medulla NBs are organized in a “beads on a string” arrangement in which the youngest columns of neurons are located close to the OPC neuroepithelium. Birth of newer neurons displaces older neurons to more medial locations adjacent to the central brain. Additionally, within each column the youngest neurons are located next to their NBs at the superficial surface of the medulla cortex, while the oldest neurons are

pushed deeper towards the neuropil (Apitz & Salecker, 2014; Hasegawa et al., 2011; Morante et al., 2011). This spatial orientation results in the arrangement of neuron subtypes expressing TF combinations corresponding with birth-order in concentric rings within the medulla cortex, and allows for the simultaneous observation of NBs at different temporal stages in their lineage progression (Hasegawa et al., 2011). In the next section, we will explore evidence showing that these mechanisms not only generate diversity, but also specify higher-order neuronal features and contribute to circuit formation.

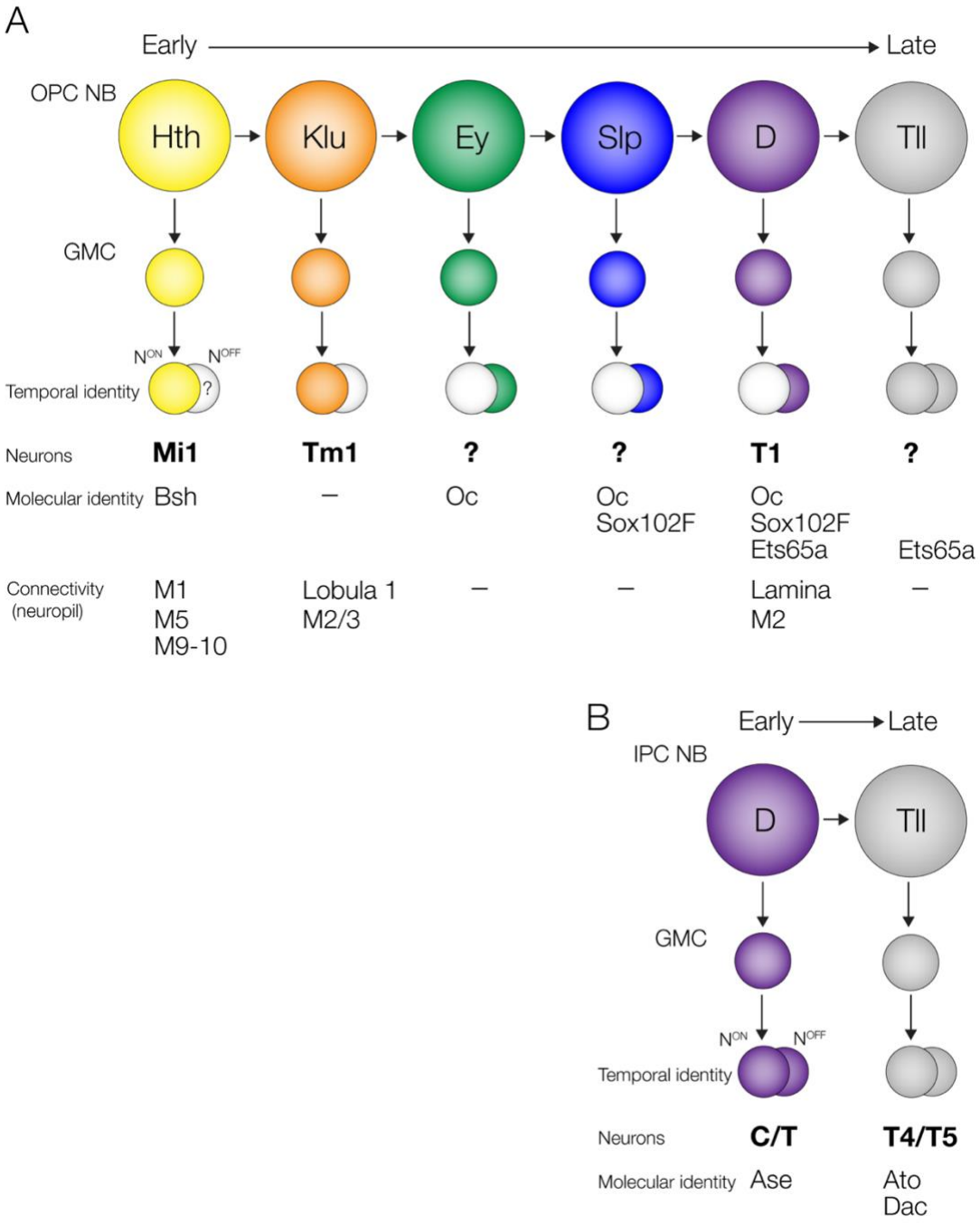

Figure 1.2. The TTF cascade in type I optic lobe NBs.
(A) OPC medulla NB TTF cascade (*first row*). During each TTF window, the NB gives rise to a GMC which undergoes a Notch-dependent terminal division to generate a pair of neurons or glia (*rows two and three*). Notch^{ON} neurons are shown on top of Notch^{OFF} neurons. Each TTF window generates unique neuronal identities, with key examples listed (*row four*). Molecular identities and target neuropils are listed for the respective neuronal subtypes (*rows five and six*). (B) IPC NB TTF cascade (*first row*). Subsequent rows as in Figure 1.1. Notch^{ON} neurons are shown on top of Notch^{OFF} neurons.

Specification of neuronal morphology and targeting by temporal patterning

Landmark studies support a role for the OL TTFs in specifying higher-order features of neuronal identity, such as morphology and connectivity. For example, the TTF Hth drives expression of the homeodomain TF Bsh, which in the Notch^{ON} hemilineage is necessary and sufficient to specify Mi1 neuron morphology: in *bsh* mutant MARCM clones the majority of neurons are converted from Mi1 local interneurons arborizing at the M1, M5 and M9-10 layers of the medulla to Tm-type projection neurons which arborize in both the medulla and lobula (Hasegawa et al., 2013). Conversely, ectopic expression of Hth in later-born NBs is sufficient to generate ectopic Bsh+ neurons (although there is a competence window in which the NB can respond to this manipulation), and in a Hth/Su(H) double-mutant background, Bsh+ progeny are lost, demonstrating the requirement for both Hth and Notch in the specification of the Bsh+ Mi1 identity (Hasegawa et al., 2011; X. Li et al., 2013). Further characterization revealed that early medulla NBs produce neurons expressing Drf, Bsh, or Run, depending on birth-order. Overexpression of Bsh using *Drf-Gal4*, to label endogenous Drf+ neurons, results in the generation of ectopic medulla intrinsic neurons that have correct arborizations in the M1, M5 and M9-10 layers, however these arborizations are not wildtype. Dual overexpression of Bsh and Hth is required to generate Mi1 neurons with wildtype arborization, not accomplishable by Hth overexpression alone. Additionally, both Hth and Bsh contribute to the regulation of Ncad expression in Mi1 neurons, which plays an important regulatory role in the correct formation of Mi1 arborizations (Hasegawa et al., 2011, 2013; Morante & Desplan, 2008). Together, these data paint a picture of a regulatory hierarchy in which the Hth TTF window gives rise to Bsh+ Mi1 neuron identity, morphology, and targeting of which is specified by the coordinate function of Hth and Bsh.

The specification of T1 neuron morphology is another example within the medulla. The specification of neuronal identity is accomplished through combinatorial TF action downstream of temporal patterning in the NB (Naidu et al., 2020). T1 neurons are born from the Notch^{OFF} hemilineage of the D temporal identity window and are distinguishable from other neurons by a combinatorial code of three TFs expressed in mature T1 neurons and not in their parental NBs: Ocelliless (Oc), Sox102F and Ets65A (Naidu et al., 2020). How does expression of these TFs in T1 neurons relate to the temporal patterning axis? Oc+ Notch^{OFF} neurons are born from the Ey TTF window and continue to be generated through the Slp and D windows, while Sox102F+

neurons are derived from the Slp and D windows and Ets65A+ neurons are born in the D and Tll windows (Figure 1.2A). The TTFs Ey, Slp and D are required to initiate the expression of Oc, Sox102F and Ets65A, respectively. For example, *ey* RNAi in the NB results in the loss of Oc+ neurons across all windows, Sox102F+ neurons are lost in *slp* mutant clones, and Ets65A+ neurons are lost in *D* mutant clones (Naidu et al. 2020). This developmental program results in the overlap of Oc, Sox102F and Ets65A expression in the neuronal progeny of the D window and results in the T1 identity (Figure 1.2A). T1 neurons are unicolumnar and connect the lamina and medulla, with cell bodies located in the medulla and characteristic "T" shaped axon branches. CRISPR-mediated knockdown of each of these TFs in T1 neurons impacts different aspects of connectivity and morphogenesis. In an *oc*-CRISPR background, T1 neurons have disorganized arborizations in the medulla while their axon projections still target the lamina, similar to wildtype. Loss of Oc does not affect Sox102F expression. Loss of Sox102F causes overexpansion of T1 medulla arborizations and eliminates wildtype axon projections to the lamina without affecting Oc expression. Lastly, loss of Ets65A causes projections to overextend to the M6 layer without affecting either Sox102F or Oc expression. These results suggest a mechanism similar to the combinatorial codes identified in *C. elegans*, in which distinct TFs act in a combinatorial fashion to specify different aspects of morphology and targeting (Hobert & Kratsios, 2019; Naidu et al., 2020). Taken together, these results support a model in which temporal patterning in OL NBs activates the expression of specific TF combinations that specify the morphology and targeting of neuronal progeny.

The role of temporal patterning in specifying connectivity in the OL is not limited to the medulla. Another example of hierarchical temporal regulation of morphological and connective features is found in the role of Dac and Ato in specifying T4/T5 lobula neuron identities derived from the IPC. IPC NBs give rise to two different neuronal subtypes, C/T and T4/T5, utilizing a truncated TTF cascade (Figure 1.2B). In the IPC, D and Tll expression define the early and late stages of neurogenesis, respectively. Young IPC NBs give rise to C/T neurons in the D window before switching to Tll expression, which upregulates the pro-neural proteins Ato and Dac to specify T4/T5 progeny (Apitz & Salecker, 2015; Mora et al., 2018). Generation of single-cell clones using IPC-specific *ato-Gal4* revealed that Ato+ NBs give rise to two distinct subtypes of direction selective neurons: the T4 and T5 neurons. Dendrites of T4 and T5 arborize within medulla layers 10 and Lo1, respectively, whereas axons project to one of four lobula plate layers

(Apitz & Salecker, 2018; Hofbauer & Campos-Ortega, 1990; Oliva et al., 2014). The function of Dac in the specification of T4/T5 identities was tested using a Dac MARCM approach, demonstrating that in the absence of Dac, T4/T5 neurons are converted to a T2/T3 morphology, with altered dendritic localization to medulla layer M9, and axons targeting lobula layers 2 and 3. Simultaneous knockdown of Dac and Ato resulted in complete absence of T4/T5 identities (Apitz & Salecker, 2018). Examination of Ato mutants in the IPC reveals that Ato is not required for neurogenesis, as Ato+ NBs still give rise to neurons, however, Ato mutant neurons show severe morphological and connectivity defects (Oliva et al., 2014). These results suggest that Ato and Dac are expressed in the Tll window of IPC NBs, where they act to specify higher-order features of the T4/T5 lobula neurons.

How does Dac/Ato function downstream of the Tll window in IPC NBs to specify the complex properties of the T4/T5 direction selective neurons? In order to identify TFs that instruct these mature morphological properties, Schilling et al. performed an RNAi screen against known TFs expressed in T4/T5 neurons, using optomotor response as an output. RNAi against either SoxN or Sox102F resulted in a severely disrupted optomotor response, implicating these factors in the function of the T4/T5 neurons, although their expression was only detected in T4/T5 neurons themselves and not in their progenitor populations. In a SoxN RNAi background T4/T5 dendrites overextended into ectopic medulla layers and showed disrupted axon targeting, demonstrating a regulatory role for these genes in specifying targeting and connectivity (Schilling et al., 2019). To determine whether these genes play a ubiquitous or cell-type specific role in the development of T4/T5 neurons, SoxN and Sox102F were knocked down in specific subsets of T4/T5s: T4a-d, T4/T5ab and T5cd, showing autonomous defects in each subtype. These guidance defects are shown to be dependent on the regulation of the adhesion molecule, Connectin, by the Sox family TFs via two distinct mechanisms. First, SoxN is required for Sox102F expression which suppresses Connectin expression. Second, SoxN is required for Connectin expression in a Sox102F-independent manner (Schilling et al., 2019). Lastly, the combined action of Ato and Dac in late IPC progenitors ensures the downstream expression of SoxN/Sox102F and thus correct target selection based on Connectin expression levels. Taken together, the results of these studies suggest hierarchical regulation of terminal neuronal features by temporal patterning events in their respective progenitors. In the case of T4/T5 neurons, IPC NBs enter a late temporal window triggered by Tll-mediated silencing of the D window, and

activation of Dac and Ato in the NB. The coordinate action of Dac and Ato activates the downstream TF effectors SoxN and Sox102F, which in turn regulate levels of the cell-surface protein, Connectin, and ensure proper axon and dendrite connectivity in each T4/T5 subtype. Although this is one example of a linear pathway, it is likely that the TTFs at the top of the regulatory hierarchy generate TF combinations that regulate neuron-specific cellular machinery necessary to ensure proper connectivity. Interestingly, previous work identified a role of another Sox family TF, SoxD, in the neurite targeting of T4/T5 neurons (Contreras et al., 2018), suggesting that multiple Sox family proteins might coordinate in a molecular code to ensure proper wiring.

To further understand the hierarchical regulation of complex morphological features of visual system neurons, a comprehensive understanding of how TTFs regulate downstream effector genes is required. The advent of single-cell RNA sequencing has allowed for an unprecedented ability to profile gene expression in distinct cell types. Application of this approach to understand how the eight T4/T5 neuron subtypes are transcriptionally established over time supports a model in which TFs specify a combinatorial code of downstream effectors in each cell type. Single-cell sequencing of T4/T5 neurons reveals that separate transcriptional programs correspond to specific features of the wiring process. Common T4/T5 features are established by a combination of TFs expressed in all eight subtypes (Lim1, Drgx, Acj6), manipulation of these factors results in gross defects to all T4/T5 dendrite and axon morphology (Kurmangaliyev et al., 2019, 2020). This overall genetic program is diversified by feature-specific transcriptional programs, with separate pathways regulating axon and dendrite specification. All T4/T5 neurons share a common function and general morphology but can be further divided into eight distinct subtypes based on their axonal targeting to the layers a-d of the lobula plate (T4a-d and T5a-d subtypes). Distinct TFs regulate the axon targeting of each of these subtypes to the appropriate layer in the lobula plate in two steps. First, binary expression of the TF, Bifid, directs T4/T5 axons to the general region of the a/b or c/d layers. Second, binary expression of Grain directs T4/T5 axons to individual target layers a and b, or c and d. Perturbation of Bifid or Grain selectively disrupts each lamination step while other common features of T4/T5 morphology are unaffected. Additionally, T4 neurons receive dendritic input in the medulla while T5 neurons receive inputs in the lobula. This choice appears to be determined by the binary expression of the Tfap-2 TF (Kurmangaliyev et al., 2019, 2020). Each

of these programs is characterized by a specific code of TFs as well as cell-surface proteins, with further analysis demonstrating unique downstream codes of immunoglobulin (Ig) superfamily proteins in each T4/T5 subtype (Kurmangaliyev et al., 2019, 2020). These modular programs support a model in which TTFs sit at the top of the hierarchy, activating separate combinatorial codes of downstream TFs in their progeny to regulate separate aspects of morphology and connectivity.

Conservation of embryonic temporal transcription factors from fly to mouse

It has been known for many decades that individual mammalian retinal and neocortical progenitors produced a diversity of neurons and glia in a stereotyped order (Angevine & Sidman, 1961; Livesey & Cepko, 2001). Cell culture experiments showed that the temporal sequence of neurons and glia could be generated in vitro, suggesting a lineage-intrinsic component to the process (Shen et al., 2006). Yet the identification of molecular mechanisms underlying this process of mammalian temporal patterning remained unknown. The first TTF cascade to be characterized was the Hb>Kr>Pdm>Cas series found in most embryonic VNC NBs (see above), making these TFs excellent candidates for specifying temporal identity in the mammalian retina and cortex. This line of research was delayed, however, by the fact that each *Drosophila* TTF is related to an expanded gene family in mammals: Hb is related to the Ikaros family; Kr is equally related to dozens of Zn finger TFs, the tandem Pdm proteins are related to many POU domain TFs, and Cas is related to many Zn finger TFs.

The first breakthrough came when one of the Ikaros family members, Ikzf1 (aka Ikaros), was shown to be necessary and sufficient for specifying early-born retinal cell types (Elliott et al., 2008). Ikzf1 mutants had reduced number of early-born retinal ganglion cells (RGCs), horizontal cells (HCs), and Amacrine cells (AM); misexpression of Ikzf1 gave the opposite phenotype of ectopic early-born cell types at the expense of later-born cell types, such as bipolar neurons (BI) (Elliott et al., 2008). Viral tracing showed that Ikzf1+ retinal progenitor cells (RPCs) produced both early-born and late-born cell types, ruling out the possibility of dedicated progenitors for early- and late-born cell types (Elliott et al., 2008). Several years later similar results were observed for Ikzf1 in specifying early-born cortical neurons (Alsio et al., 2013). Ikzf1 was detected in ventricular zone progenitors (VZPs) as they produced early-born deep layer cell types; interestingly Ikzf1 was not detected in neurons themselves, but this role was

likely taken by the closely related Ikzf2 (aka Helios) protein which is specifically detected in the deep layer 6 neurons (Alsio et al., 2013). Cre-induced tracing of Ikzf1+ VZP progeny showed that they produced both early- and late-born cell types, similar to retinal progenitors, and showing that VZPs transition from an Ikzf1+ to Ikzf1- profile (Alsio et al., 2013). Surprisingly, Ikzf1 mutants had no effect on cortical cell identities, although compensation by Ikzf2 may occur and the Ikzf1/Ikzf2 double mutant may be needed to determine the full loss of function phenotype. Conversely, Ikzf1 misexpression resulted in ectopic early-born deep layer neurons (Ctip2+ Tbr1+ Foxp2+) at the expense of later-born superficial layer neurons (Satb2+ Brn2+ Cux1+), although misexpression of Ikzf1 at late stages of cortical neurogenesis had no effect, showing that there is a limited competence window to respond to Ikzf1 (Alsio et al., 2013).

Taken together, these studies reveal a remarkable conservation of function between fly Hb and mammalian Ikaros family members. In both systems: (1) the TTF is expressed transiently in progenitors while they produce early-born cell types; (2) the TTF is necessary and sufficient for specifying early-born cell types; (3) there is a limited competence window to respond to the TTF.

The second ortholog to a fly TTF to be characterized was Casz1, an ortholog of the late TTF, Castor (Mattar et al., 2015). There are two isoforms Casz1v1 and Casz1v2. Casz1 isoforms are expressed in RPCs at increasing levels from E14.5 to P0, when late-born cell types are generated. Loss of function of both isoforms via mouse conditional mutant or retroviral clones showed a decrease in late-born rods and a corresponding increase in earlier-born HCs, AMs, and cones. Conversely, overexpression resulted in an increase in rod (Casz1v2) or BI numbers (Casz1v1) (Mattar et al., 2015). More recently the same group has shown that Casz1 has physical and genetic interactions with the NuRD complex (Mattar et al., 2021), known to promote epigenetic gene silencing, and that the NuRD complex histone deacetylase function is necessary for Casz1 function (Mattar et al., 2021). For example, Casz1 overexpression decreases rods, as mentioned above, but addition of the histone deacetylase inhibitor TSA will prevent Casz1-induced ectopic rod formation; furthermore, CRISPR knockdown of key NuRD complex members mimics the Casz1 loss of function phenotype of reduced rod numbers (Mattar et al., 2021). Taken together, fly Cas and mouse Casz1 have highly similar roles in the specification of late-born neuronal identity. For several years, Ikzf1 and Casz1 were the only two orthologs of fly

TTFs, and they provided 'book ends' as early and late TTFs, respectively -- leaving open the question of what comes between them.

More recently, two additional TTFs have been discovered to play a role in the middle stages of retinal neurogenesis following Ikzf1 and preceding Casz1. The first, Foxn4 is expressed in retinal progenitors at the time of middle-born neuron production: HCs, AMs, cones, and rods -- but not late-born BIs or Müller glia (Liu et al., 2020). Interestingly, the Drosophila ortholog of Foxn4 called Jumu is required in several embryonic neuroblast lineages to specify cell identities (Cheah et al., 2000), although it has not been tested for a role in temporal patterning. Loss of function for Foxn4 results in increased early-born retinal ganglion cells (RGCs) and loss of subsequent cell types (HCs, AMs, cones) as well as transient loss of rods. Conversely, misexpression of Foxn4 results in fewer RGCs and increased number of HCs, cones, and rods (Liu et al., 2020). Similar to *Drosophila* TTF cross-regulation, Foxn4 activates the next TTF, Casz1, and represses the previous TTF, Ikzf1 (Liu et al., 2020). The second TTF to be recently characterized is actually a pair of POU domain TFs Pou2f1/2 (formerly Oct-1/2), which are orthologs of the fly middle-born TTF Pdm. Recent work from the Cayouette lab has shown that Pou2f1/2 proteins are detected in RPCs during the middle stages of neurogenesis (E11.5-E15.5) and maintained in mid-born cones, HCs and AMs (Javed et al., 2020). Overexpression by electroporation resulted in an increase in cone numbers. Reducing Pou2f1/2 levels by RNAi, CRISPR gene lesioning, or Cre-induced conditional knock out effectively decreased Pou2f1/2 protein levels and reduced cone number while increasing late-born rod numbers (Javed et al., 2020). Furthermore, the authors show that the early TTF, Ikzf1, activates Pou2f1/2 expression, and Pou2f1/2 represses the late TTF Casz1 (Javed et al., 2020). This is somewhat different from the cross-regulatory hierarchy in *Drosophila*, in which Pdm promotes Cas expression (Grosskortenhaus et al., 2006; Tran & Doe, 2008).

The results summarized above show that the mammalian cortex and retina both use orthologs of fly VNC TTFs to generate temporal identity using remarkably similar mechanisms, although see (Sagner et al., 2021). It remains unclear whether this reflects a deep evolutionary relationship, or the more recent convergence of gene expression patterns. Despite the recent progress, many questions remain. (1) What is the relationship between Pou2f1/2 and Foxn4 in specifying "middle" temporal identity? Perhaps Pou2f1/2 act as "subtemporal" factors to subdivide the broader Foxn4 expression window. (2) The fly TTF Kr is equally related to dozens

of mammalian Zn finger TFs; which, if any, of these TFs may play a role in specifying temporal identity following Ikzf1? High temporal resolution single cell RNA-sequencing (Clark et al., 2019) may provide the best candidates from this broad TF population. (3) Casz1 is a TTF in the retina, but is not expressed in the developing cortex. What takes its place as a late TTF in the cortex? (4) How does Casz1v1 induce BPs, whereas Casz1v2 induce rods? (5) Both fly and mouse TTFs are transiently expressed; what maintains neuronal identity after the TTFs are gone? (6) Fly spatial TFs alter the epigenome to bias TTF genomic access and function (Sen et al., 2019), whereas mouse Casz1 alters the epigenome (Mattar et al., 2021), which may bias spatial TF binding and function; does each organism integrate spatial and temporal TFs differently? or might both spatial and temporal TFs act by altering the epigenome, helping to create distinct, heritable chromatin landscapes for each neural subtype? Recently there has been rapid progress in the field of temporal patterning in both flies and mice, so the answers to the questions above should soon arrive.

CHAPTER II

THE HUNCHBACK TRANSCRIPTION FACTOR DETERMINES INTERNEURON MOLECULAR IDENTITY, MORPHOLOGY AND PRESYNAPSE TARGETING

Pollington, H. Q. & Doe, C. Q. (2025). The Hunchback transcription factor determines interneuron molecular identity, morphology, and presynapse targeting in the *Drosophila* NB5-2 lineage. *PLOS Biology*. Accepted Jan 2025

Author contributions

Conceptualization: C.Q.D., H.Q.P.; Methodology: H.Q.P.; Formal analysis: H.Q.P.; Investigation: C.Q.D., H.Q.P.; Data curation: H.Q.P.; Writing – original draft: C.Q.D., H.Q.P.; Writing – review & editing: C.Q.D., H.Q.P.; Visualization: H.Q.P.; Supervision: C.Q.D.; Project administration: C.Q.D.; Funding acquisition: C.Q.D.

Introduction

During development, the generation of neuronal diversity is a crucial component in assembling proper neural circuit assembly and increases the complexity of neural circuitry and behavioral output. The central nervous system (CNS) consists of a diverse array of neurons that differ in transcription factor and neurotransmitter expression, morphology, connectivity, and electrophysiology. All these features are integrated to define unique neuron identities, enabling each neuron to form specific and stereotyped neural circuits that generate appropriate behaviors.

Neurogenesis in both Drosophila and vertebrates is initiated by spatial cues that specify progenitor identity (Luo, 2020), followed by temporally expressed transcription factors (TTFs) that diversify the progeny of each progenitor (Doe, 2017; El-Danaf et al., 2023; Holguera & Desplan, 2018). In the mouse retina, retinal progenitor cells (RPCs) sequentially generate multiple cell types necessary for retinal circuit assembly (C. L. Cepko, 1999, p. 199). RPCs express the TTF cascade: Ikaros > Pou2f1/Pou2f2 > FoxN4 > Casz1, each specifying specific cell types (El-Danaf et al., 2023). Ikaros expression is maintained in early-born RPC progeny and promotes expression of the homeodomain transcription factor, Prox-1, required to specify early-born horizonal cell fate (Elliott et al., 2008). In the developing mammalian cortex, apical

radial glia (aRGs) produce cortical neurons that settle in functionally distinct laminar layers in an inside-out fashion, generating deep layered early-born neurons and superficially located late-born neurons (El-Danaf et al., 2023; Holguera & Desplan, 2018). As in the retina, Ikaros is expressed early in neuronal progenitors of the mouse neocortex (Alsio et al., 2013). Prolonged Ikaros expression in cortical progenitors results in an increase in the number of early-born neurons expressing the early-born cortical TFs, Tbr1 and Foxp2, where it is required for early-born neuronal fate (Alsio et al., 2013). In the zebrafish spinal cord, early-born motor neurons and interneurons form a fast-swimming circuit, while later-born neurons form a slow-swimming circuit (Deska-Gauthier & Zhang, 2021). Early-born spinal cord neurons also show distinct morphological and connectivity differences compared to later-born neurons (Deska-Gauthier & Zhang, 2021). Thus, temporal patterning within progenitor lineages is an essential mechanism for generating neuronal diversity in the vertebrate CNS.

Similarly, *Drosophila* neural progenitors, called neuroblasts (NBs), sequentially produce motor neurons, interneurons, and glial cell type progeny that settle in a deep-to-superficial pattern (Isshiki et al., 2001; Kambadur et al., 1998; Mark et al., 2021; Tran & Doe, 2008), similar to mammalian cortical development (Luo, 2020). *Drosophila* NBs generate a stereotyped sequence of neurons and glia in all parts of the CNS, but here we focus on the ventral nerve cord (VNC), analogous to the vertebrate spinal cord. NBs in the VNC sequentially express the following TTF cascade: Hunchback (Hb, ortholog of Ikaros) > Krüppel (Kr) > Nubbin/Pdm2 (Pdm) > Castor (Cas; ortholog of Casz1) > Grainy head (Grh) (Doe, 2017). During each expression window, the NB asymmetrically divides to generate a smaller ganglion mother cell (GMC), which then divides to produce two post-mitotic neurons that transiently maintain the TTF expressed at the time of birth. This generates early-born neurons that express Hb, required for establishing motor neuron identity (Isshiki et al., 2001; Meng et al., 2019, 2020; Novotny et al., 2002; Pearson & Doe, 2003; A. Q. Seroka & Doe, 2019).

The role of Hb in specifying *Drosophila* motor neuron fate has been most extensively investigated in the NB3-1 and NB7-1 lineages (Isshiki et al., 2001; Meng et al., 2019, 2020; Novotny et al., 2002; Pearson & Doe, 2003; A. Q. Seroka & Doe, 2019). NB7-1 generates the U1-U5 and VO motor neurons in sequential birth-order: U1/U2 motor neurons express Hb, U3 expresses Kr, VO expresses Kr/Pdm, U4 expresses Pdm, and U5 expresses Pdm/Cas (Isshiki et al., 2001). Prolonged Hb expression in NB7-1 generates increased numbers of U1/U2 at the

expense of later-born motor neurons (Isshiki et al., 2001; Meng et al., 2019; A. Seroka et al., 2020; A. Q. Seroka & Doe, 2019). The late-born ectopic U1/U2 motor neurons lack expression of the late-born transcription factor, Zfh2, display U1/U2 morphology, and form synapses with U1/U2 dorsal muscle targets (Meng et al., 2019; A. Q. Seroka & Doe, 2019). Similarly, prolonged Hb expression in NB3-1 increases functional synapses innervating muscles targeted by early-born neurons and decreases synapse formation to muscles innervated by later-born neurons (Meng et al., 2020). Increased synaptic connections to early-born muscles increases presynaptic vesicle release; however, there is no difference in miniature-excitatory post-synaptic potential (mEPSP) amplitude, suggesting ectopic Hb motor neurons may undergo homeostatic compensation (Meng et al., 2020).

The role of Hb in generating motor neuron identity and connectivity is well characterized, yet relatively little is known about the role of TTFs in generating interneuron identity. Interneuron and motor neuron axons have different constraints on circuit formation. While motor neuron axons select a muscle target from a small pool of muscles, interneuronal axons must bypass a vast array of potential neuron partners within the synaptically dense neuropil, a much more complex environment, to form appropriate synaptic connections to partner neurons. In addition, interneuron neurites are directed by gradients of the attractant and repulsive extrinsic signaling cues: Semaphorin 1a, 2a, and 2b, Slit, and Netrin (Heckman & Doe, 2022; Keleman & Dickson, 2001; Sales et al., 2019; Simpson et al., 2000; Zlatic et al., 2009). Interneurons expressing specific guidance receptors are either attracted or repelled from discrete domains within the neuropil, directing neurites to extend to distinct neuropil regions. These extrinsic cues may contribute to interneuron morphology and connectivity; however, the role of neuron intrinsic mechanisms is not well understood.

To understand whether the mechanisms that Hb uses to specify early-born motor neuron identity are conserved in interneurons, we investigated the role of Hb in specifying interneuron identity in the NB5-2 lineage. NB5-2 predominately generates interneuron progeny, with the late-born interneurons forming a proprioceptive circuit (Heckscher et al., 2015; Mark et al., 2021). We generated a NB5-2 split Gal4 line to genetically label NB5-2 and its progeny. We found that NB5-2 expresses the canonical TTF cascade and TTF expression is transiently maintained in the interneuronal progeny. When we prolonged expression of Hb in the NB5-2 lineage, it resulted in an increased number of Hb+ NB5-2 interneurons that express early-born

TFs (Nervy, Dbx, and Nkx6) at the expense of neurons expressing late-born TFs (Runt and Zfh2). In addition, we identified several early-born Hb+ neurons with an axon/dendrite morphology distinct from that of later-born interneurons, forming a unique diagonal contralateral projection. At the synaptic level, ectopic Hb expression in late-born neurons resulted in an increase in presynapse percentage at neuropil locations normally targeted by NB5-2 Hb+ early-born neuronal presynapses. Finally, we found that prolonged NB5-2 Hb expression generates behavioral defects similar to disrupting the late-born proprioceptive circuit: decreased locomotor velocity and increased number of C-shaped body bends. In summary, we show that Hb specifies early-born NB5-2 interneuron molecular identity, axon/dendrite morphology, and presynapse targeting (essential for proper connectivity), and that proper TTF identity is necessary for appropriate behavioral output.

Results

Generation of a split-Gal4 line expressed in NB5-2 and its embryonic lineage

To create a transgene specifically expressed in the NB5-2 lineage, we constructed a split-Gal4 based on the intersection of *wingless* (*wg*), expressed in row 5 neuroectoderm, and *ventral nervous system defective* (*vnd*), expressed in medial column neuroectoderm (Figure 2.1A,B). The intersection of these two hemi-drivers defines the neuroectoderm domain that generates NB5-2, and the split-Gal4 is strongly and specifically expressed in NB5-2 and its progeny (Figure 2.1C). We refer to this split-Gal4 line alone as NB5-2-Gal4, or NB5-2>GFP when the NB5-2-Gal4 is driving expression of UAS-GFP. We note that NB5-2-Gal4 has occasional expression in the NB5-1 lineage, but this has no effect on our experiments as NB5-1 delaminates much later in embryogenesis, starts its lineage Cas+, and thus is unlikely to express earlier TTFs Hb, Kr, and Pdm (Cui & Doe, 1992). Thus, we conclude that NB5-2-Gal4 is an appropriate tool for driving gene expression in NB5-2 and its embryonic progeny.

NB5-2 expresses the canonical TTF cascade

Most VNC NB lineages sequentially expresses Hb, Kr, Pdm, Cas, and Grh and include intervals where adjacent TTFs are co-expressed (Doe, 2017). Here we determine whether NB5-2 also expresses this TTF cascade, and whether there are gene expression overlaps within the series. We found that NB5-2>GFP expression was not detected until late stage 10, and thus at earlier

stages NB5-2 was identified by its position in the NB array: the most medial row 5 NB just anterior to the row 6/7 Engrailed expression domain (Supp. Figure 2.1). Using these markers prior to stage 10, and NB5-2>GFP expression beginning at stage 10, we were able to characterize the TTF cascade in NB5-2 throughout embryogenesis (Figure 2.1D). We found that NB5-2 initially expresses Hb, low levels of Kr, and transient Pdm; brief expression of Pdm during the NB first division window has been previously observed in the NB4-2 lineage and thought to be protein inherited from the Pdm+ neuroectoderm (Bhat et al., 1995). Subsequently, NB5-2 sequentially expresses Kr, Pdm, Cas, and Grh with a period of overlap in each case (Figure 2.1D; Supp. Figure 2.1). We conclude that NB5-2 undergoes the canonical TTF cascade, with transient overlap of each TTF, resulting in nine different TTF expression windows. Most importantly for this work, Hb is detected in the earliest portion of the NB5-2 lineage.

Figure 2.1 (next page). NB5-2 expresses the canonical TTF cascade.
(A) Schematic of NB5-2 split Gal4 (green) construction using the unique NB5-2 expression combination of *wingless* (*wg*; yellow) and *ventral nervous system defective* (*vnd*; blue).
(B) Schematic of segmentally repeating NB5-2 location in early embryo. Anterior left, ventral view.
(C) NB5-2>GFP expression in stage 11 embryo in the lateral view (left panel; inset shows CNS volume from lateral view; Scale bar: 5 µm.), posterior view (middle panel; inset shows CNS volume from posterior view; Scale bar: 10 µm), and ventral view (right panel; Scale bar: 50 µm) labels NB5-2, NB5-2 neuron progeny, and a small population of neuroepithelium (ne).
(D) NB5-2 TTF expression cascade at stages 9-14. NB5-2 identification was achieved using the NB markers Deadpan (Dpn; insets in all expect stg 10) or Worniu (Wor; inset stg 10 only). Due to delayed GFP (green) expression in stage 9 and early stage 10 embryos, NB5-2 was identified as the most medially located NB, anteriorly adjacent to the Engrailed expression domain (see A GFP labeled NB5-2 was used to identify NB5-2 after early stage 10. Quantification: Stg E9 n= 16 hemisegments, 4 animals; stg 9 n= 12 hemisegments, 3 animals; stg E10 n= 20 hemisegments, 5 animals; stg 10 n= 12 hemisegments, 3 animals; stg 11 n= 8 hemisegments, 2 animals; stg 12 n= 12 hemisegments, 3 animals; stg 14 n= 12 hemisegments, 3 animals. Scale bar: 5 µm.

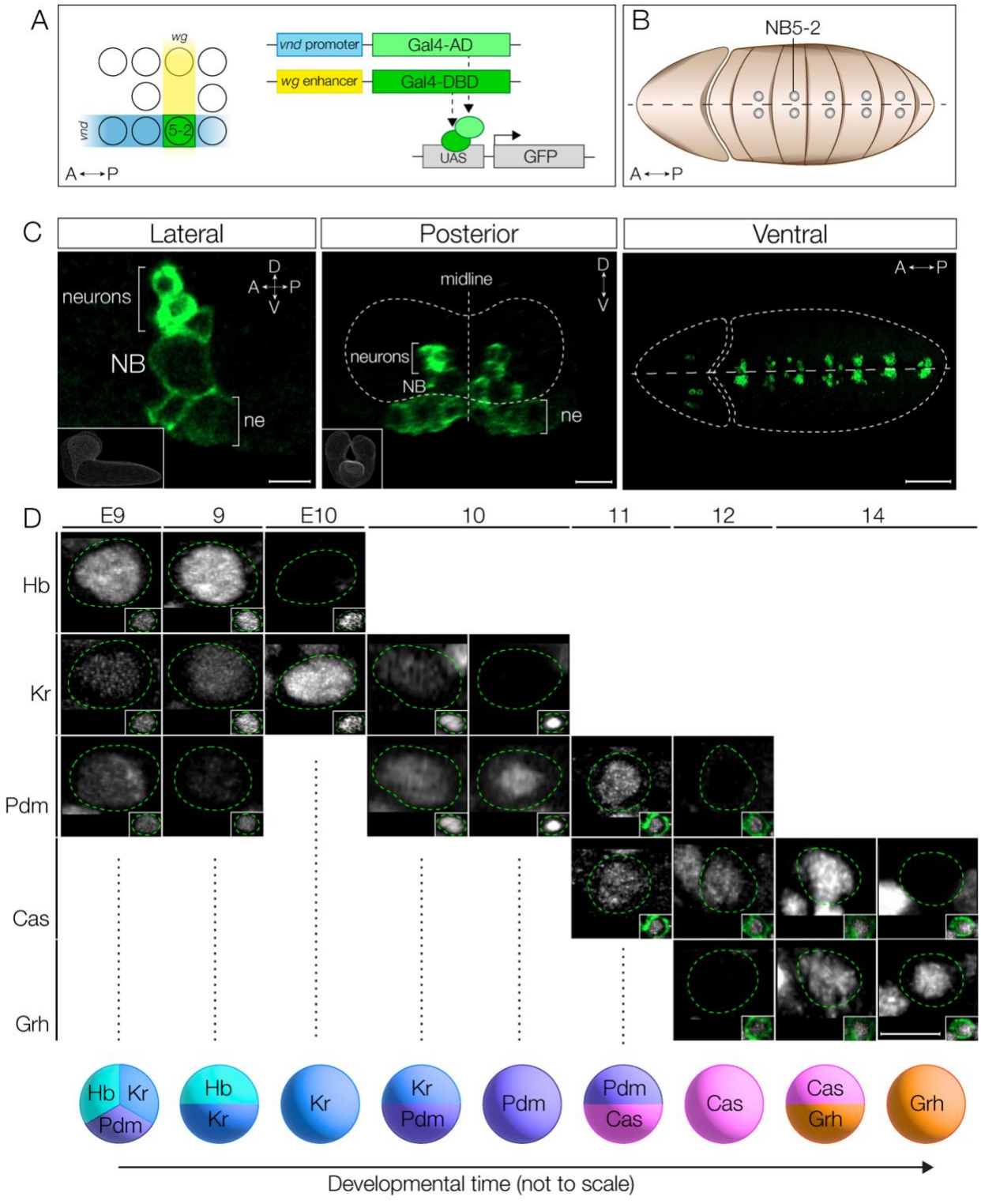
A
wg
vnd
5-2
A↔P
vnd promoter
Gal4-AD
wg enhancer
Gal4-DBD
UAS
GFP
B
NB5-2
A↔P
C
Lateral
Posterior
Ventral
neurons
NB
ne
D
A
P
V
midline
A↔P
D
E9
9
E10
10
11
12
14
Hb
Kr
Pdm
Cas
Grh
Hb Kr Pdm
Hb Kr
Kr
Kr Pdm
Pdm
Pdm Cas
Cas
Cas Grh
Grh
Developmental time (not to scale)

NB5-2 neuronal progeny express the TTF present at their time of birth

In most NB lineages, TTF expression in the NB is transiently maintained in the progeny born during each NB TTF expression window (Isshiki et al., 2001; Tran & Doe, 2008). Indeed, we find that each TTF can be detected within a subset of NB progeny (Figure 2.2A-C; quantified in D). Each window of NB expression, both single and dual gene overlap, contributes to the neuronal progeny (Figure 2.2A-C; quantified in D). Transient expression varied among TTFs: Hb, Kr, and Grh expression was maintained until the L1 larval stage (and possibly longer); Pdm expression was detectable only until embryonic stage 14; and Cas was detectable until late embryonic stage 17, with little expression observed in newly hatched larvae. Neurons expressing early TTFs are located in a deep layer closer to the neuropil, while neurons expressing later TTFs are located more superficially (Figure 2.2A-C), as expected from previous work (Isshiki et al., 2001; Mark et al., 2021; Tran & Doe, 2008). In addition, neurons from sequential TTF windows invariably have adjacent cell body positions (Figure 2.2A-C).

Interestingly, there are different numbers of neurons expressing each TTF (or TTF combination) (Figure 2.2D), which allows us to use neuron numbers as a proxy for the length of each TTF expression window. For example, at stage 14, Hb is detected in 5 neurons, which suggests that the NB Hb expression persisted for 3 divisions (each division making a Hb+ GMC that makes a pair of sibling neurons). Although we note that NB5-2-Gal4 does not begin expression until after the first neuroblast division in some animals, thus marking only 3-4 of the 5 Hb+ neurons. In this way, we infer that Kr alone has a one division window to contribute 2 neurons, Kr/Pdm has one division window (2 neurons), Pdm alone has a one division window (2 neurons), Pdm/Cas has a two division window (4 neurons), Cas alone has a two division window (4 neurons), Cas/Grh has a one division window (2 neurons), and at stage 16, Grh alone has a one division window (2 neurons) (summarized in Figure 2.2E). We also note that the average total number of NB5-2 neurons at stage 14 compared to stage 16/17 is consistent with the generation of Cas/Grh and Grh alone neurons after stage 14 (Figure 2.2F).

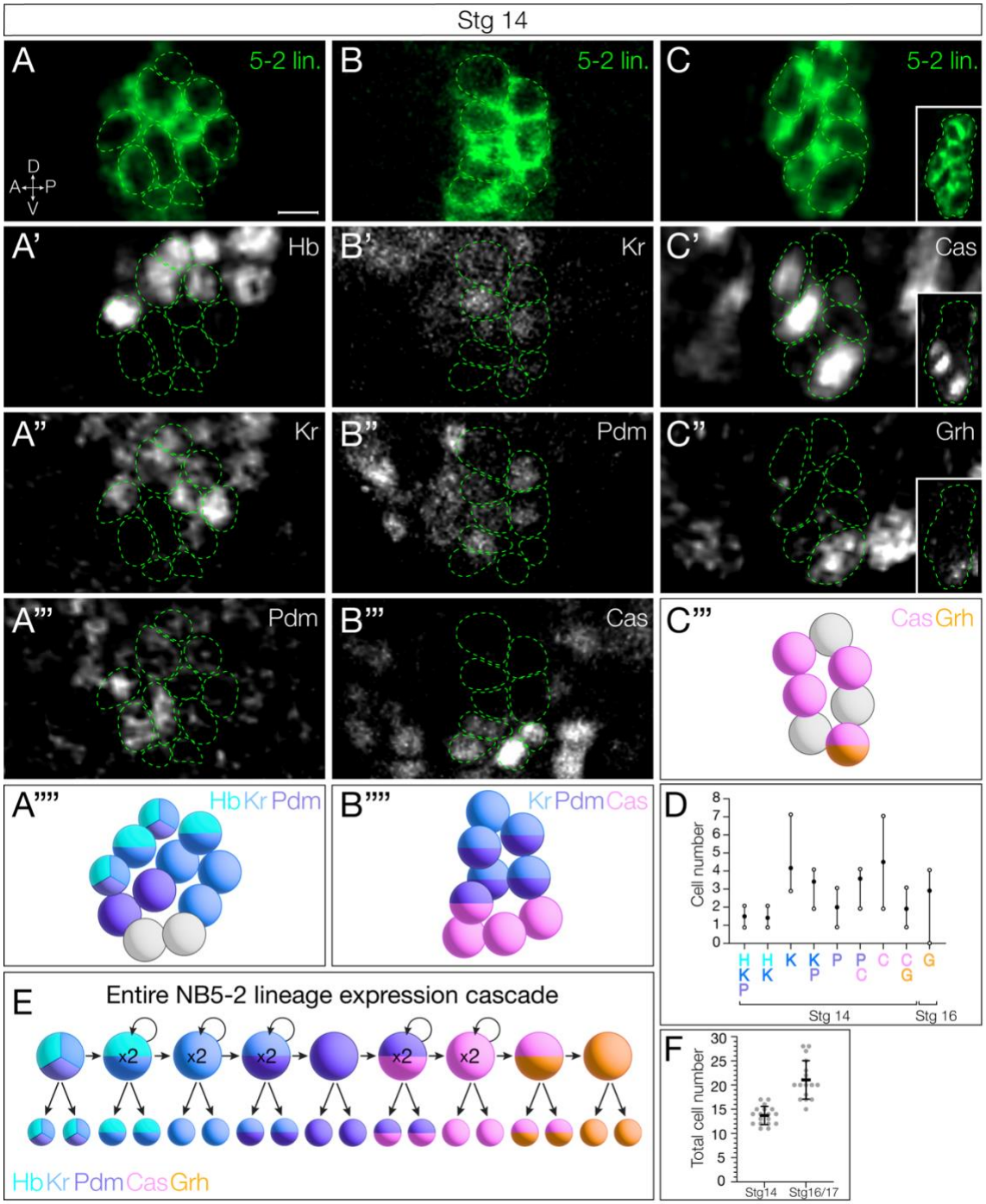

Figure 2.2. NB5-2 progeny maintain TTF expression present at time of birth.

(A) NB5-2>GFP progeny (green) stained for Hb (A'), Kr (A''), and Pdm (A''') at stage 14; A schematic summary (A''''). Anterior left, lateral view. Scale bar: 4 µm.
(B) NB5-2>GFP progeny stained for Kr (B'),
Pdm (B''), and Cas (B'''); schematic summary (B''''').

Figure 2.2. (continued). NB5-2 progeny maintain TTF expression present at time of birth.
(C) NB5-2>GFP progeny stained for Cas (C') and Grh (C'') with a low magnification image of Cas-/Grh- neurons (inset); schematic summary (C''').
(D) Quantification of NB5-2 neurons expressing each TTF singly or in combination in stage 14 (all but Grh) and 16 embryos (only Grh). Hb/Kr/Pdm avg= 1.5, Hb/Kr avg= 1.4, Kr avg = 4.2, Kr/Pdm avg= 3.4, Pdm avg= 2, Pdm/Cas= 3.6, Cas avg= 4.5, Cas/Grh avg= 1.9, Grh avg= 2.9; n = 12 hemisegments, 3 animals.
(E) Schematic of NB5-2 divisions during each TTF expression window throughout embryogenesis.
(F) Quantification of total NB5-2 neurons in stage 14 embryos (avg = 13.9, n=18 hemisegments, 5 animals) and 16 (avg= 21.1, n=17 hemisegments, 5 animals). The data underlying the graphs in the figure can be found in S1 Data.

Neuronal settling position is correlated with birth-order

Previous work has shown that early-born Hb+ neurons reside closest to the neuropil, being physically displaced into more dorsal regions by later-born neurons. Conversely, later-born Cas+ neurons take more superficial positions (Isshiki et al., 2001; Kambadur et al., 1998; Mark et al., 2021; Tran & Doe, 2008). To determine if NB5-2 progeny settling position is correlated with birth-order, we mapped the deep-to-superficial position of the NB5-2 progeny. We found that Hb+ and Kr+ neurons are located in overlapping deep layers (Figure 2.3A). Pdm neurons are positioned more superficially (Figure 2.3A-B), with some overlap with both Hb and Kr, consistent with overlapping expression patterns seen in NB5-2 (Figure 2.1). Lastly, both Cas+ and Grh+ neuron populations are located in the most superficial layers (Figure 2.3B-C). We conclude that (1) neuronal settling position is correlated with birth-order in the NB5-2 lineage (Figure 2.3D), and (2) that TTF expression, neuronal settling position, and birth-order are tightly correlated. These findings all support a model in which each TTF is inherited by the neuronal progeny born during each TTF expression window, with little migration or movement, resulting in early-born neurons located in deep layers and late-born neurons located in superficial layers.

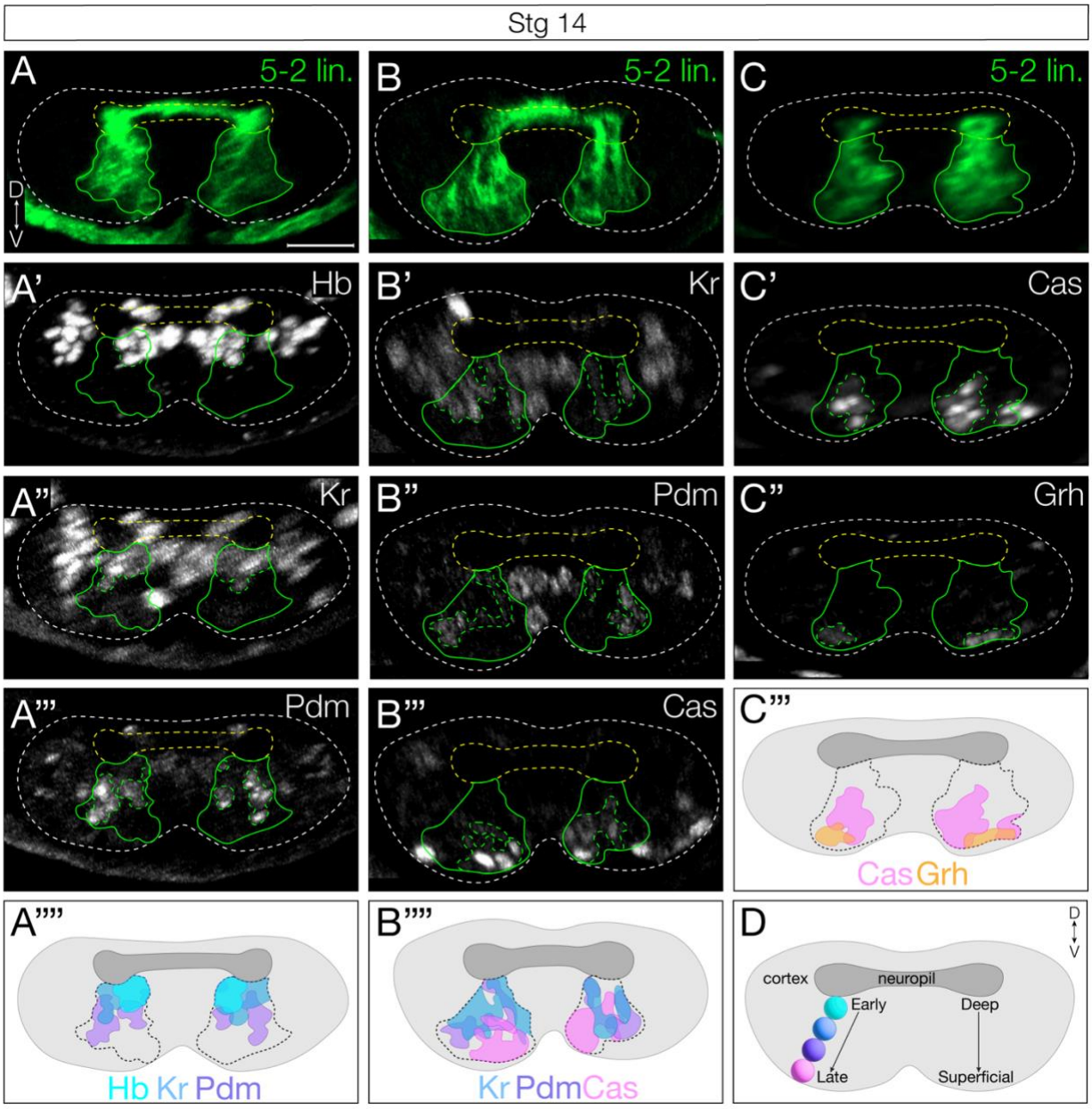

Figure 2.3. NB5-2 progeny deep-superficial settling position is correlated with birth-order.
(A) NB5-2>GFP progeny (green) settling position of neurons expressing Hb (A'), Kr (A''), and Pdm (A'''); schematic summary (A''''). Dorsal up, posterior view. n= 6 segments, 3 animals. Scale bar: 10 µm.
(B) NB5-2>GFP progeny settling position of neurons expressing Kr (B'), Pdm (B''), and Cas (B'''); schematic summary (B'''').
(C) NB5-2>GFP progeny settling position of neurons expressing Cas (C') and Grh (C''); schematic summary (C''').
(D) Cartoon of stereotypical early-to-late born cell body positions within the VNC cortex.

Prolonged Hunchback expression in NB5-2 prevents late TTF expression

To distinguish the relative importance of birth-order and TTF expression in specifying interneuronal identity, we broke their correlation by mis-expressing Hb in the NB5-2 lineage, which allowed us to determine which -- birth-order or TTF identity -- is more important for neuronal identity. We used NB5-2-Gal4 to specifically misexpress Hb throughout the lineage, and assay for alterations in the expression of later-born TTFs. If time of birth is used to generate interneuron diversity, we would expect little effect of Hb misexpression; in contrast, if the TTF identity is causal for interneuron identity, we would expect to see a clear transformation of late-born to early-born interneuron identity. In the following sections we determine the effect of Hb misexpression on interneuronal molecular identity, axon/dendrite morphology, and presynapse targeting within the dense neuropil.

We first validated the ability of Hb misexpression to repress later NB TTFs; in other NB lineages, misexpression of Hb can result in delayed or absent expression of late TTFs (Isshiki et al., 2001). The timing of Hb misexpression is also important: NBs have a relatively short competence window for responding to Hb (Kohwi et al., 2013; Pearson & Doe, 2004). We found that NB5-2-Gal4 drives misexpression of Hb beginning at early stage 10, soon after the termination of endogenous Hb expression (Figure 2.4A), and prior to the termination of the competence window at stage 12 (Kohwi et al., 2013). Importantly, we found that misexpression of Hb in the NB5-2 lineage resulted in a highly penetrant loss of expression of all later-born TTFs (Figure 2.4A; summarized in B), a prerequisite for subsequent experiments.

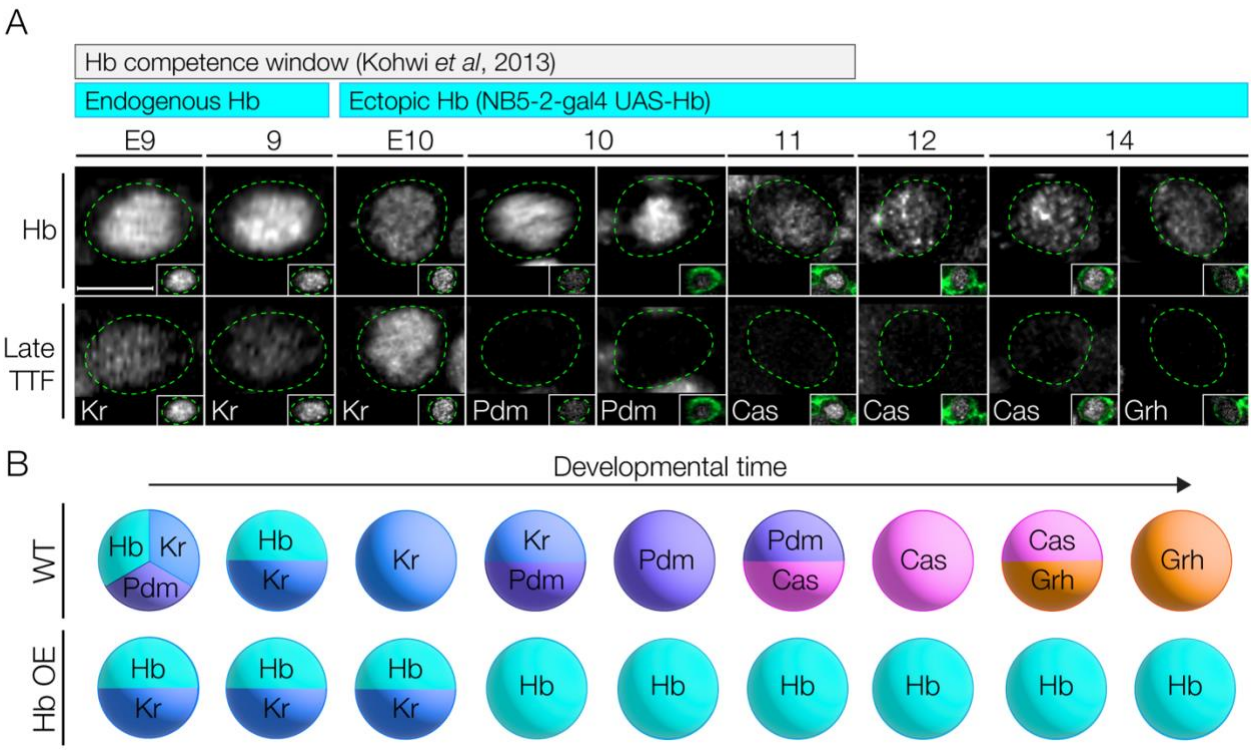

Figure 2.4. Prolonged Hunchback expression in NB5-2 delays expression of late TTFs.
(A) NB5-2>Hb progeny expressing Hb (top panels) and later TTFs (bottom panels) at stages 9-14. Bars show developmental length of known Hb competence window in other NBs (gray) and endogenous and ectopic NB5-2 Hb expression (cyan). NB5-2 identification was achieved as in Supplemental Figure 2.1; a combination of GFP (green) and Dpn was used to identify NB5-2 after stage 10 (insets). Quantification: stg E9 n= 20 hemisegments, 5 animals; stg E10 n= 24 hemisegments, 6 animals; stg 10 n= 16 hemisegments, 4 animals; stg 11 n= 8 hemisegments, 2 animals; stg 12 n= 12 hemisegments, 3 animals; stg 14 n= 12 hemisegments, 3 animals. Scale bar: 5 µm
(B) Schematic of wildtype and Hb overexpression in NB5-2.

Hunchback specifies early-born interneuron molecular identity

Next, we wanted to determine if loss of later-born TTFs due to prolonged Hb expression extended to NB5-2 progeny. We quantified the number of NB5-2 neurons expressing each TTF following Hb misexpression. As expected, we observed a significant increase in the number of Hb+ neurons in the NB5-2 lineage (Figure 2.5E-F, quantified in Q). We also found an increase in Hb+/Kr+, and Hb/+Pdm+ co-expressing neurons (Supp. Figure 2.2A-B, quantified in D-G), consistent with co-expression observed in wildtype NB5-2 neurons (Figure 2.2A). We note that

while NB Pdm expression is repressed by Hb misexpression, we see an increase in Hb+/Pdm+ NB5-2 progeny; the discrepancy in Pdm expression from NB to progeny is unclear. Conversely, we observed a striking decrease in Cas+ and Grh+ neurons, of which NB5-2 Hb+ neurons have no overlapping expression (Figure 2.5K-L, quantified in U; Supp. Figure 2.2C, quantified in H). We conclude that NB5-2>Hb is an effective tool for prolonging Hb expression throughout the NB5-2 lineage, and that prolonged Hb expression is highly effective at repressing NB expression of all later TTFs.

Figure 2.5 (next page). Prolonged Hunchback expression in NB5-2 generates ectopic early-born interneurons at the expense of late-born neurons

(A, C, E, G, I, K, M, O) Wildtype NB5-2>GFP progeny (green; dashed outline) stained for the indicated markers. Stage 16/17 (unless stated otherwise), anterior left, lateral view. Scale bar: 4 μm.

(B, D, F, H, J, L, N, P) NB5-2>Hb (green; dashed outline) stained for the indicated markers. Stage 17, anterior left, lateral view. Scale bar: 4 μm.

(Q-X) Quantification. The data underlying the graphs in the figure can be found in S2 Data.

(Q) Hb neurons. Stage 14. WT avg=2.75, n=12 hemisegments, 3 animals; HbOE avg=16.27, n=11 hemisegments, 3 animals.

(R) Nervy neurons. WT NB5-2 avg=3.11, n=28 hemisegments, 7 animals; HbOE avg=9.63, n=27 hemisegments, 7 animals.

(S) Dbx neurons. WT NB5-2 avg=2.09, n=22 hemisegments, 6 animals; HbOE avg=7.76, n=25 hemisegments, 7 animals.

(T) Nkx6 neurons. WT NB5-2 avg=2.31, n=19 hemisegments, 5 animals; HbOE avg=6.35, n=23 hemisegments, 6 animals.

(U) Castor neurons. WT NB5-2 avg=7.67, n=12 hemisegments, 3 animals; HbOE avg=2.67, n=12 hemisegments, 3 animals.

(V) Runt neurons. WT NB5-2 avg=8.52, n=21 hemisegments, 6 animals; HbOE NB5-2 avg=4.79, n=24 hemisegments, 6 animals.

(W) Zfh2 neurons. WT NB5-2 avg=7.57, n=21 hemisegments, 6 animals; HbOE NB5-2 avg=2.7, n=20 hemisegments, 6 animals.

(X) Total NB5-2 progeny number. WT avg=21.10, n=21 hemisegments, 6 animals; HbOE avg=22.75, n=24 hemisegments, 6 animals.

(Y) Schematic summary.

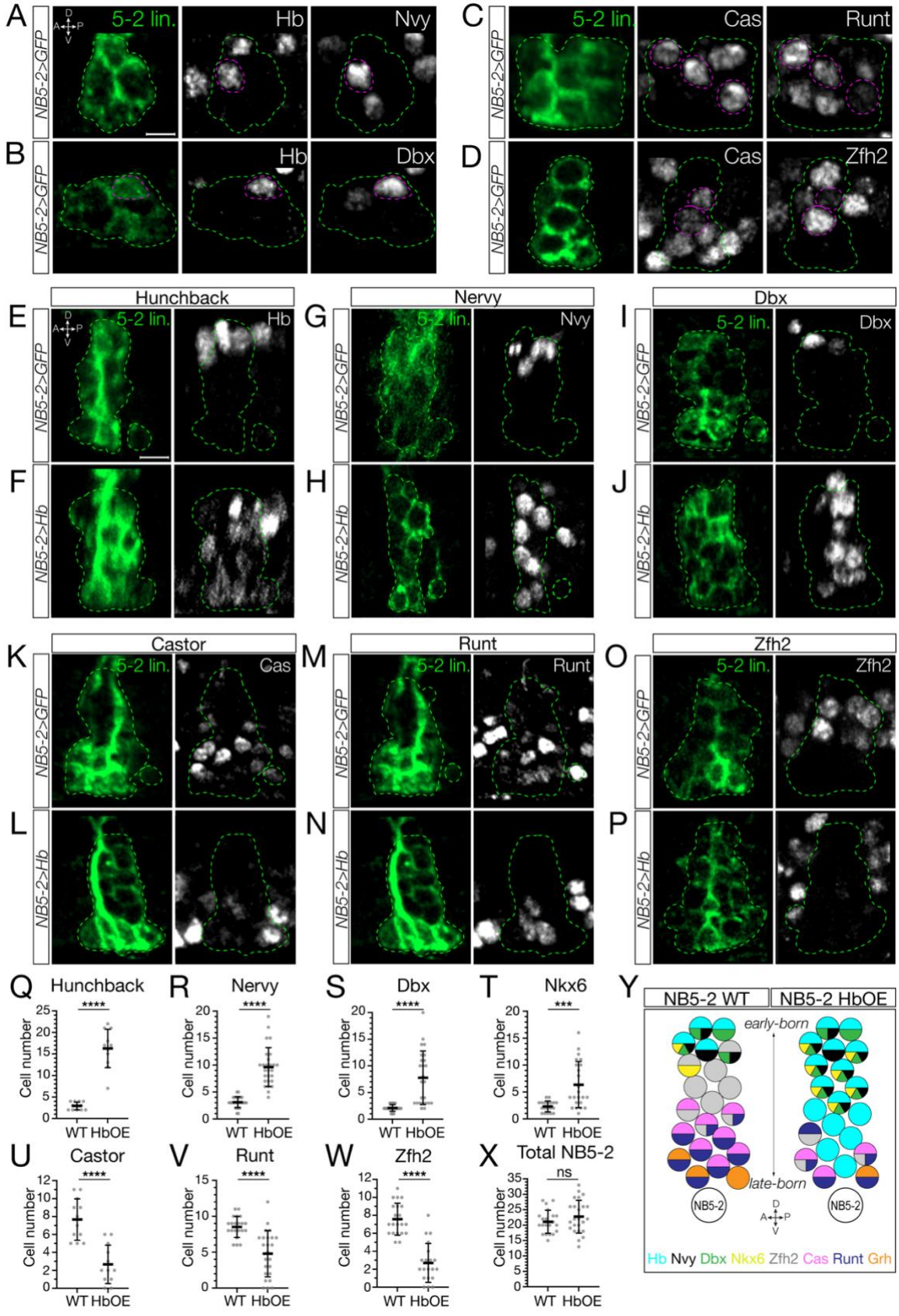
A
NB5-2>GFP
5-2 lin.
Hb
Nvy
B
Hb
Dbx
C
5-2 lin
Cas
Runt
D
Cas
Zfh2
Hunchback
E
5-2 lin.
Hb
F
NB5-2>Hb
Nervy
G
Nvy
H
Dbx
I
Dbx
J
Castor
K
Cas
L
Runt
M
Runt
N
Zfh2
O
Zfh2
P
Q Hunchback
R Nervy
S Dbx
T Nkx6
U Castor
V Runt
W Zfh2
X Total NB5-2
Cell number
WT HbOE
****
***
ns
Y
NB5-2 WT
NB5-2 HbOE
early-born
late-born
NB5-2
Hb Nvy Dbx Nkx6 Zfh2 Cas Runt Grh

To determine the role of Hb in specifying interneuron molecular identity downstream of TTF expression, we needed to identify molecular markers for early-born Hb+ and late-born Hb-negative interneurons in the NB5-2 lineage. We screened a collection of transcription factor antibodies, and identified Nervy, Dbx, and Nkx6 as early-born TFs expressed in Hb+ neurons but not in Cas+ neurons (Figure 2.5A,B and Supp. Figure 2.3A). Conversely, we identified Runt and Zfh2 as late-born TFs expressed in Cas+ neurons, but not in Hb+ neurons (Figure 2.5C,D). Next, we prolonged Hb expression in the NB5-2 lineage and assayed for changes in TF expression. We found that Hb misexpression resulted in an expansion of early-born Hb+, Nervy+, Dbx+, and Nkx6+ neurons that spanned the deep-superficial axis of the NB5-2 lineage (Figure 2.5E-J and Supp. Figure 2.3B,C; quantified in Q-T). Furthermore, prolonged Hb expression resulted in a striking loss of late-born Cas+, Runt+, and Zfh2+ neurons (Figure 2.5K-P; quantified in U-W). Importantly, there was no significant difference in the total number of NB5-2 neurons per hemisegments (Figure 2.5X), showing that late-born neurons are transformed into neurons with an early-born molecular identity, rather than undergoing cell death. We conclude that Hb is sufficient to specify early-born interneuron molecular identity at the expense of late-born neurons, and that temporal identity is more important than birth-order in specifying early-born interneuron molecular identity.

Hunchback+ early-born interneurons have a distinct morphology compared to later-born interneurons

To determine the role of Hb in specifying NB5-2 early-born interneuron axon/dendrite morphology, we needed to identify the individual neuron morphology of both early-born Hb+ and late-born Hb-negative interneurons. We showed above that NB5-2 makes five Hb+ neurons (Figure 2.2). Here we design a genetic method for identifying the morphology of each Hb+ neuron in the NB5-2 lineage. We used intersectional genetics to stochastically label individual neurons that were both Hb+ and derived from NB5-2. We call this intersectional approach "Hb+ filtered NB5-2 neurons" (Figure 2.6A). Using this method, we identified five Hb+ neurons in the NB5-2 lineage: MN12 (Figure 2.6B), and four interneurons that we name "Idun1-Idun4" (Figure 2.6C-F). Each Idun neuron has a similar but unique morphology. Based on deep-superficial cell body position, we propose that the first NB5-2 derived GMC (GMC-1) makes MN12/Idun1 siblings, GMC-2 makes Idun2/Idun3 siblings, and GMC-3 makes Idun4 and a sibling that may

undergo apoptosis, as we have never detected a sixth Hb+ neuron in the lineage. Subsequently we focus on the four Hb+ Idun interneurons.

We previously used the open-source transmission electron microscopy (TEM) volume of the first instar larval CNS (Ohyama et al., 2015) to reconstruct all of the neurons within the NB5-2 lineage in both segment A1L and A1R (Mark et al., 2021), but it was unknown which neurons in the whole lineage reconstruction were Hb+. To identify the morphology of the Hb+ neurons in the lineage, we used the intersectional genetics method described above to label "Hb+ filtered NB5-2 neurons" with a membrane-bound reporter (Figure 2.6A). We were able to identify all four Hb+ Idun interneurons as well as MN12 based on a clear match in neuron morphology (Figure 2.6B-F). All Hb+ Idun interneurons are unique, but there are a few shared features. (1) All Idun interneurons have a cell body position in a deep layer close to the neuropil. (2) All Idun interneurons have an ascending or descending intersegmental projection. (3) With the exception of Idun4, all Idun interneurons have a contralateral projection that crosses the midline with a diagonal trajectory, from ventral-medial to dorso-lateral, clearly visible in a posterior view.

Figure 2.6 (next page). Hunchback+ early-born interneurons have a distinct morphology compared to later-born neurons.
(A) Intersectional genetics was used to stochastically label NB5-2 Hb+ neurons. See methods for details.
(B-F) Single cell morphology for the indicated neurons in L1 (0-3hr ALH) larvae. Top panels, TEM reconstruction; left, left, posterior view, right dorsal view. Dotted line marks VNC border; grey surface, neuropil. Bottom panels, MCFO single neuron labeling of the indicated neurons. Left, posterior view, dotted lines mark the VNC and the neuropil, inset shows Hb expression in each neuron; right, dorsal view; dotted lines indicate the VNC borders and the midline.
(G) TEM reconstruction (top panels) and Hb+ ∩ NB5-2 lineage labeling (bottom panels) of all Hb+ NB5-2 neurons.

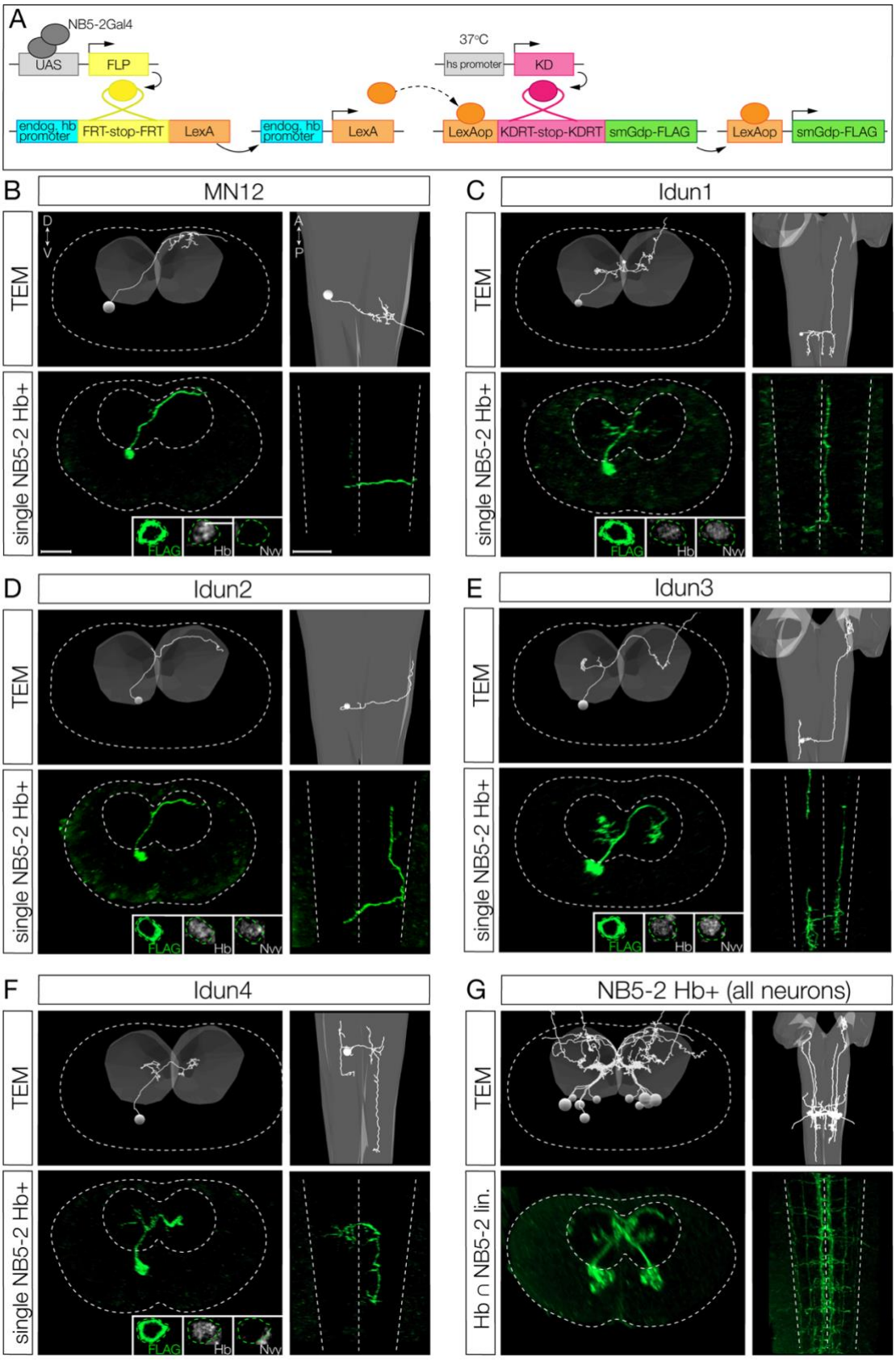
A
NB5-2Gal4
UAS
FLP
endog. hb promoter
FRT-stop-FRT
LexA
endog. hb promoter
LexA
37°C
hs promoter
KD
LexAop
KDRT-stop-KDRT
smGdp-FLAG
LexAop
smGdp-FLAG
B
MN12
C
Idun1
D
Idun2
E
Idun3
F
Idun4
G
NB5-2 Hb+ (all neurons)
TEM
single NB5-2 Hb+
Hb ∩ NB5-2 lin.
D
V
A
P
FLAG
Hb
Nvy

We found that the formation of a diagonal contralateral projection was unique to the early-born neurons; TEM reconstruction of all neurons in the lineage only found this trajectory in Idun1, Idun2, Idun3 and MN12. These shared morphological features can be observed when all five Hb+ neurons in the lineage are labeled together by light or electron microscopy (Figure 2.6G). In conclusion, we have identified four Hb+ interneurons in the NB5-2 lineage and matched them to the same four interneurons within the TEM reconstruction. Importantly, these early-born interneuron morphologies are clearly different from late-born interneuron morphology (Supp. Figure 2.4). In addition to identifying morphological differences in early-born and late-born interneurons, mapping the Idun interneurons in the TEM volume allows us to quantify presynapse and postsynapse position for each Idun neuron - a prerequisite for characterization of Idun presynapse neuropil targeting (see below).

Hunchback specifies early-born interneuron morphology

We showed above that Hb determines early-born interneuron molecular identity based on early and late-born TF expression. Here we ask whether Hb determines early-born interneuron axon/dendrite morphology. We wanted to distinguish between two possible mechanisms, as we did for interneuron molecular identity. First, *birth-order* may be critical for determining neuronal morphology, perhaps each neuron born at a different time encounters a changing environment which directs the appropriate projection. Second, *TTF expression* may determine neuronal morphology, perhaps via TTF-regulated guidance cues. To determine the relative importance of birth-order and TTF expression, we misexpressed Hb in the NB5-2 lineage and asked whether late-born neurons persisted in generating late-born neuronal morphology (birth-order model) or whether they acquired early-born neuronal morphology (TTF model). The latter was found to be important in the motor neurons of the NB7-1 lineage (Meng et al., 2019; A. Q. Seroka & Doe, 2019); here we ask whether this mechanism is extended to the interneurons, where axons and dendrites remain within the synaptically dense neuropil of the CNS.

We focus on Idun1, Idun2, and Idun3, as these interneurons have a unique diagonal commissural crossing projection not observed in later-born neurons, with the addition of Idun1 possessing the most medial ascending projection and Idun2 possessing the most lateral ascending projection among NB5-2 progeny (Figure 2.7). NB5-2>GFP labels three types of contralateral projections: dorsal, ventral, and diagonal, that are best seen in a posterior view (Figure 2.7A),

plus ascending/descending projections that are best seen in a dorsal view (Figure 2.7A'). In contrast to controls, Hb misexpression shows a striking loss of the dorsal and ventral contralateral projections and an increase in the diagonal projections (Figure 2.7B; posterior view) as well as a loss of ascending/descending projections (Figure 2.7B'). These phenotypes are due to a change in late-born neuron morphology, and not the death of late-born neurons, as there are the same number of neurons in control and experimental NB5-2 lineages (Figure 2.5X).

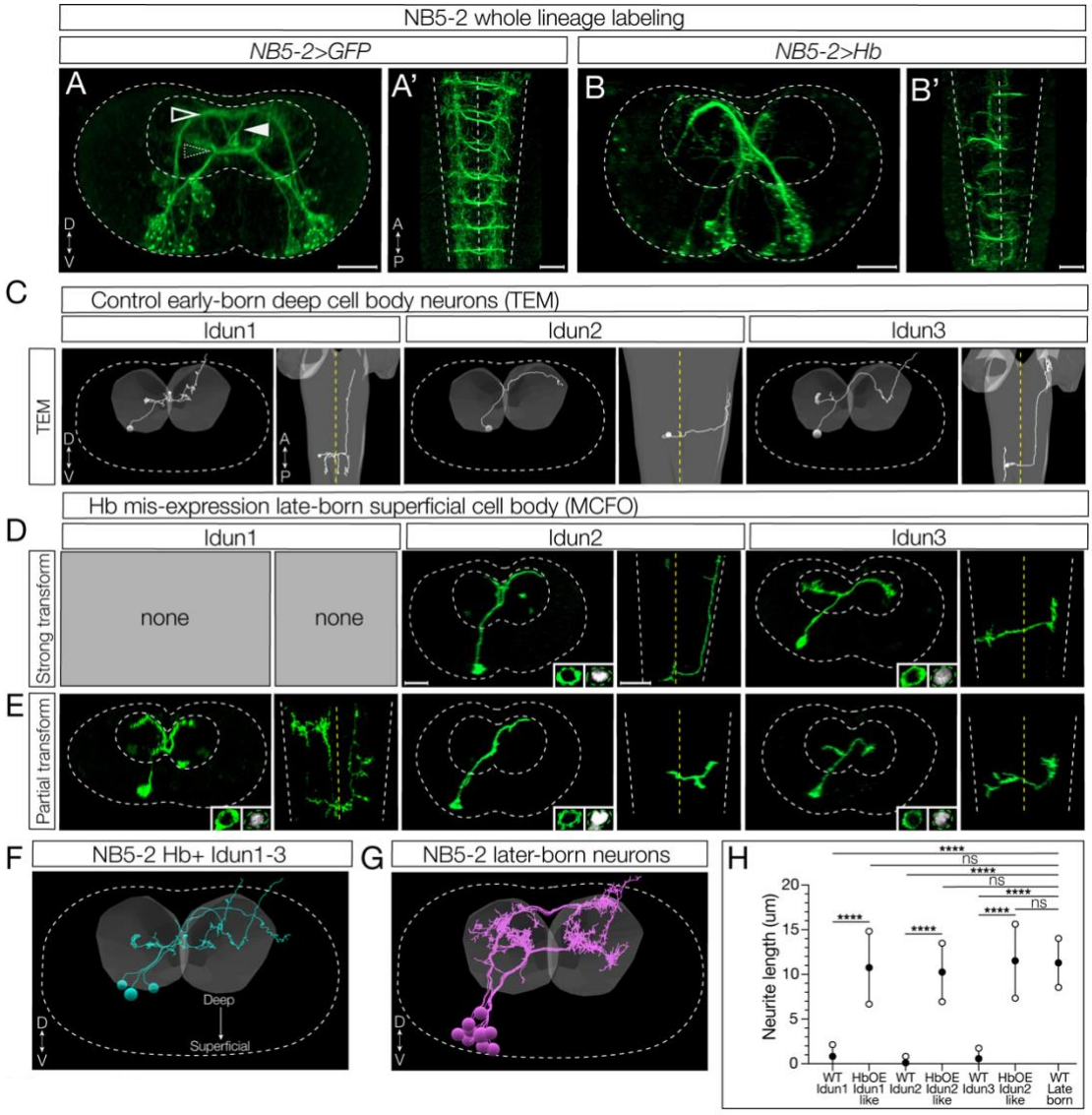

Figure 2.7. Hunchback determines early-born neuron morphology.
(A) Whole lineage labeling of L1 (0-3hr ALH) wildtype (WT) NB5-2>GFP (green) axon/dendrite morphology displaying dorsal (outlined arrow), ventral (dotted arrow), and diagonal (filled arrow) neurite projections within the A1/A2 VNC neuropil. (A) Dorsal up, posterior view; (A') Anterior up, ventral view. Scale bar: 10 µm.

Figure 2.7 (continued). Hunchback determines early-born neuron morphology.
(B) Whole lineage labeling of NB5-2>Hb morphology within the A1/A2 VNC neuropil. (B) Dorsal up, posterior view; (B') Anterior up, ventral view.
(C) TEM reconstruction of WT Idun1 (left two panels), Idun2 (middle two panels), and Idun3 (right two panels) morphology and cell body position relative to the neuropil (grey). Left panel, dorsal up, posterior view; Right panel, anterior up, ventral view. VNC border (white dotted line); VNC midline (yellow dotted line).
(D) L1 (0-3hrs ALH) NB5-2>Hb late-born neurons, labeled using MultiColor FlipOut (MCFO; green), displaying strong Idun1 (left two panels), Idun2 (middle two panels), and Idun3 (right two panels) morphology with Hb (right inset) expression in the cell body (left inset). Left panel, dorsal up, posterior view; Right panel, anterior up, ventral view. Scale bar: 10 µm.
(E) NB5-2>Hb late-born neurons displaying partial Idun1 (left two panels), Idun2 (middle two panels), and Idun3 (right two panels) morphology and Hb (right inset) expression in the cell body (left inset).
(F) TEM reconstruction of WT NB5-2 Hb+ neuron morphology from a single A1 hemisegment.
(G) TEM reconstruction of WT NB5-2 later-born neuron morphology from a single A1 hemisegment.
(H) Quantification of WT Idun1-3, late-born transformed Idun1-3 NB5-2>Hb (HbOE Idun1-like/ Idun2-like/ Idun3-like), and WT late-born neurite length (WT Idun1 avg=0.83, n=8; WT Idun2 avg=0.11, n=7; WT Idun3 avg=0.58, n=5; HbOE Idun1-like avg=10.76, n=9; HbOE Idun2-like avg=10.25, n=10; HbOE Idun3-like avg=11.52, n=8; WT late-born avg=11.29, n=19; one-way ANOVA *p-values*: WT Idun1 vs HbOE Idun1-like *p-value* <0.0001, WT Idun2 vs HbOE Idun2-like *p-value* <0.0001, WT Idun3 vs HbOE Idun3-like *p-value* <0.0001, WT Idun1 vs. WT late-born *p-value*<0.0001, WT Idun2 vs. WT late-born *p-value*<0.0001, WT Idun3 vs. WT late-born *p-value*<0.0001, HbOE Idun1-like vs. WT late-born *p-value*=0.99 (n.s), HbOE Idun2-like vs. WT late-born *p-value*=0.97 (n.s), HbOE Idun3-like vs. WT late-born *p-value*>0.99 (n.s)). The data underlying the graphs in the figure can be found in S3 Data.

To prove that Hb misexpression reprograms late-born interneurons to generate an axon/dendrite morphology characteristic of early-born neurons, we labeled single neurons in the NB5-2 lineage using multicolored flip out (MCFO) (Pfeiffer et al., 2008) in a wild type or Hb misexpression background. Following Hb misexpression, we identified late-born interneurons based on their superficial cell body position (see Figure 2.3) (Mark et al., 2021), and confirmed that they were Hb+ despite their superficial position (Figure 2.7D-E). We found that these late-born neurons expressing Hb had an early-born axon/dendrite morphology, including a diagonal contralateral projection and ascending/descending intersegmental projections similar to the TEM reconstruction of Idun1-3 neurons (Figure 2.7C-E); we call these "strongly" transformed

neurons. In addition, we also observed "partially" transformed late-born neurons, characterized by the expected diagonal commissural projection but lacking ascending or descending projections (Figure 2.7E). Why there are two phenotypic classes is not clear (see Discussion).

To gain additional evidence for the Hb-mediated transformation of late-born neurons into neurons with morphological features characteristic of early-born neurons, we measured soma-neuropil distance as a proxy for birth-order (see Figure 2.3) (Mark et al., 2021). As expected, wild type early-born Idun1, Idun2, and Idun3 neurons had cell bodies close to the neuropil, with very short soma-neuropil distance (Figure 2.7F, quantified in H). Also as expected, wild type Hb-negative late-born neurons had superficial locations and a large soma-neuropil distance (Figure 2.7G, quantified in H). Importantly, Hb misexpression resulted in neurons with a diagonal commissural projection, characteristic of early-born neurons, yet showing a large soma-neuropil distance (Figure 2.7H). This shows that late-born, superficially located neurons can be efficiently transformed into neurons with early-born morphology following prolonged Hb expression. We conclude that Hb is sufficient to induce early-born interneuron morphology. This is consistent with the "TTF model" for specifying interneuron morphology.

Hunchback determines interneuron presynapse targeting within the neuropil

We next wanted to determine if Hb played a role in early-born interneuron presynaptic targeting, which is particularly interesting due to the dense packing of synapses in the neuropil. We first sought to determine the presynapse localization of Idun1-3 within the neuropil, a critical first step in establishing proper connectivity to downstream early-born partners. We used the TEM dataset to predict the neuropil volume occupied by Idun1, Idun2, and Idun3 presynapses (Figure 2.8A), as well as for all NB5-2 neuronal presynapses (Figure 2.8B). The neuropil position of presynapses differed for each neuron, which we label as i1, i2, and i3 for Idun1-3, respectively. We then used Hb filtered genetics (Figure 2.8C) to express Bruchpilot (Brp), an inactive presynaptic marker, in the Idun1-3 neurons and mapped the coordinates for the three volumes to the neuropil. Importantly, in controls, the Brp puncta targeted the same three volumes in both light and electron microscopy, which can be seen for both Hb+ neurons (Figure 2.8D) and all NB5-2 progeny neurons (Figure 2.8E). Note that left and right hemisegments were treated as independent data and mirrored to show only left hemisegments. Overexpression of Hb in the NB5-2 derived neurons results in several phenotypes. (1) There is a higher percentage of Brp

puncta targeting i1 and i2 (compare Figures 2.8E and F; quantified in Figure 2.8G), consistent with late-born neurons being transformed to early-born Idun1 and Idun2 neurons, and targeting to their characteristic Idun1/2 neuropil volumes. (2) There is a loss of Brp puncta from late-born neurons (Figure H' and I'), also consistent with late-born neurons being transformed to early-born Idun1 and Idun2 neurons. (3) There is a decrease in the percentage of Brp puncta that target the i3 volume. (4) There are Brp puncta abnormally positioned between the i2 and i3 volumes (Figure 2.8F; yellow arrows). Our results provide support for a model in which the early TTF Hb can reprogram late-born neurons, driving them to target their presynapses to neuropil volumes normally targeted by presynapses of early-born neurons.

To test these conclusions, we performed an additional analysis using custom Python code (Newstein, 2024) to create a neuropil template, align our images to the template, and create a shared coordinate system across all images of all genotypes. As described above and in Figure 2.8D, D' we mapped Hb+ NB5-2 lineage derived presynapses into three Hb+ neuropil volumes (i1-i3); those outside these domains were presynapses of late-born NB5-2 derived neurons (Supp Figure 2.6). In controls, we observed presynapses in the three Hb+ domains (Figure 2.8H, cyan puncta) as well as in the late-born domains (Figure 2.8H, magenta puncta). In contrast, overexpression of Hb in the NB5-2 derived neurons resulted in a higher percentage of presynapses in two Hb+ neuropil domains (Figure 2.8I, quantified in 2.8J), similar to our manual registration findings (Figure 2.8D-G). Importantly, we find no significant difference in the total number of presynapses between controls and Hb misexpression using our manual registration analysis and only a slight difference using our computational registration approach (quantified in Figure 2.8K). We conclude that Hb overexpression can drive late-born presynapses into Hb+ neuropil domains, based on both manual and computationally defined presynapse localization.

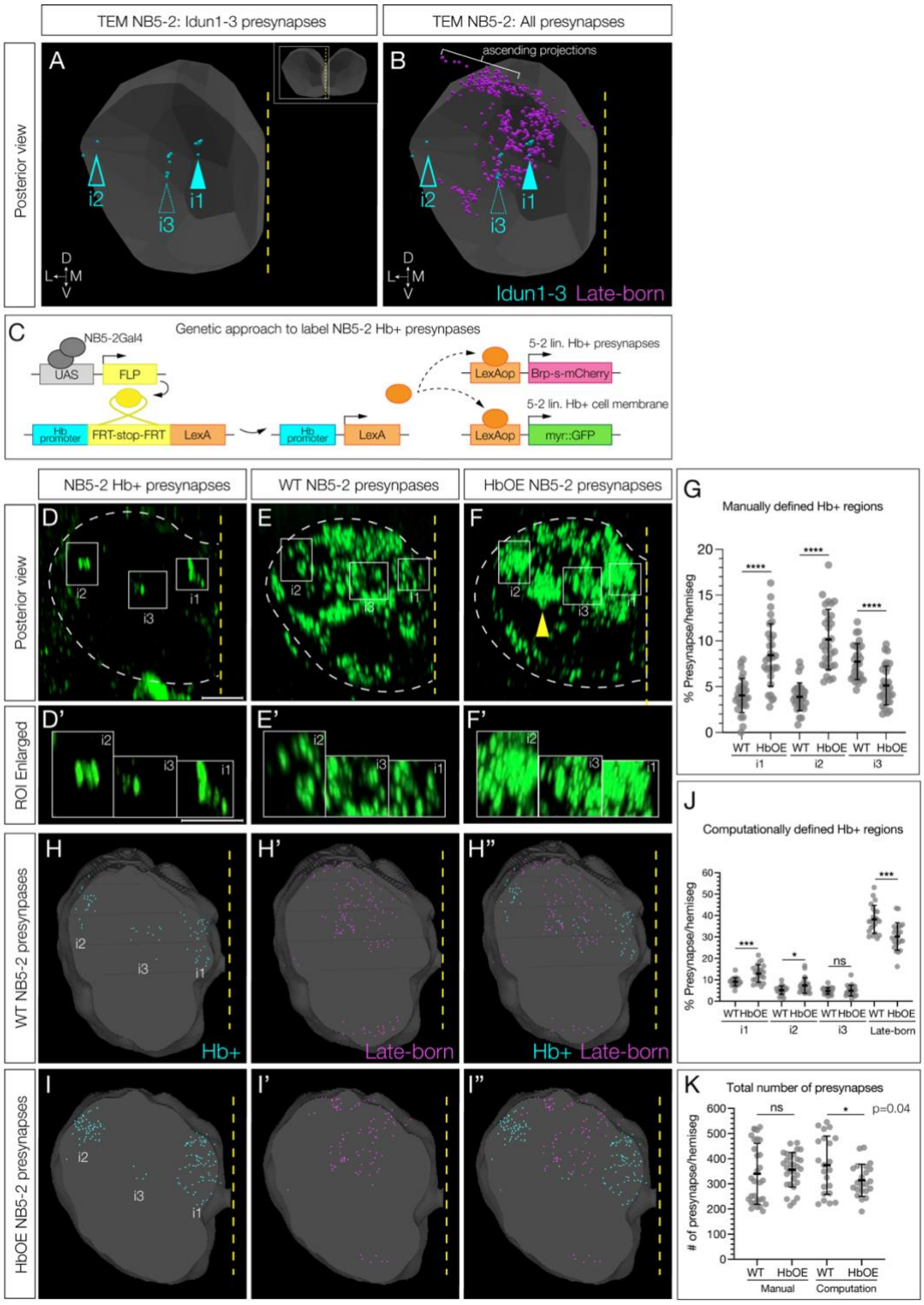

Figure 2.8. Hunchback determines interneuron presynapse localization
(A) TEM reconstruction of NB5-2 Hb+ Idun1 (i1), Idun2 (i2) and Idun3 (i3) presynapse positions in the A1 left hemisegment neuropil (grey). Dorsal up, posterior view.

Figure 2.8 (continued). Hunchback determines interneuron presynapse localization
(B) TEM reconstruction of NB5-2 Hb+ Idun1-3 (cyan) and late-born neuron (magenta) presynapses in the left A1 neuropil hemisegment.
(C) NB5-2 Hb-filtered presynapse genetics. An intersectional genetics approach to drive expression of Brp exclusively in NB5-2 Hb expressing neurons. NB5-2 Gal4 (grey) drives expression of Flipase (FLP, yellow) to promote excision of a stop codon inserted downstream of the endogenous Hb promoter (cyan) and upstream of a LexA transgene (orange), allowing for LexA expression exclusively in NB5-2 Hb expressing neurons. LexA then drives expression of a truncated Brp conjugated to mCherry (Brp-s-mCherry, magenta) and GFP (myr::GFP, green).
(D) NB5-2 Hb+ presynapses labeled by Brp expression (green) using intersectional genetics. Idun1-3 positions are outlined (white) in the left hemisegment neuropil (dotted outline) according to average location found from hemisegment centroid position (see Methods) Dorsal up, posterior view. Scale bar: 5 μm. Idun1-3 regions enlarged (D'). Scale bar: 3 μm.
(E) WT NB5-2 presynapses labeled by endogenous Brp expression conjugated to a V5 epitope tag (green). Idun1-3 (i1-i3) positions are outlined; (E') enlargement of boxed regions in E.
(F) NB5-2>Hb presynapses with Idun1-3 (i1-i3) positions outlined with a possible Idun3 mistargeting location (yellow arrow; see Discussion); (F') enlargement of boxed regions in F.
(G) Quantification of WT NB5-2 and NB5-2>Hb (HbOE) larval presynapse percentage per hemisegment, found using manual registration, in neuropil positions i1 (WT avg= 4.05, HbOE avg= 8.45, n= 30, *p-value*<0.0001), i2 (WT avg= 3.90, HbOE avg= 10.16, n= 30, *p-value*<0.0001), and i3 (WT avg= 7.74, HbOE avg= 5.13, n= 30, *p-value*<0.0001).
(H) WT NB5-2 presynapses in Hb+ (cyan) and late-born (H', magenta) regions defined by computational registration. Merged image of Hb+ and late-born regions (H''). Images generated using Nepari (https://napari.org/).
(I) HbOE NB5-2 presynapses in Hb+ (cyan) and late-born (I', magenta) regions defined by computational registration. Merged image of Hb+ and late-born regions (I''). Images generated using Nepari (https://napari.org/).
(J) Quantification of NB5-2 WT and HbOE larval presynapse percentage per hemisegment, found using computational registration, in neuropil positions i1 (WT avg= 9.11, HbOE avg= 12.93, n= 22, *p-value*= 0.0002), i2 (WT avg= 5.19, HbOE avg= 7.35, n= 22, *p-value*= 0.0161), i3 (WT avg= 4.79, HbOE avg= 4.98, n= 22, *p-value*= 0.76), and late-born regions (WT avg= 38.31, HbOE avg= 30.23, n= 22, *p-value*= 0.0002).
(K) Quantification of all NB5-2 WT and HbOE larval presynapses per hemisegment found using manual and computation registration analyses (Manual WT avg= 340.2, Manual HbOE avg= 356, n= 30, *p-value* = n.s.; Computation WT avg= 374, Computation HbOE avg= 314.2, n= 22, *p-value*= 0.04). The data underlying the graphs in the figure can be found in S4 Data.

Hunchback misexpression phenocopies loss of a proprioceptive behavior circuit

Drosophila larvae have a well-characterized proprioceptive circuit: proprioceptive sensory neurons > Jaam1-3 > Eve+ interneurons > Saaghi1-3 > motor neurons (Heckscher et al., 2015; Wreden et al., 2017). Ablation of the Eve+ interneurons in the proprioceptive circuit results in decreased larval crawling speed and increased C-shaped body bends (Heckscher et al., 2015). Importantly, both Jaams and Saaghis are late-born neurons in the NB5-2 lineage (Mark et al., 2021). This raises the question: if Hb misexpression transforms late-born Jaam and Saaghi neurons into an early-born identity, will they maintain or lose their connectivity to the proprioceptive circuit neurons? If Hb misexpression can drive late-born neurons into a circuit with endogenous early-born neurons, we would expect a loss of proprioceptive behavior. Thus, we misexpressed Hb throughout the NB5-2 lineage and measured these two behaviors. Qualitatively, experimental larvae showed a strong uncoordinated crawling pattern (compare SuppMovie 1 and SuppMovie 2). Quantitatively, we observed significantly decreased forward locomotor velocity and increased C-shaped body bends, compared to controls (Figure 2.9A,B). We conclude that transformation of late-born NB5-2 interneurons to an early-born identity disrupts late-born proprioceptive circuit assembly or function.

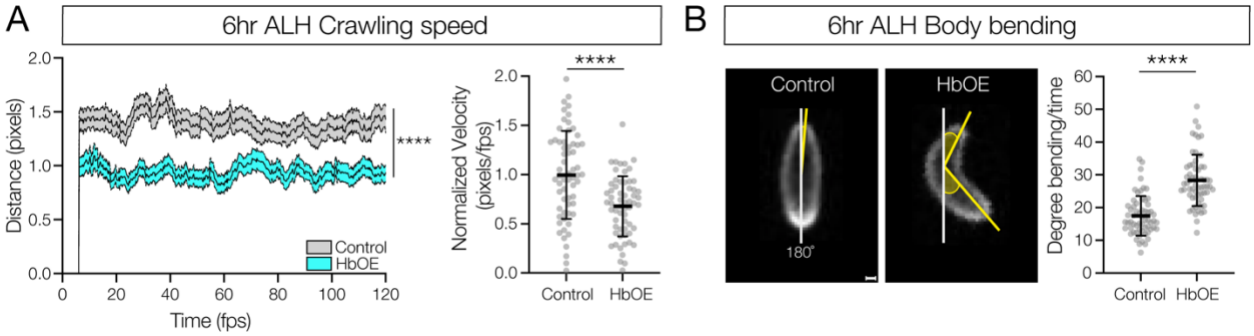

Figure 2.9. Prolonged Hunchback expression disrupts late-born proprioceptive circuit connectivity.

(A) Crawling speed of newly hatched WT NB5-2>GFP (Control; grey, avg AUC=159, n=61)) and NB5-2>Hb (HbOE; cyan, avg AUC=106.9, n=62) larvae (0-4hrs ALH) (*p-value*<0.0001); Normalized crawling speed of WT (control, avg=0.99) and HbOE (avg=0.68) larvae (*p-value*<0.0001).

(B) WT NB5-2 (control, avg=17.47, n=61) and HbOE (avg=28.31, n=62) body bend posture determined by the angle of degree (yellow shaded) from 180˚ (white line); Quantification of body-bend degree from 180˚ (*p-value*<0.0001). Scale bar: 40 µm. The data underlying the graphs in the figure can be found in S5 Data.

Discussion

During neurogenesis, intrinsic mechanisms play a vital role in determining neuron identity. The role of Hb in specifying motor neuron identity has been well studied in NB3-1 and NB7-1 (Grosskortenhaus et al., 2006; Isshiki et al., 2001; Kanai et al., 2005; Novotny et al., 2002; Pearson & Doe, 2003; Tran et al., 2010). Our study provides a comprehensive analysis of Hb in specifying NB5-2 interneuron identity. We found that the TTF cascade is expressed sequentially in NB5-2 (Hb > Kr > Pdm > Cas > Grh) and is transiently maintained in the post-mitotic progeny with single or multiple gene overlap combinations. This expression pattern is consistent with the previously characterized NB3-1 and NB7-1 and is further support of a conserved, intrinsic TTF mechanism among VNC NBs (Doe, 2017). To determine the role of Hb in specifying interneuron identity we prolonged Hb expression in NB5-2 and analyzed three aspects of neuron identity: molecular identity, axon/dendrite morphology, and presynapse targeting (required for proper connectivity), and then assessed behavioral output due to changes in neuron identity.

We found that prolonged Hb expression prevented expression of late-born TTFs and increased the number of interneuron progeny with an early-born molecular identity (Nervy+ Dbx+ Nkx6+) at the expense of late-born progeny. In NB3-1, prolonged Hb expression increases the number of RP1/RP4 motor neurons with an early-born Zfh2-/Cut- molecular identity (Meng et al., 2020; Tran & Doe, 2008). Similarly, NB7-1 Hb misexpression increases motor neuron progeny with an early-born U1/U2 molecular identity (Eve+/Zfh2-) (Meng et al., 2019; A. Q. Seroka & Doe, 2019). In NB5-6 and NB7-4, both of which generate interneuron progeny, Hb binds NB specific loci in each NB, suggesting differential expression of downstream genes (Sen et al., 2019). Previous work has also shown that the late TTF Cas window of expression can be subdivided by "sub-temporal" genes to specify four distinct Apterous+ (Ap+) interneurons in the NB5-6T lineage. Ap+ neurons are uniquely specified through activation of the transcription factor Collier/Knot (Col) and a series of feedforward loops (Baumgardt, Karlsson, Terriente, Diaz-Benjumea, et al., 2009; Stratmann et al., 2016). The combinatorial expression of Kr/Pdm has also been shown to be crucial for the Nkx6+ molecular identity of the VO MN, derived from NB7-1 (A. Seroka et al., 2020). Thus, the combinatorial expression of multiple TTFs may be important in promoting individual neuronal molecular identities. In the NB5-2 lineage, Hb

induced expression of the early-born TFs (Nervy, Dbx, and Nkx6) suggests that Hb may promote specification of distinct interneurons through differential expression of unique TF combinations.

To understand if Hb is required for proper NB5-2 interneuron morphology, we first identified the unique morphology of the NB5-2 Hb+ interneurons, Idun1-4, and then found that late-born neurons expressing Hb displayed a strikingly similar early-born diagonal neurite morphology. We found that late-born neurons displaying early-born morphology fell into two phenotypic classes: strongly transformed, where late-born neurons possessed a diagonal and ascending projection and partially transformed, in which the late-born neuron displayed a diagonal projection but lacked an ascending projection. We propose three explanations for these phenotypic classes: (1) partially transformed late-born neurons do not experience the same developmental environment as early-born neurons and thus lack the environmental signals to extend ascending and descending projections. (2) Late-born neurons inherently have less time to form long projecting neurites. Assaying morphology at later time points may allow for the formation of ascending projections. (3) Neurons may require a separate mechanism to form long projecting neurites, not present in some late-born neurons.

Prolonged Hb expression in NB7-1 results in a late-born to early-born transformation of U1/U2 early-born dendrite morphology (Meng et al., 2020; A. Q. Seroka & Doe, 2019). The expression of extrinsic signaling ligand/receptors, such as Sema/Plexin or Slit/Robo, allows a neuron to respond to a given attractant or repulsive signaling gradient within the neuropil (Zlatic et al., 2009); differential expression of one or more receptor in early- or late-born neurons may determine differences in presynaptic or postsynaptic neuropil targeting. A transcriptomic study of *Drosophila* olfactory projection neurons (PNs) revealed that transcriptomes of PN subtypes shows the highest amount of TF and cell-surface molecule diversity during circuit assembly (H. Li et al., 2017). In future studies, identifying and functionally testing downstream Hb targets such as guidance ligands/receptors will be an important next step in understanding how connectivity within the *Drosophila* CNS is established.

To understand if Hb promotes functional connectivity, we would ideally like to optogenetically simulate Idun1-3 presynaptic partners (or Idun1-3 directly) following Hb misexpression. A TTX-insensitive increase in GCaMP activity in putative downstream partners would functionally validate monosynaptic connectivity. Unfortunately, TEM connectivity data revealed that many Idun2 and Idun3 pre- and post-synaptic partners are unknown neurons,

meaning we do not currently possess genetic access to these neurons. Idun1 shows pre- and post-synaptic connections to the well characterized Moonwalking Descending Neuron (MDN) (Bidaye et al., 2014; Carreira-Rosario et al., 2018; K. Lee & Doe, 2021; K. M. Lee et al., 2022). The connectivity between MDN and Idun1 is the most ideal connection among the NB5-2 Hb+ neurons because we have genetic access to MDN, and Idun1 expresses GABA (Supp. Figure 2.5), suggesting it functions as an inhibitory neuron; however, there are two additional late-born NB5-2 neurons that also form synapses with MDN, making an excitation response between endogenous and transformed late-born neurons impossible to distinguish.

Although genetic limitations prevented us from testing whether Hb transformed late-born neurons acquire functional connectivity matching that of early-born neurons, we performed two experiments that both support a Hb-induced switch in late-born neuron connectivity. First, we asked if Hb misexpression in late-born neurons induces them to form presynapses in neuropil domains normally targeted by endogenous early-born neurons. To achieve this, we use two complementary analyses of manual and computational registration to locate NB5-2 Hb+ neuropil subregions. We found a significant increase in the percentage of presynapses that target Idun1 and Idun2 subregions following Hb misexpression, consistent with the transformed neurons acquiring the same connectivity as the endogenous early-born neurons. However, we also observed a significant decrease or no change in presynapses in the i3 volume and an abnormally positioned cluster of presynapses between i2 and i3 (Figure 2.8F; yellow arrows). These results may be consistent with Idun3 being transformed to Idun1 or Idun2; alternatively, the Idun3 presynapse region contains some late-born presynapses, and thus it is possible that these neurons are transformed into Idun1/2 identity. In the future, direct genetic assess to Idun1-3 will allow us to explore these possibilities.

Second, we asked if Hb misexpression in late-born neurons disrupted their normal connectivity, leading to slow locomotion and increased C-shaped body bends, hallmarks of defective proprioceptive behavior (Heckscher et al., 2015). Indeed, Hb misexpression resulted in the same behavioral defects as ablation of proprioceptive circuit neurons, consistent with reprograming late-born neuron connectivity to neurons of the proprioceptive circuit to a new connectivity that is unable to generate normal proprioceptive behavior. These findings are consistent with Hb misexpression abolishing normal late-born neuron connectivity. Note that the role of TTFs in establishing connectivity has been previously shown for embryonic motor

neurons (Meng et al., 2019, 2020; A. Q. Seroka & Doe, 2019) and there are strong correlations between neuronal birth-order and wiring specificity in *Drosophila* olfactory projection neurons and mushroom body Kenyon cells (T. Lee & Luo, 1999).

In *Caenorhabditis elegans*, the *hb* homolog, *hbl-1*, specifies early-born seam cell fate (Lin et al., 2003). In addition, combinatorial expression of homeodomain proteins specify specific neuron types (Reilly et al., 2020). Our data show that Hb is sufficient to promote the expression of two homeodomain proteins, Nkx6 and Dbx, in early-born NB5-2 progeny, and repress homeodomain Zfh2 expression. Hb repression of Zfh2 is also observed in early-born NB3-1 and NB7-1 neurons (Meng et al., 2019, 2020; A. Q. Seroka & Doe, 2019; Tran & Doe, 2008). Taken together, this may place Hb as a hierarchical transcription factor that promotes/represses the expression of downstream homeodomain proteins, which then generate unique, lineage specific TF combinations to specify distinct aspects of individual neuron identity.

In both flies and mammals, neuron settling position is correlated with neuronal birth-order. For example, early-born Hb+ neurons are located deep in the VNC cortex and late-born Cas+ are located superficially. In mammals, cortical projection neurons in different layers project to distinct regions of the CNS (Haubensak et al., 2004; Molyneaux et al., 2007). Progeny generated from apical radial glia (aRG) settle in a similar birth-order dependent manner, early-born neurons located in deep cortical layers while later-born neurons migrate to settle more superficially (Luo, 2020). The Hb mammalian ortholog, Ikaros (Ikzf1), is expressed early in aRGs and is necessary and sufficient to generate early-born progeny (Alsio et al., 2013; Elliott et al., 2008). Prolonged Ikzf1 expression in aRGs increases the number of deep layer early-born cells, identified by early-born TFs (Ctip2+Tbr1+Foxp2+) (Alsio et al., 2013). Similarly, Ikzf1 is expressed in early retinal progenitor cells (RPC) and promotes the production of early-born neuron identities derived from RPCs. Misexpression of Ikzf1in RPCs increases the number of early-born horizontal cells and amacrine cells at the expense of late-born bipolar neurons (Elliott et al., 2008). In addition, the Cas mammalian ortholog, Casz1, is expressed in later cell divisions of RPCs and promotes the production of late-born rod cells (Mattar et al., 2015, 2018).
Our data shows that Hb expression in NB5-2 is sufficient to specify early-born interneuron identity at the molecular, morphological, presynapse targeting, and behavioral levels. The correlations in *Drosophila* NBs and mammalian aRGs and RPCs suggests there is a conserved mechanism in which intrinsic TTF expression in progenitor cells is, in part, an initial requirement

to diversify individual progenitor lineages. This leads to many open questions: how does Hb promote lineage-specific early-born neuron identity? What is the function of TFs downstream of Hb? Is the role of Hb in specifying interneuron identity conserved across multiple species? Does Ikzf1 promote/repress the expression of specific TFs important for distinct aspects of early-born cortical or retinal cell identity? These will be exciting avenues to explore in future studies.

Materials and Methods

Fly Stocks

Male and female *Drosophila melanogaster* were used. The chromosomes and insertion sites of transgenes (if known) are shown next to genotypes.

Table 1. Genotypes utilized to obtain results for the Figure(s) indicated in Chapter II

Genotype	Figure(s)
vnd-VP16; R16H05-Gal4 DBD/10xUAS-IVS-myr::sfGFP-THS-10xUAS(FRT.stop)myr::smGdP-HA	Figure 2.1, 2.2, and 2.3
vnd-VP16/10xUAS-IVS-myr::GFP; R16H05-Gal4 DBD	Figure 2.5, 2.7, and 2.9
vnd-VP16/10xUAS-IVS-myr::GFP; R16H05-Gal4 DBD/UAS-Hunchback	Figure 2.4, 2.5, 2.7 and 2.9
hs-KD, 3xUAS-FlpG5; vnd-VP16/ 13xlexAop(KDRT-stop)SmGdp-Flag; R16H05-Gal4 DBD/hb(FRT.stop)lexA-T2A-ORF	Figure 2.6
20xUAS-Flp; vnd-VP16/13xLexAop2-IVS-myr::sfGFP, 8xLexAop-Brp-short-mCherry; R16H05-Gal4 DBD/hbP(FRT.myr::smGdP-cMyc.stop)LexA:p65-T2A-hb	Figure 2.6 and 2.8
hs-FLPG5.PEST; vnd-VP16; R16H05-Gal4 DBD/ 10xUAS(FRT.stop)myr::smGdP-	Figure 2.7

OLLAS 10xUAS(FRT.stop)myr::smGdP-HA 10xUAS(FRT.stop)myr::smGdP-V5-THS-10xUAS(FRT.stop)myr::smGdP-FLAG	
hs-FLPG5.PEST; vnd-VP16/UAS-Hunchback; R16H05-Gal4 DBD/ 10xUAS(FRT.stop)myr::smGdP-OLLAS 10xUAS(FRT.stop)myr::smGdP-HA 10xUAS(FRT.stop)myr::smGdP-V5-THS-10xUAS(FRT.stop)myr::smGdP-FLAG	Figure 2.7
vnd-VP16/UAS-FLP, 79C23S-GS(FRT-stop)smFPV5-2A-LexAVP16 ; R16H05-Gal4 DBD	Figure 2.8
vnd-VP16/UAS-FLP, 79C23S-GS(FRT-stop)smFPV5-2A-LexAVP16 ; R16H05-Gal4 DBD/UAS-Hunchback	Figure 2.8

Gal4 lines, mutants and reporters used were:

vnd-VP16 (2R, VK1, 59D3) (Mark et al., 2021)

R16H05-Gal4 DBD (3L, P2, 68A4) (this work)

10XUAS-IVS-myr::sfGFP-THS-10xUAS(FRT.stop)myr::smGdP-HA (RRID:BDSC_62127)

10xUAS-IVS-myr::GFP (BDSC_32198)

UAS-Hunchback (III) (Isshiki et al., 2001)

hs-KD (BDSC_56167)

3xUAS-FLPG5 (BDSC_55808)

13xlexAop(KDRT-stop)SmGdp-Flag (BDSC_62111)

hbP(FRT.myr::smGdP-cMyc.stop)LexA:p65-T2A-hb (Mark et al., 2021)

hs-FLPG5.PEST.Opt (RRID:BDSC_77140)

10xUAS(FRT.stop)myr::smGdP-OLLAS 10xUAS(FRT.stop)myr::smGdP-HA 10xUAS(FRT.stop)myr::smGdP-V5-THS-10xUAS(FRT.stop)myr::smGdP-FLAG (RRID:BDSC_64086)

20xUAS-FLP (BDSC_55807)

13xLexAop2-IVS-myr::sfGFP (this work)

8xLexAop-Brp-short-mCherry (J. Li et al., 2018)

UAS-FLP (BDSC_4540)

79C23S-GS(FRT-stop)smFPV5-2A-LexAVP16 (Xu et al., 2019)

Hb+ filtered NB5-2 intersectional genetics

We used an intersectional genetics approach to label single NB5-2 Hb+ progeny (Figure 2.6A). Our NB5-2-Gal4 drove expression of UAS-Flipase (UAS-FLP) specifically in NB5-2, where it then bound to Flipase Recombination Target (FRT) cis-regulatory sites to promote excision of a stop codon downstream of the endogenous Hb promoter. Excision of the stop codon enabled LexA expression downstream of the *hb* promoter to be expressed following transcription of the endogenous *hb* gene. Stage 17 embryos were heat-shocked (see methods below) to promote expression of the KD recombinase (Nern et al., 2011) and excision of a stop codon downstream of the LexAop cis-regulatory site. The combination of FLP and KD excised stop codons promoted expression of spaghetti-monsterGFP conjugated with a FLAG epitope tag (smGdp-FLAG) specifically in NB5-2 derived Hb+ progeny.

Embryos were aged to stage 17 at 25˚C for 18 hours. Embryos were then heat-shocked in a 37˚C water bath for 12 minutes, placed in an 18˚C room for 12 minutes, and placed back at 25˚C until larval hatching. First instar larval (L1; 0-3hrs ALH) brains were then dissected and fixed following the fixation protocol (See Immunostaining and Imaging section).

Manual Presynapse Analysis (Figure 2.8C-G)

NB5-2 Hb+ presynapses were labeled using a similar approach to the Hb filtered NB5-2 intersectional genetics (see above), to drive expression of a truncated, inactive version of the presynaptic marker, Bruchpilot (Brp), conjugated with an mCherry epitope tag (Brp-short-mCherry), and the cell membrane marker, myristoylated GFP (myr::GFP), in NB5-2 Hb+ progeny (Figure 2.8C), hereafter referred to as “Hb-filtered presynapses”. Wild-type (WT) NB5-2 control and HbOE NB5-2 presynapses were labeled using the NB5-2-Gal4 driver and Synaptic Tagging with Recombination (STaR) (Y. Chen et al., 2014).

L1 (0-3hrs ALH) larval of each genotype (Hb-filtered presynapses, WT NB5-2 control, and HbOE NB5-2) brains were dissected and fixed (see Immunostaining and Imaging section).

WT and HbOE presynapses were imaged using a laser intensity of 0.14 mW to capture all WT presynapses while also minimizing high fluorescent signal clusters observed in HbOE animals, to keep both in the lineage range.

Neuropil volume was labeled using N-Cadherin antibody staining. To define neuropil borders we made a surface object using Imaris 10.0.1 software. We then defined a centroid in each hemisegment by measuring the length, height, and depth of a single abdominal hemisegment, focusing our analysis on abdominal segments 1 and 2 (A1 and A2) (Supp. Figure 2.7). For Hb+ neuropil volumes i1-i3, presynapses distribute along the anterior-to-posterior axis, spanning the depth of a single hemisegment. To control for segmental depth, we used the transcription factor marker Even-skipped (Eve) to locate the U1 motor neurons and defined segmental borders according to their location (i.e. the U1 motor neuron position in thoracic segment 3 defined the A1 anterior border; the U1 position in A1 define the posterior border).

To isolate individual presynapses, we used the Imaris 10.0.1 spots tool, defining the size of an average presynapse spot for NB5-2 Hb-filtered (XY diameter: 0.31µm, Z diameter: 1.71µm) and WT and HbOE presynapses (XY diameter: 0.41µm, Z diameter: 1.46µm) and setting a minimum threshold intensity between 7-12AU. We then found the average center of each Hb+ position (i1 n=10 animals, 20 hemisegments; i2 n=10 animals, 20 hemisegments; i3 n=4 animals; 9 hemisegments). To find the average distance of centroid to each center of the Hb+ regions, we measured and averaged the distances along the medial-lateral and dorsal-ventral axes from the centroid. A volume for each position was then created using Imaris 10.0.1 custom surface tool, spanning the depth of the hemisegment. The size of each volume was determined by the average center distance plus/minus 2 standard deviations. To validate this approach, we applied the averaged measurements of the i2 volume (the furthest Hb+ volume from the centroid) back to individual NB5-2 Hb-filtered presynapse hemisegments. We found that 5/6 hemisegments (3 animals) captured the labeled Hb+ presynapses in the i2 region. Total presynapse number per hemisegment was found using the Imaris 10.0.1 manual select tool and selecting all presynapse spots within a single hemisegment. Centroid position and Hb+ volumes for individual hemisegments were then found in WT control and HbOE hemisegments. Individual presynapses were isolated using the Imaris 10.0.1 spots tool (described above). Presynapses that fell within each Hb+ volume where then manually quantified. Presynapse percentages were calculated using the quantified presynapse numbers in Hb+ volumes and the

total presynapse number in the corresponding hemisegment to minimize variance in Brp presynapse labeling between animals.

Computational Presynapse Analysis (Figure 2.8H-K)

To complement our manual analysis, we also compared confocal images from different animals on the same set of coordinates using the technique of template registration. Images of segments labeling NB5-2 Hb-filtered presynapses (n= 2 segments) and NB5-2 WT (n= 4 segments) and HbOE (n= 4 segments) presynapses were combined to make a "template" neuropil by overlaying and aligning segmented N-Cad stained neuropils using Computational Morphometry Toolkit (CMTK) Software (https://www.nitrc.org/projects/cmtk), Nepari (https://napari.org/), and custom Python code (Newstein, 2024). Individual images that successfully aligned with the "template" were selected for further analysis. Each hemisegment was analyzed separately by defining a transformation matrix which overlays left and right neuropils.

To define NB5-2 Hb+ presynapse regions within the neuropil, NB5-2 Hb+ presynapses from 17 A1/A2 hemisegments (8 animals) were isolated using the Imaris 10.0.1 spots tool and aligned to the "template" neuropil. After aligning to the hemisegment template, presynapse spots were blurred using a 1μm gaussian filter and thresholded so that 95% of the presynapses were included in the volume. Hb+ presynapse subregions (i1-i3) were then defined manually based on position on the medial-lateral axis.

Late-born NB5-2 presynapse regions were then defined by taking 2 randomly selected WT NB5-2 presynapse images and using the same gaussian filter to create a volume where pixel intensity corresponds to nearby presence of WT NB5-2 presynapses (Supp. Figure 2.6). Due to the difference in total presynapse number between Hb-filtered and WT presynapse images, Hb-filtered pixel intensity was scaled by a factor of 10 to equate pixel intensity to that in WT presynapse images. To exclude regions with many Hb+ presynapses, the WT presynapse volume was subtracted from the Hb-filtered volume. To quantify NB5-2 WT (n= 22 hemisegments, 5 animals) and HbOE (n = 22 hemisegments, 5 animals) presynapses, presynapse spots were defined using Imaris 10.0.1 spots tool for each genotype and aligned to the "template" neuropil. Presynapse spots that fell within the Hb+ and late-born regions in the left hemisegment were then quantified.

Neuron naming

We named the early-born Hb+ interneurons in the NB5-2 lineage Idun1-4 after *Iðunn*, the Norse god of youth.

Immunostaining and Imaging

Primary antibodies were: chicken anti-GFP (1:1000, RRID:AB_2307313, Aves Labs, Davis, CA), mouse anti-engrailed (5ug/mL, DSHB 4D9-Eng, RRID: AB_528224), mouse anti-Hunchback (1:100, Abcam, F18-1G10.2), rabbit anti-Hunchback #5-27 (1:400) (Tran & Doe, 2008), guinea pig anti-Kr (1:500, Doe lab), rat anti-Pdm2 (1:100, abcam, ab201325, Cambridge, MA), rabbit anti-Castor (1:1000, Doe lab), rat anti-Grainy head (1:400, a gift from Stefan Thor, University of Queensland), rat anti-Deadpan (1:20, abcam, ab195173), rabbit anti-Worniu (1:1000; abcam, ab196362), rabbit anti-Nervy (1:300, gift from Richard Mann, Columbia University), Guinea pig anti-Dbx (1:200, Doe lab), rat anti-Nkx6 (1:500, gift from J. Skeath, Washington University, St. Louis), guinea pig anti-Runt (1:1000, gift from C. Desplan, New York University), rat anti-Zfh2 (1:250, Doe lab), rat anti-FLAG (1:400, Novus NBP1-06712), rat anti-HA (1:1000, MilliporeSigma, 11867423001, St. Louis, MO), chicken anti-V5 (1:800, Bethyl Laboratories, Inc. A190-118A, Centennial, CO), rabbit anti-mCherry (1:500, Novus, NBP2-25157), mouse anti-Eve (5ug/mL, DSHB 2B8), rat anti-N-cadherin (0.168ug/mL, DSHB DN-Ex #8), and fluorophores-conjugated secondary antibodies were from Jackson ImmunoResearch (West Grove, PA) and were used at 1:300 for embryos and 1:400 for larval brains.

Embryos were fixed in 4% paraformaldehyde or formaldehyde for 20 min and stained as previously described (Mark et al., 2021). Larval brains were dissected in PBS, fixed in 4% paraformaldehyde, and then stained by following protocols as described (Sullivan et al., 2019). The samples were DPX mounted.

Images were captured with a Zeiss LSM 900 confocal microscope with a *z*-resolution of 0.22 μm. Due to the complex 3-dimensional pattern of each marker assayed, we could not show NB5-2 progeny marker expression in a maximum intensity projection, because irrelevant neurons in the z-axis obscured the neurons of interest; thus, NB5-2 progeny were montaged from their unique z-axis position while preserving their X-Y position. Images were processed using Imaris (Bitplane, Zurich, Switzerland) to generate three dimensional reconstructions and level

adjustments. Any level adjustment was applied to the entire image. Figures were assembled in Adobe Illustrator (Adobe, San Jose, CA).

Behavior

We recorded behavior in newly hatched larvae (4-6hr). Behavior arenas were made with 1.2% agar, 2 mm thick. Arenas were placed on a Functional Independence Measure (FIM) table (Risse, Thomas, Otto, Lopmeier, et al., 2013) for recording. Larvae were transferred to the agar arena and given 2 min to acclimate before recording. Behavior was recoded for 2 min (125 fps) at 24˚C and 60% humidity using a Basler acA2040-25gm camera with a Computer TEC-V7X 1.1" 7X Macro Zoom Telecentric lens and Pylon Viewer software. Recordings were edited in Fiji to eliminate arena borders, adjust the brightness-to-contrast ratio to increase larvae visibility (Min:15-19, Max:57-64), and saved at 25fps. Larval locomotion speed and body bends were calculated using FIMTrack 2.0 software.

Statistics

Statistical significance is denoted by asterisks: ****$p<0.0001$; ***$p<0.001$; **$p<0.01$; *$p<0.05$; n.s., not significant. The following statistical tests were performed: Welch's t-test (normal distribution, non-parametric) (two-tailed p value) (Figures 2.5Q-X, 2.8G, 2.8J-K, 2.9A-B) and one-way ANOVA (Figures 2.7H). All analyses were performed using Prism8 (GraphPad). The results are stated as mean ± s.d., unless otherwise noted.

BRIDGE

In Chapter II, we provide strong evidence that the early expressed TTF, Hunchback (Hb), determines many aspects of early-born NB5-2 interneuron identity. We show that prolonged NB5-2 Hb expression transforms the molecular identity, morphology, and presynapse targeting of late-born interneurons to an early-born fate. This transformation disrupts the circuit function of the late-born EL proprioceptive circuit at the behavioral level. Thus, TTF identity may be a vital component required for proper circuit formation and function.

We next wondered whether proper TTF identity of the NB5-2 late-born neurons, Saahgi1-3 (SA1-3) and Jaam1-3 (JA1-3), is required for proper pre- and post-synaptic connectivity within the EL proprioceptive circuit. We hypothesized that SA1-3 and JA1-3 are Castor expressing neurons, as previous work has shown the SA1 is Cas+ (Mark et al., 2021). Castor is known to repress Pdm expression during the NB TTF cascade (Cleary & Doe, 2006; Grosskortenhaus, 2006; Grosskortenhaus et al., 2005; Isshiki et al., 2001), but evidence of its role in promoting aspects of interneuron identity are sparse. Thus, we aimed to determine if Castor is required to specify aspects of NB5-2 late-born interneuron identity.

CHAPTER III

DETERMINING THE ROLE OF CASTOR IN LATE-BORN NB5-2 INTERNEURON IDENTITY AND CONNECTIVITY

Authors currently contributing to this work: Pollington, H. Q., Lee, K. M., Hirono, K., and Doe, C. Q.

Author contributions

Conceptualization: C.Q.D., H.Q.P.; Methodology: H.Q.P.; Formal analysis: Figure 3.1 H.Q.P. and K.H, Figure 3.2 K.M.L, Figure 3.3 H.Q.P.; Investigation: C.Q.D., H.Q.P., K.M.L, K.H.; Data curation: Figure 3.1 K.H., Figure 3.2 K.M.L, Figure 3.3 H.Q.P.; Writing – original draft: H.Q.P.; Writing – review & editing: H.Q.P., K.M.L; Visualization: H.Q.P., K.H.; Supervision: C.Q.D.; Project administration: C.Q.D.; Funding acquisition: C.Q.D.

Introduction

The ability to generate complex behaviors is a key element to the survival of any organism. Appropriate behavioral responses to environmental stimuli are enabled by proper circuit assembly within the central nervous system (CNS). CNS interneurons are pivotal in integrating sensory input to generate proper motor output. Interneuron-to-interneuron connectivity also increases circuit complexity, facilitating more precise circuit functions and behavioral output. However, the precise mechanisms that promote interneuron connectivity are poorly understood.

In vertebrates and invertebrates, birth-order appears to play a defining role in circuit establishment. In the mice neocortex, previous work has shown that neurons derived from the same radial ganglion progenitor preferentially form synaptic connections with sibling neurons compared with non-sibling neurons of close proximity (Y.-C. Yu et al., 2009). In zebrafish neurogenesis, early-born neurons preferentially connect to form a fast swim circuit, while later-born neurons contribute to a slow swim circuit (Deska-Gauthier & Zhang, 2021). In *Drosophila*, the neural progenitor, NB3-3, generates a population of Even-skipped lateral (EL) neurons that contribute to two separate neural circuits, divided by birth-order. Early-born ELs contribute to a mechanosensory escape roll circuit and late-born ELs contribute to a proprioceptive circuit (Heckscher et al., 2015; Wreden et al., 2017). The late-born EL proprioceptive circuit is also comprised of synaptic connections with late-born NB5-2 neurons, Jaam1-3 (JA1-3) and Saaghi1-3 (SA1-3) (Heckscher et al., 2015; Mark et al., 2021; Wreden et al., 2017). The correlation of

circuit association with birth-order connectivity from two separate NB lineages supports a hypothesis that birth-order is an essential component to circuit assembly.

During development, vertebrate and *Drosophila* neurogenesis is initiated by spatial cues that specify neural progenitor identity (Luo, 2020), which then express a series of temporally regulated transcription factors (TTFs) that diversify neuron progeny by temporal identity and thus, birth-order. Neurons derived from a neural progenitor cell express unique combinations of transcription factors (TFs; molecular identity), possess distinct morphological features, and targets synapses to precise subregions within the CNS. In the mouse neocortex, apical radial glia (aRG) generate neuronal progeny that form 6 laminar layers, each expressing laminar-specific transcription factors (TFs) and show unique axon/dendrite projection patterns (Kumamoto & Hanashima, 2014). In mouse retinal development, retinal progenitor cells (RPCs) express the TTF cascade: Ikaros > Pou2f1/Pou2f2 > FoxN4 > Casz1, to specify the generation of seven unique cell types (Cepko, 2014). Casz1, the *Drosophila* Castor ortholog, is expressed in mid/late stages in RPCs and has been shown to specify late-born bipolar and rod photoreceptor fate (Mattar et al., 2015). Retroviral knockout of *Casz1* in RPCs increases production of earlier-born amacrine, horizontal and cone cells at the expense of rod photoreceptors; however, *Casz1* misexpression results in increased late-born bipolar and rod photoreceptors (Mattar et al., 2015).

In *Drosophila*, neural progenitors (neuroblasts; NBs) of the ventral nerve cord (VNC) undergo sequential expression of the TTF cascade: Hunchback (Hb)> Krüppel (Kr)> Pdm> Castor (Cas)> Grainyhead (Grh) (Doe, 2017). The expression of each TTF is transiently maintained in neuron progeny from the expression window of its birth (i.e. early-born neurons express Hb and late-born neurons express Castor) (Doe, 2017). Many studies have shown that the early TTF, Hb, plays a dominant role in specifying multiple aspects of motor and interneuron identity (Grosskortenhaus, 2006; Meng et al., 2019; Seroka & Doe, 2019; Pollington & Doe, 2025). However, in order to categorize TTFs as a class of molecules that diversify and specify neuron identity, more evidence is needed on the functional role of late-born TTFs.

The *Casz1 Drosophila* ortholog, Castor, has been shown to play an important role in regulating expression of the preceding and subsequent TTFs, Pdm and Grh, in many NB lineages (Baumgardt, et al., 2009; Grosskortenhaus, 2006; Isshiki et al., 2001; Meng et al., 2020; Tran & Doe, 2008), but it's role in specifying aspects of interneuron identity remains minimal. In combination with Pdm, Castor has been shown to specify late-born motor neuron identity in the

NB7-1 lineage. NB7-1 produces a population of U motor neurons (MNs) with unique temporal identities; U1 and U2 express Hb/Kr, U3 expresses Kr, U4 expresses Pdm, and U5 expresses Pdm/Cas+, followed by the production of several Cas+ interneurons (Isshiki et al., 2001).Co-misexpression of Pdm/Cas significantly increases the number of U5 MNs, while misexpression of Cas alone results in a loss U4 and U5 MNs (Grosskortenhaus, 2006; Meng et al., 2020). The authors speculate that early NB7-1 Cas expression truncates MN production and promotes early Cas+ interneuron generation (Meng et al., 2020). In addition, Castor expression diversifies a population of late-born peptidergic neurons and is required to specify peptidergic identity generated from NB5-5 and promotes downstream expression of the subtemporal genes *klumpfuss* (*klu*) and *nab* (Benito-Sipos, et al., 2010).

To understand if Castor specifies late-born interneuron identity, we are currently investigating the role of Castor in promoting aspects of late-born interneuron identity in the NB5-2 lineage. Specifically, we focus on the role of Castor in specifying aspects of late-born JA1-3 and SA1-3 identity. Previous work has shown that SA1 expresses Cas and that NB5-2 generates eight Cas+ interneurons (Mark et al., 2021; Pollington & Doe, 2025). We hypothesized that JA1-3 and SA2-3 are born during the Cas expression window given that, like SA1, they form connections in the late-born proprioceptive circuit and all cell-bodies reside adjacent to SA1. We first wanted to test this hypothesis using a lineage specific intersectional genetics approach to stochastically label signal neurons that both express Cas and were derived from NB5-2. Thus far, we have confirmed that JA3, SA1, and SA3 express Cas. We also wanted to understand if Cas misexpression disrupts proprioceptive behavior. Last, we aim to understand if Cas specifies molecular and morphological identity of NB5-2 interneurons. However, as of the writing of this dissertation, this study is currently ongoing and thus, more work is needed to formulate any conclusions from this work.

Results

NB5-2 Saaghi-1, Saaghi-3, and Jaam-3 interneurons express Castor

To understand if Castor is required for proprioceptive connectivity we first needed to identify if JA1-3 and SA1-3 express Castor. We designed a genetic method using an intersectional genetics approach to stochastically label individual neurons that both express Castor and were derived from NB5-2 (see Material and Methods). We refer to this intersectional approach as “Cas+

filtered NB5-2 neurons" (Figure 3.1A). We then compared the morphology of single labeled neurons to the open-source TEM volume (Ohyama et al., 2015). Using this comparison thus far, we have found that three of six SAs/JAs express Castor: SA1, SA3 and JA3 (Figure 3.1B-D). SA1 and SA3 both project to the dorsal neuropil domain but possess unique morphological differences. SA1 possess complex ipsilateral neurite branching and a contralateral neurite that initially projects laterally, then curves back to the midline. In comparison, SA3 shows much simpler morphology. In contrast, JA3 neurites project to the ventral neuropil with complex contralateral neurite branching. We conclude, thus far, that at least half of the neurons that contribute to the late-born EL proprioceptive circuit express Castor. However, at the time of this dissertation, this experiment is currently ongoing and thus, we cannot confidently state whether SA2, JA1, and 2 express Castor.

Cell-body proximity in the VNC cortex is often used as an approximation of birth-order and TTF identity, relative to other neuron progeny derived from the same NB. Interestingly, TEM reconstruction data reveals that SA1-3 and JA1-3 cell bodies cluster tightly together (Figure 3.1E), suggesting that SA2, JA1, and JA2 may possess the same TTF identity as SA1, SA3, and JA3. However, further work is needed to definitively conclude this hypothesis (See Discussion).

Figure 3.1 (next page). NB5-2 pre-motor SA1 and SA3 and post-sensory JA3 interneurons express Castor.
(A) An intersectional genetics method was used to stochastically label single NB5-2 Cas+ neurons (see Methods for details).
(B-D) Single cell morphology of SA1 (B; n= 15 animals), SA3 (C; n= 6) and JA3 (D; n=17) in L1 (0-3hr) larvae. Top panels, TEM reconstruction; left posterior view, right dorsal view. Dotted line outlines VNC border with neuropil (grey). Middle panels, Cas-filtered genetic labeling of the indicated neuron; left posterior view; right dorsal view. Dotted lines outline the VNC and neuropil borders. Bottom panels, filament tracing of Cas-filtered labeled neuron of the indicated neuron; left posterior view; right dorsal view. Dotted lines outline the VNC and neuropil borders. Scale bar: 10 µm.
(E) TEM reconstruction of all NB5-2 neurons (top panel) and JA1-3 and SA1-3 (bottom panel).

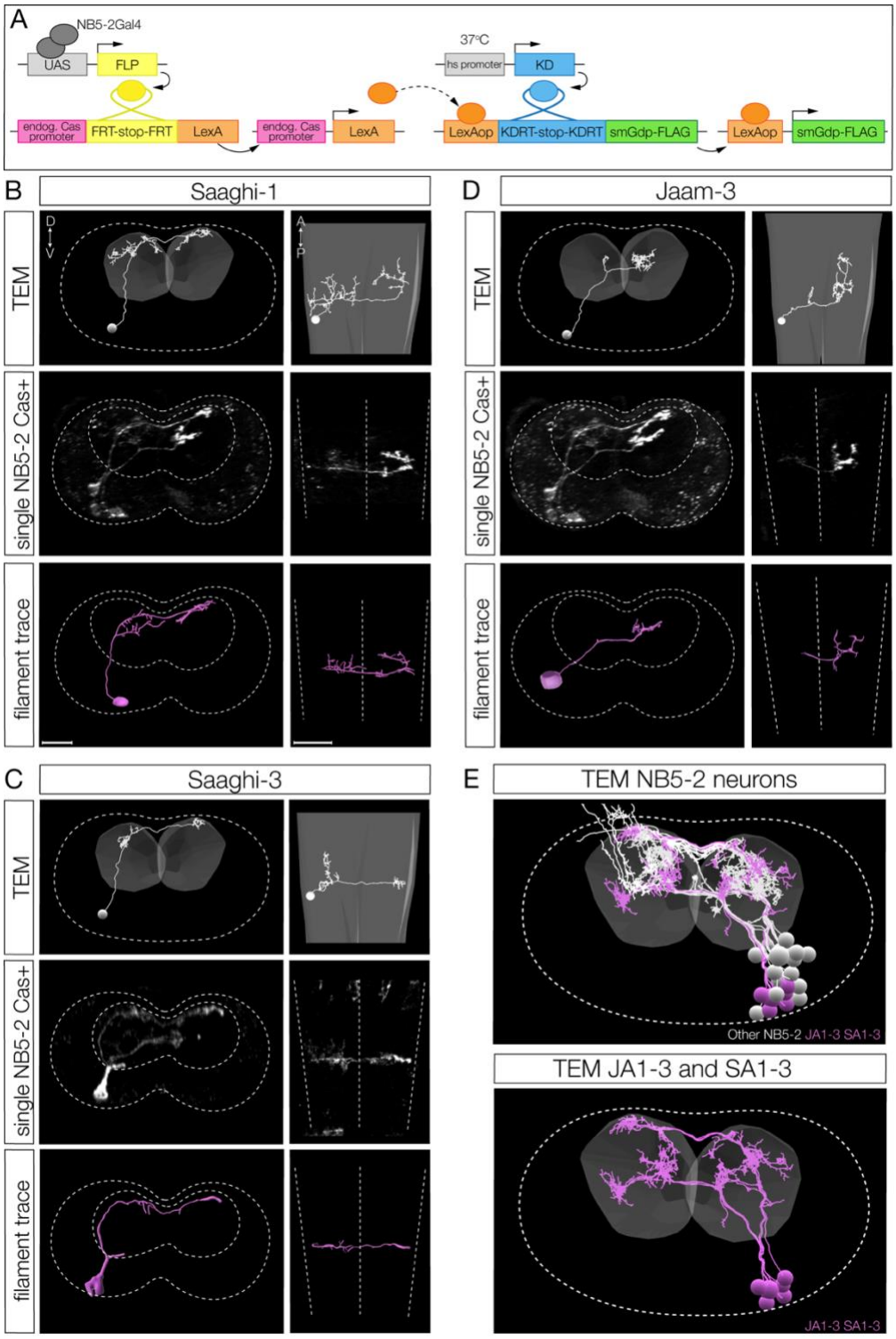

Castor misexpression disrupts EL proprioceptive circuit behavior.

Above we show that three of the six SA/JA neurons that contribute to the EL proprioceptive circuit express Cas. Here we ask whether Cas is required for proper EL proprioceptive circuit assembly. Ablation of the Eve+ interneurons in the proprioceptive circuit results in decreased larval crawling speed and an increase in a C-shaped body bend (Heckscher et al., 2015). In addition, previous studies have shown that misexpression of Cas inhibits Pdm expression (Baumgardt, Karlsson, Terriente, Díaz-Benjumea, et al., 2009; Benito-Sipos, et al., 2010; Meng et al., 2020). We predicted that misexpression of Cas in NB5-2 may inhibit Pdm expression, promoting Pdm neurons to express Cas and form connections with neurons in the EL proprioceptive circuit, thus, disrupting proprioceptive behavior due to an increase in neuronal connections.

To test this, we used a NB5-2 split-Gal4 (Pollington & Doe, 2025) and misexpressed Cas specifically in NB5-2 (NB5-2 split-Gal4; UAS-Cas), subsequently called NB5-2>Cas. We then assayed for behavioral phenotypes in control (NB5-2 split-Gal4; UAS-LacZ) and NB5-2>Cas first instar larvae (4-6hrs ALH). Qualitatively, NB5-2>Cas larvae showed noticeable non-linear crawling trajectories compared to control (Figure 3.2A). To assay for disruptions in proprioceptive behavior we quantified larval crawling speed, total distance traveled, and body posture phenotypes over a 3-minute period. We observed that NB5-2>Cas larvae crawled consistently slower and traveled shorter distances over time compared to control (Figure 3.2B-D). Consistent with our qualitative observations, NB5-2>Cas larvae also showed a significant increase in the amount of time turning (Figure 3.2E). When assessing body posture, we observed that NB5-2>Cas larvae spend less time in a straight heading position and more time in a C-shaped body bend (Figure 3.2F-G). To confirm that C-shaped body bends were not due to increased incidences of larvae rolling, we quantified the percentage of time larvae spent rolling and found no significant difference (Figure 3.2H). Thus, we conclude that Cas misexpression disrupts proprioceptive behavior.

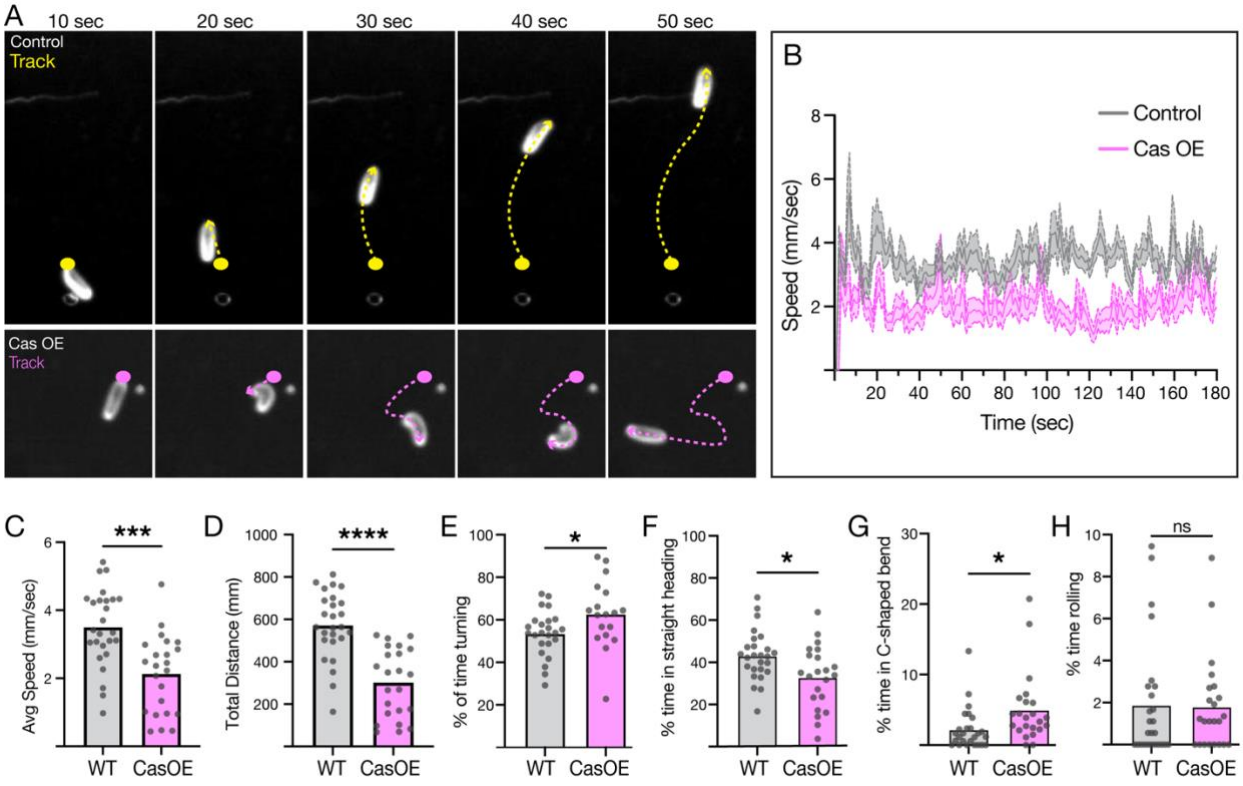

Figure 3.2 Castor misexpression disrupts proprioceptive circuit behavior
(A) Representative L1 (4-6hr ALH) WT control (dotted yellow) and NB5-2>Cas (CasOE; dotted magenta) larval crawling trajectory from a start point (filled circle) to end point (arrow) over a 3-minute time period.
(B) L1 larval crawling speed of WT control (grey) and CasOE (magenta) over time. (WT n= 26, CasOE n= 23)
(C) Quantification of average crawling speed of individual L1 larvae. WT avg= 3.5, n=26; CasOE avg= 2.1, n= 23 (*p-value*=0.001).
(D) Quantification of total distance traveled. WT avg= 572, n= 26; CasOE avg= 301, n= 23 (*p-value*<0.0001).
(E) Quantification of percentage of time turning (turning: >10˚ angle from 0˚ and average crawling speed). WT avg= 54, n= 24; CasOE avg= 63, n= 18 (*p-value*=0.03).
(F) Quantification of percentage of time in a straight heading (straight heading: <10˚ angle from 0˚). WT avg= 43, n= 26; CasOE avg= 33, n= 22 (*p-value*=0.01).
(G) Quantification of percentage of time in a C-shaped body bend (C-shaped bend: >65˚ angle from head to tail and lack of crawling for <1 mm/sec). WT avg= 2, n= 26; CasOE avg= 5, n= 23 (*p-value*=0.02).
(H) Quantification of percent time rolling (rolling: >65˚ angle from head to tail and moving twice the average speed for individual larvae). WT avg= 1.9, n= 26; CasOE avg= 1.8, n= 23 (*p-value*= 0.91).

Castor is required to terminate NB5-2 Pdm expression but is not sufficient to inhibit Pdm

The wild-type NB5-2 sequentially expresses the TTF cascade, Hb>Kr>Pdm>Cas>Grh throughout embryogenesis (Figure 3.3A). To determine if Cas is necessary to specify late-born interneuron identity, we first wanted to understand the role of Cas in regulating the NB5-2 TTF cascade. We labeled NB5-2 and it's progeny using a NB5-2 split-Gal4 (Pollington & Doe, 2025) and drove expression of a cell membrane tag conjugated with an HA epitope, which we refer to as NB5-2>HA. To achieve Cas loss of function, we used a combination of a *cas* mutant (Cui & Doe, 1992) and a Castor flipase-dependent transgene (*cas*^{24}/Cas-promoter-frt-stop-frt-LexA-ORF; See Materials and Methods), which we call "*cas* null" embryos. We focused our analysis of TTF expression in *cas* null embryos beginning at stage 11 because this stage marks the onset of the wild-type NB5-2 Cas expression window. In *cas* null embryos, we observed prolonged NB5-2 Pdm expression from stages 10-15 and a lack of Grh expression through stage 15 (Figure 3.3B). We did not characterize TTF expression in stage 16 and 17 embryos because we were not confident in our ability to identify NB5-2 at these later stages. We conclude that Cas is required to terminate the NB5-2 Pdm expression window, consistent with other NBs (Baumgardt, et al., 2009; Benito-Sipos, et al., 2010; Grosskortenhaus, 2006; Isshiki et al., 2001; Meng et al., 2020; Tran & Doe, 2008), and is required for progression of the TTF cascade to the Grh expression window.

To understand if Cas is sufficient to inhibit NB5-2 Pdm expression we misexpressed Cas in NB5-2. Using NB5-2Gal4>HA, the NB5-2 cell membrane is not labeled until late stage 10 (Pollington & Doe, 2025). To identify NB5-2 at earlier embryonic stages, we used a combination of the NB marker, Asense (Ase), and the segmental marker Engrailed (En). NB5-2 was identified as the most medial Ase+En- NB, anteriorly adjacent to the En expression domain (Pollington & Doe, 2025). In NB5-2>Cas embryos, Cas expression was first observed at early stage 10, during the wild-type Kr/Pdm expression window and extended through the Grh expression window (Figure 3.3C). In addition to Cas, Kr/Pdm expression was present in NB5-2 at early stage 10 and Pdm expression persisted to stage 11. Similar to wild-type, Grh expression began at stage 14 and continued to stage 15. Thus far, we conclude that Cas does not inhibit Pdm expression in NB5-2. It is possible that a single UAS-Cas transgene does not produce an adequate amount of Cas to inhibit endogenous Pdm expression or NB5-2 Pdm regulation differs from other NBs (see Discussion).

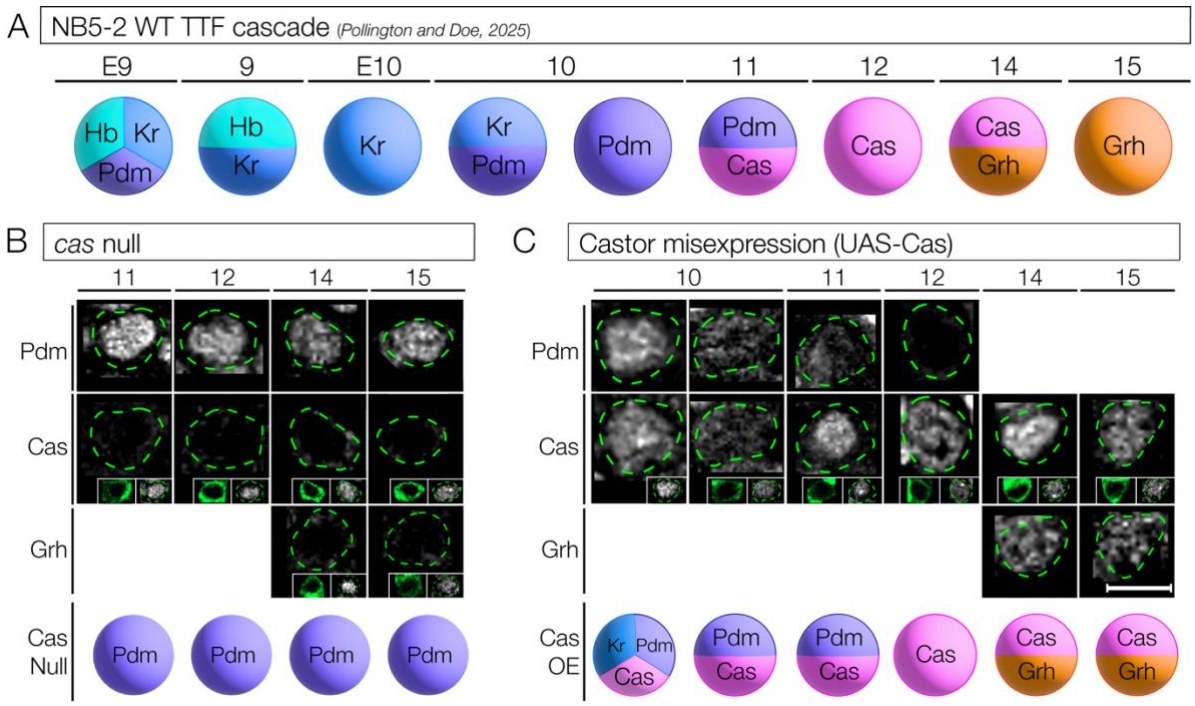

Figure 3.3 Loss of Castor prolongs the NB5-2 Pdm expression window but Castor misexpression does not disrupt the TTF cascade
(A) Schematic summary of the WT NB5-2 TTF cascade throughout embryogenesis (Pollington & Doe, 2025).
(B) *cas* null (*cas*^{24} x Cas-filtered) NB5-2 expression of Pdm (top panels), Cas (middle panels), and Grh (bottom panels) in stage 11-15 embryos. NB5-2 was identified using NB5-2>HA (left inset) and the NB marker Asense (Ase; right inset). Schematic summary of *cas* null NB5-2 TTF expression (bottom row). Quantification: Stg 11 n= 4 hemisegments, 1 animal; stg 12 n= 4 hemisegments, 1 animal; stg 14 n> 12 hemisegments, 3 animals; stg 15 n> 8 hemisegments, 2 animals.
(C) NB5-2>Cas (Cas OE) NB5-2 expression of Pdm, Cas, and Grh in stage 10-15 embryos. Due to delayed cell membrane labeling before stage 10, NB5-2 stage 10 embryos were identified as the most medially located NB, anteriorly adjacent to the row 6/7 Engrailed expression domain (Pollington & Doe, 2025). Following stg 10, NB5-2 was identified as described above (see B). Quantification: Stg 10 n> 6 hemisegments, 2 animals; stg 11 n= 35 hemisegments, 10 animals; stg 12 n= 16 hemisegments, 4 animals; stg 14 n= 16 hemisegments, 4 animals; stg 15 n= 8 hemisegments, 2 animals. Scale bar: 5µm.

Discussion

During development, intrinsic cues promote the generation of unique neuron identity, facilitating proper circuit assembly. The role of Castor in regulating the expression of the preceding and subsequent TTFs, Pdm and Grh, has been well studied in multiple NBs

(Baumgardt, et al., 2009; Benito-Sipos, et al., 2010; Grosskortenhaus, 2006; Meng et al., 2020; Tran & Doe, 2008). Castor is expressed in many late stage NBs and is transiently maintained in interneuron post-mitotic progeny (Doe, 2017); however, it remains unknown if Castor functions to specify aspects of late-born interneuron identity.

This study describes efforts thus far in elucidating the role of Castor in specifying aspects of interneuron identity. Although this work is currently ongoing, we have identified the NB5-2 interneurons, SA1, SA3, and JA3 as late-born Castor expressing neurons. This is promising evidence that lineally related interneurons with the same TTF identity contribute to the same circuit. Neurite length has been shown to be a reliable proxy for categorizing neurons into temporal cohorts, and previous work has categorized JA1-3 and SA1-3 into late-born temporal cohorts (Mark, et al. 2021). Thus, we hypothesize that JA1-3 and SA1-3 all express Cas. However, our intersectional genetics approach has resulted in an over-representation of JA3 and SA1 and will need further optimization in the future. Previous work has shown that NB5-2 generates eight Cas+ interneurons by embryonic stage 16 (Pollington & Doe, 2025). Although we have only identified one other NB5-2 neuron that expresses Cas, Jaam6 (Supp. Figure 3.1). Therefore, not all Cas+ neurons in the lineage have been identified using our genetic approach. Thus, more work is needed to identify all Cas+ neurons in the NB5-2 linage.

To test if Castor plays a role in circuit assembly, we misexpressed Castor in NB5-2 and assayed for disruptions in proprioceptive behavior. We observed that Cas misexpression results in decreased larval crawling speed and an increase in a C-shaped body bend, phenocopying behavior observed when the late-born EL interneurons are overstimulated or ablated (Heckscher et al., 2015). Recent work has also shown that transformation of late-born NB5-2 interneurons to an early-born Hb identity disrupts proprioceptive behavior (Pollington & Doe, 2025). Together, these results may suggest that TTF identity is essential for proper connectivity.

We hypothesized that disruptions in proprioceptive behavior may be due to Castor induced suppression of Pdm in NB5-2, resulting in increased Cas+ neurons that form synaptic connections into the late-born proprioceptive circuit. To test this, we misexpressed Cas in NB5-2 and assayed for NB5-2 TTF expression. Interestingly, we found that Cas misexpression did not effectively suppress Pdm; however, *cas* null embryos showed prolonged Pdm expression, consistent with previous studies (Baumgardt, et al., 2009; Benito-Sipos, et al., 2010; Grosskortenhaus, 2006; Tran & Doe, 2008). We provide three explanations for these results: 1)

Our genetic manipulation was not sufficient to accumulate the necessary concentration of Cas needed to suppress NB5-2 Pdm expression, 2) Cas regulation differs in NBs that generate interneurons versus MNs, or 3) Cas plays a more predominate role in the post-mitotic neuron.

To address the first possibility, we plan to increase the number of UAS-Cas transgenes used to increase the concentration of Cas early in NB5-2 neurogenesis. If Cas successfully represses Pdm it is likely the Cas misexpression phenotype observed was due to technical insufficiency; however, if we still observe a lack of Pdm repression, the second possibility may be more likely. To confirm Cas regulation differs in NBs that preferentially generate different neuron types, it will be essential to expand this study to multiple NB lineages. To test the third possibility, it will be important to identify NB5-2 Cas-negative late-born interneurons and TFs associated with Cas-negative and Cas-positive NB5-2 neurons. If Cas plays an important role in post-mitotic interneurons, we hypothesize Cas misexpression will result in an increase in post-mitotic NB5-2 interneurons expressing Cas-positive TFs at the expense of Cas-negative TFs.

In NB5-5, Cas activates expression of the subtemporal genes, *klu* and *nab* and specifies abdominal leucokinergic neurons (ABLKs) (Benito-Sipos, et al., 2010). Pan-neuronal misexpression of Cas using *elav*-Gal4 doubles the number of ABLKs present in each hemisegment compared to control. However, Cas misexpression using NB-specific drivers (*inscuteable*-Gal4 or *worniu*-Gal4) resulted in relatively mild phenotypes (Benito-Sipos, et al., 2010). The discrepancy between pan-neuronal and NB specific misexpression of Cas may suggest that Cas plays an essential role in the postmitotic neurons to promote downstream expression of sub temporal genes. Cas also promotes the fate of four late-born Apterous (Ap) neurons, derived from NB5-6T (Baumgardt, et al., 2009). NB5-6T Cas expression promotes a Collier/Knot (col) dependent feedforward loop to specify the first Ap neuron. Cas induced accumulation of Nab in NB5-6T following generation of the first Ap neuron then inhibits the col feedforward loop and further subdivides Ap neuron identity (Baumgardt, et al., 2009). Interestingly, the authors emphasize an important division of mechanisms in which col-dependent feedforward signaling must only occur in the post-mitotic Ap neuron and Nab accumulation must occur in the NB in order for proper Ap neuron specification to occur (Baumgardt, et al., 2009). This would suggest that Castor may function at multiple levels during neurogenesis to specify unique neuron identity. This will be an exciting avenue to explore in the future.

Materials and Methods

Fly Stocks

Male and female *Drosophila melanogaster* were used. The transgene insertion sites (if known) are shown next to the respective genotypes.

Table 2. Genotypes utilized to obtain results for the Figure(s) indicated in Chapter III

Genotype	Figure(s)
hs-KD, 3xUAS-FlpG5; vnd-VP16/ 13xlexAop(KDRT-stop)myr::SmGdp-FLAG; R16H05-Gal4 DBD/ CasP(FRT.myr::smGdP-cMyc.stop)LexA:p65-T2A-CasORF	Figure 3.1
10xUAS-myr-smGdP.HA; vnd-VP16; R16H05-Gal4 DBD/UAS-LacZ	Figure 3.2
10xUAS-myr-smGdP.HA; vnd-VP16; R16H05-Gal4 DBD/UAS-Castor	Figure 3.2 and 3.3
10xUAS-myr-smGdP.HA; vnd-VP16, DBD-T2A-wg; 13xLexAop2(KDRT.stop)myr::smGdP-FLAG;CasP(FRT.myr::smGdP-cMyc.stop)LexA:p65-T2A-CasORF/ *cas*^{24}	Figure 3.3

Gal4 lines, mutants and reporters used were:
10xUAS-myr-smGdP.HA (I) (BDSC_64092)
vnd-VP16 (2R, VK1, 59D3) (Mark et al., 2021)

R16H05-Gal4 DBD (3L, P2, 68A4) [Pollington & Doe, 2025]

DBD-T2A-wg (27F1) (this work)
UAS-Cas (III) [Odenwald, W.]
cas^{24} (III) [(Cui & Doe, 1992b)]
hs-KD (BDSC_56167)
3xUAS-FLPG5 (BDSC_55808)
13xLexAop2(KDRT.stop)myr::smGdP-FLAG (BDSC_62111)

CasP(FRT.myr::smGdP-cMyc.stop)LexA:p65-T2A-CasORF (III) (this work)

Immunostaining and Imaging

Primary antibodies were: mouse anti-FLAG (1:100, Sigma F1804), mouse anti-HA (1:100, RRID: AB_2687407), mouse anti-engrailed (5ug/mL, DSHB 4D9-Eng, RRID: AB_528224), guinea pig anti-Asense (1:500, PMID: 24550111), rat anti-Pdm2 (1:100, abcam, ab201325, Cambridge, MA), rabbit anti-Castor (1:1000, Doe lab), rat anti-Grainy head (1:400, a gift from Stefan Thor, University of Queensland) and fluorophores-conjugated secondary antibodies were from Jackson ImmunoResearch (West Grove, PA) and were used at 1:300 for embryos and 1:400 for larval brains.

Embryos were fixed in 4% formaldehyde for 20 min and stained as previously described (Mark et al., 2021). Larval brains were dissected in 1xPBS, fixed in 4% paraformaldehyde, and stained by following protocols as described (Sullivan et al., 2019). The samples were then DPX mounted.

Images were captured with a Zeiss LSM 900 confocal microscope with a *z*-resolution of 0.22 µm. Images were processed using Imaris (Bitplane, Zurich, Switzerland) to generate three dimensional reconstructions and level adjustments. When level adjustment were made, adjustments were applied to the entire image. Figures were assembled and annotated in Adobe Illustrator (Adobe, San Jose, CA).

Cas+ filtered NB5-2 intersectional genetics

We used an intersectional genetics approach to label single NB5-2 Cas+ progeny (Figure 3.1 and Supp. Figure 3.1). NB5-2 split-Gal4 drove expression of UAS-Flipase (UAS-FLP) in NB5-2, where it bound to Flipase Recombination Target (FRT) cis-regulatory sites to promote excision of a stop codon downstream of the endogenous *cas* promoter. Stop codon excision induced LexA expression downstream of the *cas* promoter following transcription of the endogenous *cas* gene. Embryos were heat-shocked (see methods below) to promote expression of the KD recombinase (Nern et al., 2011) and excision of a stop codon downstream of the LexAop cis-regulatory site. The combination of FLP and KD excised stop codons promoted expression of spaghetti-monsterGFP conjugated with a FLAG epitope tag (smGdp-FLAG) specifically in NB5-2 derived Cas+ progeny.

Embryos of all stages were aged at 25˚C for 18 hours. Embryos were then heat-shocked for 5-10 minutes by direct contact in a 37˚ water bath, placed in an 18˚C room for 5-10 minutes,

and placed back at 25˚C until larval hatching. First instar larval (L1; 0-3hrs ALH) brains were then dissected and fixed following the fixation protocol (See Immunostaining and Imaging section).

Behavior

We recorded behavior of newly hatch first instar larvae (4-6hrs ALH). Behavior arenas consisted of 1.2% agar, approximately 2 mm thick. Areas were placed on a Functional Independence Measure (FIM) table (Risse, Thomas, Otto, Löpmeier, et al., 2013) for recording. L1 larvae were placed on the arena and given a 2 min acclimation period. Behavior was then recorded for 3 min (4 frames per second (fps)) at 24˚C and 60% humidity using a Basler acA2040-25gm camera with a Computer TEC-V7X 1.1" 7X Macro Zoom Telecentric lens and Pylon Viewer software. The brightness-to-contrast ratio of individual recordings was edited in Fiji to increase larvae visibility, and saved at 4 fps. Larval behaviors were then captured and analyzed using FIMTrack 3.0 software. Average speed and total distance were calculated for individual larvae from 3 separate experimental replicates for each genotype. Percent time turning was determined by the percentage of time larvae displayed a >10˚ body angle from 0˚ (0˚ = straight body) while crawling at an average speed for that individual larva. Body angle was measured using a central body point to the head of the larva. Straight heading was calculated by the amount of time larvae body angle was <10˚ from 0˚ and traveling at an average speed. C-shaped body bends were calculated by the time larvae displayed >65˚ angle from head to tail and lacked crawling for <1 mm/sec. Larval rolling was determined by a body angle >65˚ from head to tail and moving at least twice the average speed for that individual larva.

Statistics

Statistical significance is denoted by asterisks: ****p<0.0001; ***p<0.001; **p<0.01; *p<0.05; n.s., not significant. The following statistical tests were performed: Welch's t-test (normal distribution, non-parametric) (two-tailed p value) (Figures 3.2). All analyses were performed using Prism8 (GraphPad). The results are stated as mean ± s.e., unless otherwise noted.

BRIDGE

While our investigations on the role of Castor in specifying NB5-2 late-born interneurons are ongoing. Our behavioral data indicates that Castor functions at some level during neurogenesis to direct proper late-born interneuron connectivity. However, TTF identity is not the only intrinsic mechanism that may be promoting aspects of interneuron identity. During GMC division, the Notch inhibiting molecule, Numb, polarizes to one side of the cell and generates two sibling neurons, one with active Notch signaling ($Notch^{ON}$; N^{ON}) and the other with inhibited Notch signaling ($Notch^{OFF}$; N^{OFF}), due to the presence of Numb.

Notch signaling has been shown to promote dorsal neuropil targeting of neurons from multiple VNC NB lineages, subdividing lineages into dorsal/ventral hemilineages (Mark et al., 2021). Yet the downstream mechanisms promoted by Notch dorsal/ventral neurite targeting remain unknown. During VNC development, many extrinsic guidance cues form expression gradients within the neuropil, guiding neurites through repulsive/attractive responses. The Semaphorin (Sema) guidance molecules, Sema1a and 2a, create expression gradients along the dorsal/ventral neuropil axis (Zlatic et al., 2009). Thus, we hypothesized that differential Notch signaling may regulate the expression of the Sema receptors, PlexinA and/or PlexinB, to inform interneurons and guide neurites to the proper neuropil subdomains.

CHAPTER IV

CHARACTERIZATION TO INVESTIGATE THE FUNCTIONAL ROLE OF NOTCH IN NB5-2 INTERNEURON NEUROPIL TARGETING

Author contributions

Conceptualization: C.Q.D., H.Q.P.; Methodology: H.Q.P.; Formal analysis: H.Q.P.; Investigation: C.Q.D., H.Q.P.; Data curation: H.Q.P.; Writing – original draft: H.Q.P.; Writing – review & editing: H.Q.P.; Visualization: H.Q.P.; Supervision: C.Q.D.; Project administration: C.Q.D.; Funding acquisition: C.Q.D.

Introduction

Neural circuit assembly requires the generation of a diverse population for neuron progeny from a small pool of neural progenitor cells (NPCs). During central nervous system (CNS) neurogenesis, NPCs asymmetrically divide to produce two daughter cells with differential Notch signaling. Invertebrates and vertebrate studies have shown that Notch signaling is widely used during development with context dependent roles, such as maintaining progenitor cell state, promoting cell fate specification, and facilitating axon guidance (Giniger, 2012; K. Yoon & Gaiano, 2005). The polarization of the Notch inhibitor, Numb, during neural progenitor cell (NPC) division is required for proper cell fate specification of sibling daughter cells (Chapman et al., 2006; Couturier et al., 2012; Johnson et al., 2016; Rhyu et al., 1994; Spana & Doe, 1996).

In *Drosophila*, many studies have highlighted the role of Notch signaling in regulating neuron identity and axon/dendrite targeting (Li, *et al.* 2018). In the optic lobe, olfactory receptor neurons (ORNs), derived from the same progenitor, asymmetrically differentiate to form $N^{ON/OFF}$ sibling neurons, show distinct axon pathfinding trajectories, and target $N^{ON/OFF}$-specific glomeruli in the antennal lobe (Endo et al., 2007). Systematic analysis of mutants for the Notch coactivator, *mastermind* (*mam*), or *numb* in multiple clonal clusters revealed that differential Notch signaling anatomically subdivides $N^{ON/OFF}$ glomeruli, N^{ON} glomeruli residing in peripheral regions and N^{OFF} glomeruli in the central antennal lobe (Endo et al., 2007). In addition, using olfactory receptor Gal4 drivers, *mam* and *numb* mutants revealed that Notch signaling promotes

odorant receptor expression. Notch signaling is also required to specify L4 lamina neuron fate and is activated by L1 Delta expression in the first ganglion of the optic lobe (Xu et al., 2024).

In the *Drosophila* ventral nerve cord (VNC), differential Notch signaling specifies neuron sibling fate, in neurons derived from neuroblasts (NBs) NB1-1, NB4-2, NB7-1, and MP2 (Skeath & Doe, 1998; Spana & Doe, 1996). Notch signaling is also required in longitudinal pioneer axons to extend neurite projections into successive VNC segments by promoting formation of growth cone filopodia (Giniger, 1998; Kuzina et al., 2011).

Recently, neuronal lineages derived from NB1-2, NB4-1, NB5-2, and NB7-1 of the VNC have been observed to generate two morphologically distinct classes of neuron progeny, one class targeting neurites to the dorsal motor neuropil and another that targets the ventral sensory neuropil (Mark et al., 2021). A lineage specific Notch signaling reporter revealed that N^{ON} neuron progeny from NB5-2 or NB7-1 exclusively target the dorsal neuropil domain. Misexpression of the constitutively active Notch intracellular domain in NB1-2, NB5-2, or NB7-1 resulted in a loss of ventral neurite projections, conservation of dorsal neurite projections, and no significant difference in total cell number (Mark et al., 2021). Thus, these data suggest that Notch signaling promotes dorsal neuropil targeting and differential Notch signaling subdivides NB lineages into $N^{ON/OFF}$ hemilineages that differentially target the dorsal/ventral neuropil domains. This differential Notch signaling may provide important insight into understanding the developmental mechanisms that promote CNS organization and interneuron circuit assembly. Yet, little is known how Notch signaling functions to promote differential neurite targeting in the VNC.

Interestingly, the Semaphorin (Sema1a, 2a, and 2b) extrinsic signaling molecules and their receptors, PlexinA (PlexA) and PlexinB (PlexB) have shown direct associations and strong correlations with Notch signaling. Notch signaling is known to repress expression of Sema2b in ORNs (Joo et al., 2013). Sema2b, an attraction ligand to PlexB expressing neurites, is highly concentrated in the ventromedial antennal lobe and absent in the dorsolateral region (Alto & Terman, 2018; Joo et al., 2013). Axon-Axon interactions promoted by Sema2b/PlexB signaling is required in ventromedial N^{OFF} ORN classes to promote correct trajectory pathfinding along the ventromedial periphery of the developing antennal lobe and terminal glomeruli targeting (Endo et al., 2007; Joo et al., 2013). Sparse labeling of ORN $N^{ON/OFF}$ sibling pairs revealed that Sema2b expression is only enriched in N^{OFF} sibling neurons (Joo et al., 2013). However, Sema2b

expression was observed in both sibling ORNs in mutants of the Notch coactivator, *mastermind* (*mam*), suggesting the Notch inhibits Sema2b expression. ORN sibling axons of *Sema2b-/-, mam-/-* double mutants preferentially extended along the dorsolateral antennal lobe, suggesting that Sema2b signaling functions downstream of Notch signaling in ORN trajectory choice (Joo et al., 2013).

The repulsive Sema1a/PlexA signaling is also an important guidance cue for proper trajectory choice of late-born ORN axons. Sema1a and PlexA expression is highly expressed in ORN axons along the periphery of the antennal lobe and are required to promote axon-axon repulsion for proper axon trajectory and glomeruli termination (Sweeney et al., 2007). In *Drosophila* embryos, Sema1a/PlexA axon repulsion promotes proper axon targeting for motor neurons and may facilitate axon defasciculation and repulsion from the intersegmental nerve (ISN) to promote proper muscle target connectivity (Ayoob, 2004; Winberg et al., 1998; H.-H. Yu et al., 1998).

In the VNC, Sema1a concentration is highest in the dorsal neuropil where it is expressed in dorsally positioned motor neurons and GABAergic interneurons and forms a decreasing concentration gradient along the dorsal/ventral axis. Sema2a forms a concentration gradient along the central midline in the medial/lateral direction (Zlatic et al., 2009). In wildtype embryos, sensory nociceptive class IV multidendritic (md) axons terminate in the most ventral neuropil domain and both PlexA and PlexB receptors are required for proper terminal axon neuropil positioning. Combinations of mutant (*sema 1a/+; plex B/+, sema 2a/+; plex B/+,* or *plex B/plex A*) embryos all result in similar dorsal projecting neurite phenotypes. Further, nociceptive axon terminals in mutant embryos remain relatively uniform along the anterior/posterior axis, suggesting that Sema1a/PlexA and Sema2a/PlexB repulsive guidance only instructs neurite trajectory along the dorsal/ventral axis. Together, dorsal/ventral $N^{ON/OFF}$ targeting and Sema1a/2a concentration gradients in the VNC neuropil show a strong correlation that Notch signaling may regulate interneuron hemilineage targeting by promoting differential Plexin receptor expression, directing neurites to dorsal/ventral neuropil domains in response to extrinsic Sema signaling cues.

Here, we are currently in the process of testing the hypothesis that Notch signaling inhibits the expression and/or activation of Sema/Plexin signaling to promote differential dorsal/ventral targeting of VNC interneurons. To test this, we are using NB5-2, as it

predominately generates interneuron progeny (Mark et al., 2021). In wild-type, NB5-2 neurons target dorsal and ventral neuropil domains. Previous work done by our group has shown that NB5-2 Notch misexpression promotes all neurons to target the dorsal neuropil (Mark et al., 2021). We followed up on these findings using NB5-2 specific Notch loss of function (UAS-NotchRNAi) and observed that all neurites targeted the ventral neuropil domain (Figure 4.1). To investigate the role of Notch in inhibiting Sema/Plexin signaling we first verified Sema1a/2a expression gradients and characterized a Sema2b expression gradient along the dorsal/ventral neuropil axis. We then compared high Sema concentration domains with NB5-2 dorsal/ventral terminal neurite locations. Although much work is needed to make any conclusions from this data, the characterizations and associations discussed serve as great steppingstones to determine the role of Notch signaling in interneuron hemilineage identity and/or neurite targeting.

Results

Notch signaling promotes dorsal neurite targeting in NB5-2 interneurons

To follow up on previous work and strengthen evidence that Notch signaling promotes dorsal neurite targeting we wanted to manipulate Notch signaling in all NB5-2 progeny and assay for neurite targeting. To observed wild-type NB5-2 neurite targeting, we used the NB5-2 split-Gal4 to drive expression of UAS-GFP, subsequently called NB5-2Gal4>GFP. We observed three distinct contralateral neurite fascicles (dorsal, diagonal, and ventral) projecting to either the dorsal or ventral neuropil domains (Figure 4.1). We then expressed the active Notch intracellular domain (UAS-N[intra]) in NB5-2, subsequently called NB5-2Gal4>N[intra] and observed that all NB5-2 progeny target the dorsal neuropil domain, reproducing previous findings (Mark et al., 2021). We also note that NB5-2Gal4>N[intra] dorsal and diagonal fascicles appear fully conserved but there was a complete loss of the ventral fascicle (Figure 4.1). In contrast, Notch loss of function (NB5-2Gal4; UAS-NotchRNAi) resulted in ventral targeting of all NB5-2 progeny and a loss of the dorsal and diagonal fascicles (Figure 4.1). Reproducing the NB5-2Gal4>N[intra] phenotype and extending this study using Notch loss of function strengthens previous conclusions that Notch signaling promotes NB5-2 interneuron dorsal neurite targeting (Mark et al., 2021).

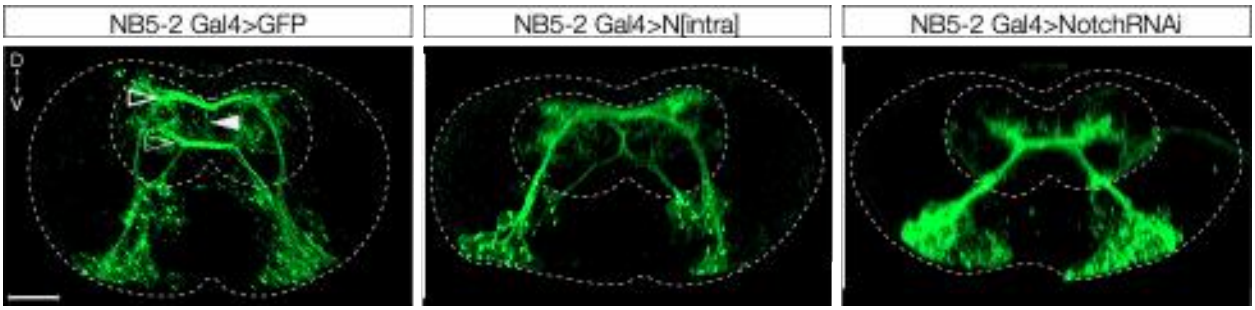

Figure 4.1. Notch gain and loss of function promote dorsal/ventral NB5-2 interneuron neurite targeting.
Whole lineage labeling in the A1 VNC of L1 (0-3hr ALH) wild-type NB5-2 (NB5-2>GFP; left panel, n= 10 animals), Notch intracellular domain misexpression (NB5-2>N[intra]; middle panel, n= 10), and Notch loss of function (NB5-2>NotchRNAi; right panel, n= 18) dorsal (outline arrow), ventral (dotted arrow), and diagonal (filled arrow) neurite fascicles in the VNC neuropil. Dotted lines indicate VNC cortex and neuropil borders. Dorsal up, posterior view. Scale bar: 10 μm.

Semaphorin 1a, 2a, and 2b are expressed in distinct regions of the VNC neuropil and NB5-2 dorsal neurites reside in a high Sema1a domain.

To understand if NB5-2 hemilineage targeting promoted by Notch signaling was locationally correlated with Semaphorin expression gradients we needed to identify the *Drosophila* Sema1a, 2a, and 2b concentration gradients in the neuropil and observe overlaps with NB5-2 dorsal/ventral neurites. Previous work has described that Sema1a expression is high in the dorsal neuropil and Sema2a is expressed along the central neuropil region in stage 17 embryos (Zlatic et al., 2009). Using immunohistochemistry, we confirmed these observations, finding that Sema1a expression was highest in the dorsal neuropil while high Sema2a expression was located in the central region of the neuropil (Figure 4.2A-B). However, we observed that high Sema1a dorsal expression is unique to the posterior commissure and is highest in the ventral region of the anterior commissure (Supp. Figure 4.1A). How this difference in location of Sema1a gradients between commissures may relate to Notch hemilineage targeting is unclear. NB5-2 neurites all target the posterior commissure and we observed that NB5-2 dorsal neurites infiltrate the high Sema1a dorsal domain (Figure 4.2A), while NB5-2 ventral neurites resided within the central Sema2a expression domain (Supp. Figure 4.1B). Interestingly, we found that PlexA expression is also high in the dorsal neuropil in stage 17 embryos but shows a lateral-to-medial expression pattern overlapping NB5-2 ventral neurites in first instar larvae (0-3hr ALH) (Figure 4.2D-E). Lastly, Sema2b expression is robustly expressed in the longitudinal tracts and shows weaker

expression in the commissures, consistent with previous observations (Wu et al., 2011). Along the dorsal/ventral axis we observed that Sema2b expression is consistently high in the ventral neuropil and NB5-2 ventral neurites reside on the dorsal border of the Sema2b expression domain. (Figure 4.2C and Supp. Figure 4.1C). We conclude that Sema1a, 2a, and 2b are expressed in discrete subregions along the dorsal/ventral neuropil axis and that NB5-2 hemilineage neurites overlap with separate Sema expression domains.

Figure 4.2 (next page). NB5-2 neurite location in relation to Sema and PlexA expression domains.
(A) Sema-1a expression gradient and NB5-2>GFP (A') overlapping regions (A'') in the A1 VNC neuropil of a stage 16/17 embryo. Dorsal up, posterior view. White dotted lines indicate neuropil border. Yellow dotted lines indicate high Sema expression domain (n = 8 animals). Scale bar: 5µm.
(B) Sema-2a expression gradient and NB5-2>GFP (B') overlapping regions (B'') (n= 8).
(C) Sema-2b expression gradient and NB5-2>GFP (C') overlapping regions (C'') (n= 6).
(D) PlexA expression and NB5-2>GFP (D') overlapping regions (D') of a stage 16/17 embryo (n= 15 animals). Yellow dotted lines indicate high PlexA expression domain. Scale bar: 5µm.
(E) PlexA expression and NB5-2>GFP (E') overlapping regions (E') of a L1 (0-3hr ALH) larva (n= 7 animals). Scale bar: 10µm.

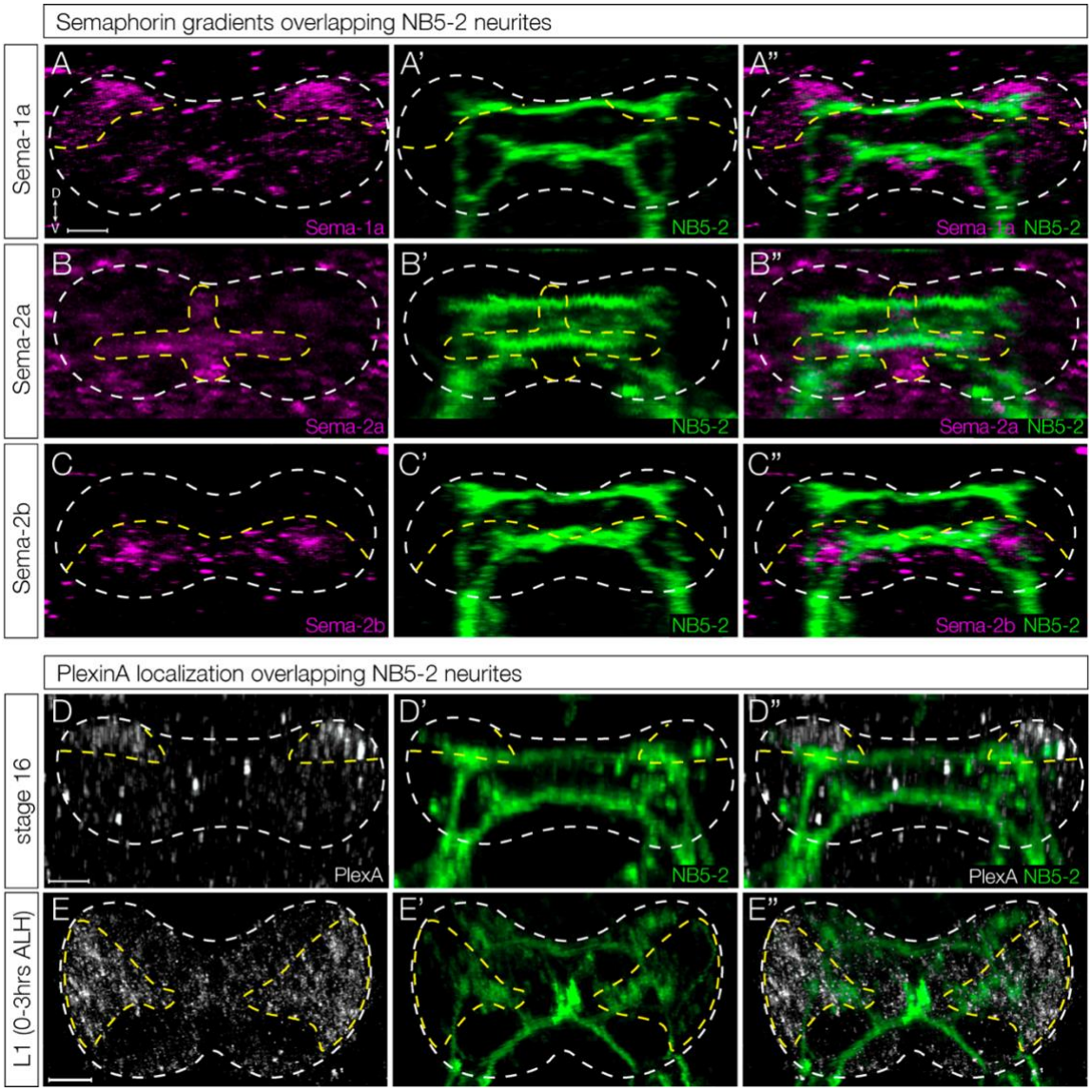

NB5-2 neurites do not show distinct dorsal/ventral fascicles until late embryogenesis

To investigate the role of Semas in directing neurite targeting we first wanted to understand the pathfinding trajectory of NB5-2 neurites throughout development. To achieve this, we tracked the development and localization of NB5-2 neurites at three developmental stages. Global neurite extension begins at approximately embryonic stage 12 (Goodman & Doe, 1993). We first observed NB5-2 neurite contralateral projections in the neuropil in stage 14 embryos (Figure 4.3A). Notably, stage 14 NB5-2 neurites form a single fascicle. In stage 15 embryos, we observed a small separation of NB5-2 dorsal/ventral fascicles, but they consistently lacked clear

and distinct separation, particularly at the midline (Figure 4.3B, yellow arrow). By stage 16, clear and distinct dorsal/ventral fascicles could be identified (Figure 4.3C). We hypothesize that this progression of dorsal/ventral fascicle resolution throughout development may require mechanisms that promote defasciculating (see Discussion).

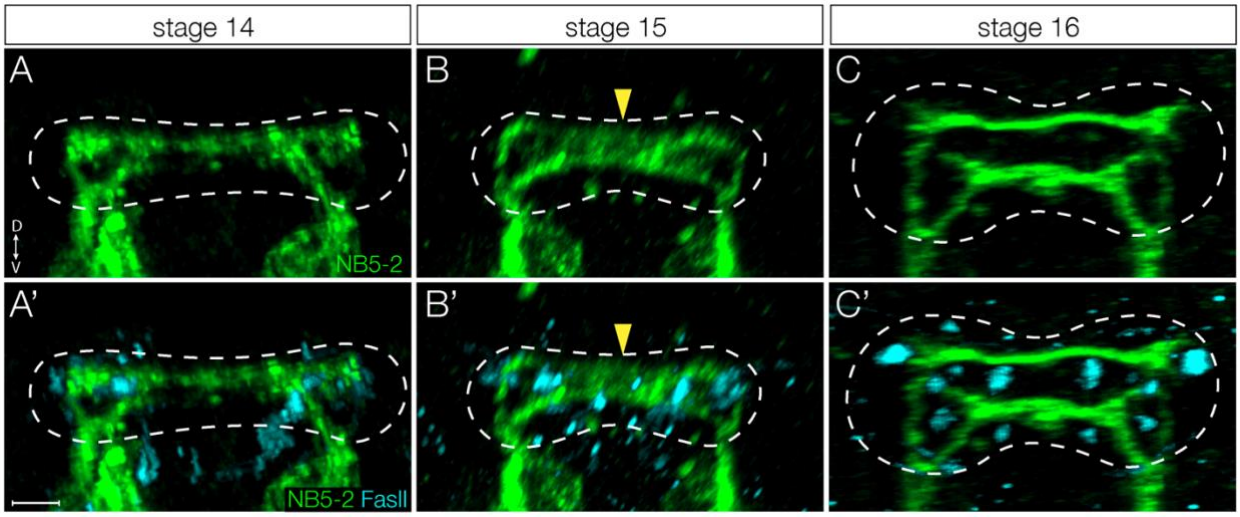

Figure 4.3. NB5-2 neurite morphology throughout embryogenesis.
(A) NB5-2>GFP (green) neurites with labeled FasII (A', cyan) fascicles in a stage 14 embryo. White dotted lines indicate neuropil border. Dorsal up, posterior view. Scale bar: 10 µm.
(B) NB5-2>GFP neurites with labeled FasII (B') fascicles in a stage 15 embryo.
(C) NB5-2>GFP neurites with labeled FasII (C') fascicles in a stage 16 embryo.

Discussion

Understanding the developmental mechanisms that promote proper organization of the CNS is essential to understanding how interneuron connectivity and proper circuit assembly are achieved. Here we lay the groundwork required to investigate the functional role of Notch signaling in hemilineage interneuron targeting. Previous findings have demonstrated that misexpression of the Notch intracellular domain promotes all NB5-2 neurons to the dorsal neuropil domain (Mark et al., 2021). Here we show that loss of Notch results in the opposite phenotype, driving all NB5-2 neurites to the ventral neuropil, thus strengthening our conclusion that differential Notch signaling among sibling neurons regulates dorsal/ventral hemilineage targeting. Yet, the downstream mechanisms promoting dorsal/ventral hemilineage targeting remains unknown.

Notch signaling is abundant throughout neurogenesis, promoting the maintenance of progenitor cells, neuron identity specification, and axon targeting (Giniger, 2012; K. Yoon & Gaiano, 2005). It is therefore imperative that we aim to differentiate whether Notch specifies neuron fate, promotes dorsal axon targeting separate form neuron fate, or informs both processes. Notch signaling is known to promote differentiation of dMP2 (Odd+) and vMP2 (Odd-) interneurons, derived from the MP2 progenitor (Spana & Doe, 1996). As pioneering neurons, dMP2 and vMP2 axon extension initiates the formation of the MP fascicle and extends longitudinal axons between successive neuromeres (Goodman & Doe, 1993). Temperature sensitive Notch mutants (N^{ts1}) fail to extend axons between successive neuromeres (Giniger, 1998; Kuzina et al., 2011). However, restricting Notch loss of function to the time of neuron identity choice, using a temperature sensitive mutation, and then restoring Notch signaling before axon extension (N^{ts1};*elav-GAL4*;*UAS-Notch*) increased Odd+ cell number but restored the MP fascicle (Giniger, 1998). This evidence may suggest that Notch signaling functions at two developmental time points, first to specify neuron identity, then later to guide neurite trajectory. Disentangling the two developmental processes in future work will allow us to better understand the mechanisms that promote differential interneuron hemilineage targeting.

To investigate the downstream mechanisms that may be promoted by hemilineage Notch signaling we focused on Sema/Plexin signaling. To begin this, we first needed to characterize Semaphorin expression gradients along the dorsal/ventral axis. We achieved reproduction of previous observations of high dorsal Sema1a and central Sema2a expression gradients (Zlatic et al., 2009) and characterized a Sema2b ventral expression gradient. Further, localization of NB5-2 dorsal neurites reside in the high Sema1a expression domain, while ventral neurites localize within the Sema2a expression region and at the dorsal border of the Sema2b expression domain. Yet, localization of Sema expression gradients reveals little about how these molecules function to direct interneuron neurite targeting.

Previous studies have shown that extending neurites expressing PlexA or PlexB are repelled from regions of high Sema1a or Sema2a concentration, respectively, while Sema2b attracts neurites expressing PlexB (Ayoob, 2004, 2006; Joo et al., 2013; Sweeney et al., 2007; Winberg et al., 1998; Zlatic et al., 2009). Therefore, we predict that PlexA expressing neurites in the VNC are likely repelled from the Sema1a dorsal domain and PlexB neurites are repelled from the Sema2a central domain and attracted toward the Sema2b ventral domain. Thus, Notch

signaling may inhibit Plexin expression in N^{ON} hemilineage neurons, allowing neurites to infiltrate the highly concentrated Sema1a dorsal domain. In contrast, Notch inhibition in N^{OFF} sibling neurons may promote PlexA/B expression to repel neurites from the dorsal neuropil and direct neurites toward the more ventrally located domain. Furthermore, a combination of PlexA/B expression in N^{OFF} neurons may be required for precise NB5-2 ventral neurite targeting, given ventral neurites terminate along the Sema2a/2b expression borders. Thus, in future work it will be important to determine: 1) if Plexin receptors are differentially expressed in $N^{ON/OFF}$ hemilineages, 2) if Notch functions to inhibit Plexin expression, and 3) if differential PlexA or PlexB expression is required for NB5-2 dorsal/ventral neuropil targeting.

However, a body of evidence investigating the interactive mix of Sema/Plexin signaling mechanisms in multiple regions of the developing *Drosophila* CNS emphasizes the complexity and possibly context dependent roles these extrinsic cues play during axon guidance (see Chapter V: Discussion). Therefore, the interactions of Sema/Plexin signaling may be more complex than our predicted model and future Sema and Plexin loss and gain of function studies will provide a better insight into whether hemilineage targeting is instructed by Sema/Plexin guidance.

To better understand the pathfinding trajectories of dorsal/ventral NB5-2 neurites, we tracked neurite localization over three developmental time points. Surprisingly, we did not observe distinct dorsal/ventral fascicles until stage 16. Stage 14 embryos only show a single neurite fascicle, while stage 15 embryos displayed separation in the lateral portions of neurite projections but a centrally fused region. It is not likely that these differences in fascicle morphology across developmental stages is due to a difference in early and late-born neurite targeting, as $N^{ON/OFF}$ neurons are sibling pairs and are expected to differentiate at the same time. One possible explanation is that during initial extension, NB5-2 neurites fasciculate as one axon bundle, and later defasciculate as axonal Notch signaling or Sema1a expression increases in the dorsal neuropil. Notch and Sema1a/PlexA signaling have been shown to promote defasciculation of motor neurons that initially extend along the intersegmental nerve (ISN) and must bifurcate to form the intersegmental nerve b branch (ISNb) (Ayoob, 2004, 2006; Giniger, 1998; Kuzina et al., 2011; Winberg et al., 1998; H.-H. Yu et al., 1998). Therefore, delayed Notch activation until stage 15 may promote defasciculation of $N^{ON/OFF}$ neurites, separating the dorsal/ventral fascicles as the neuropil develops.

Notch and Sema/Plexin signaling are both highly conserved developmental mechanisms. In the vertebrate CNS, Notch expression levels have been shown to differentiate progenitor maintenance and interneuronal functional identity (i.e. inhibitory vs excitatory) (Mizuguchi et al., 2006; Zhang et al., 2021). Notch signaling has been shown to be essential in generating interneuron diversity in the developing spinal cord of mice, chick, and zebrafish, and promote proper axon/dendrite guidance of commissural, cortical, and hippocampal interneurons (Alberi et al., 2011; Peng et al., 2007; Redmond et al., 2000; Salama-Cohen et al., 2005; Šestan et al., 1999; Shi et al., 2011). In addition, Sema/Plexin signaling is an ancient signaling mechanism that is crucial for the development of many species. *Drosophila* possess five different Semaphorins, three of which are expressed in the CNS, while humans express more than 20 paralogs (Alto & Terman, 2018; Rozbesky et al., 2019). Semaphorins in the vertebrate CNS induce cell migration of cortical and cerebellar neurons and instruct interneuron pathfinding trajectories that form the spinal cord commissural tracts (Chen et al., 2008; Faulkner et al., 2008; Kerjan et al., 2005; Leighton et al., 2001; Marín, 2016; Rünker et al., 2008; Zou et al., 2000). The evolutionary conservation and abundance of these two signaling mechanisms places a clear emphasis on the important roles they play in CNS development. In future work, it will be intriguing to investigate whether there are different Notch signaling pathways that are temporally separated to specify interneuron molecular identity and neurite guidance or if the two are in inexplicably linked. Furthermore, identifying the downstream mechanisms promoted by Notch signaling, such as Sema/Plexin signaling, may provide valuable insight into how intrinsic cues inform an interneurons response to external signals to shape the CNS and promote neural circuit assembly.

Materials and Methods

Fly Stocks

Male and female *Drosophila melanogaster* were used. The transgene insertion sites (if known) are shown next to the respective genotypes.

Table 3. Genotypes utilized to obtain results for the Figure(s) indicated in Chapter IV

Genotype	Figure(s)
vnd-VP16; R16H05-Gal4 DBD/10xUAS-IVS-myr::sfGFP-THS-10xUAS(FRT.stop)myr::smGdP-HA	Figure 4.1, 4.2, 4.3
vnd-VP16/UAS-Notch[intra]; R16H05-Gal4 DBD/10xUAS-IVS-myr::sfGFP-THS-10xUAS(FRT.stop)myr::smGdP-HA	Figure 4.1
vnd-VP16/10xUAS-IVS-myr::GFP; R16H05-Gal4 DBD/ UAS-NotchRNAi	Figure 4.1

Gal4 lines, mutants and reporters used were:

vnd-VP16 (2R, VK1, 59D3) (Mark et al., 2021)

R16H05-Gal4 DBD (3L, P2, 68A4) [Pollington & Doe, 2025]

UAS-Notch[intra] (Struhl & Greenwald, 2001)

UAS-NotchRNAi (BDSC_33611)

10xUAS-IVS-myr::GFP (BDSC_32198)

Immunostaining and Imaging

Primary antibodies were: chicken anti-GFP (1:1000, RRID:AB_2307313, Aves Labs, Davis, CA), rabbit anti-Sema-1a (1:1000, gift from Alex Kolodkin, Johns Hopkins School of Medicine), mouse anti-Sema-2a (4µg/mL, DSHB 19C2), rabbit Sema-2b (1:2000, gift from Alex Kolodkin, Johns Hopkins School of Medicine), rabbit anti-PlexA (1:500) (Sweeney et al., 2007).

Embryos were fixed in 4% paraformaldehyde for 20 min and stained as previously described (Mark et al., 2021). Larval brains were dissected in PBS, fixed in 4% paraformaldehyde, and then stained by following protocols as described (Sullivan et al., 2019). The samples were then DPX mounted.

CHAPTER V

DISCUSSION

The proper establishment of neural circuits within the central nervous system (CNS) is vital to generate appropriate behavioral responses. During CNS development, a small pool of neural progenitor cells produces a diverse array of interneurons, each with a unique identity. Neuron identity consists of the integration of multiple aspects that include combinatorial expression of transcription factors (TFs; i.e. molecular identity), morphology, connectivity, neurotransmitter expression, and electrophysiology. In vertebrates and *Drosophila*, many neural progenitor cells sequentially express a temporal transcription factor (TTF) cascade that generates early and late born neurons with different TTF identities (Doe, 2017; Holguera & Desplan, 2018). Additionally, ganglion mother cells (GMCs) that maintain TTF identity, produce two sibling neurons with differential Notch signaling. Disruptions in TTF expression and Notch signaling have been shown to impact many aspects of neuron identity (Doe, 2017; Mark et al., 2021; Pollington et al., 2023). Thus, investigating the role of TTFs and Notch signaling in specifying aspects of interneuronal identity is crucial in understanding how CNS neural circuits are established. Importantly, the outstanding gap in knowledge is our understanding of how TTFs and Notch signaling are integrated to specify specific aspects of neuron identity. This dissertation investigates the role of the TTFs, Hunchback and Castor, and Notch signaling in promoting aspects of interneuron identity (Figure 5.1). We further characterize the spatial expression gradients of the *Drosophila* Semaphorins, Sema1a, 2a, and 2b in the ventral nerve cord (VNC) that may function in shaping morphology and neurite guidance. Below we discuss and hypothesize how TTFs and Notch identity may promote individual interneuron identity and inform a neuron's response to extrinsic signaling cues.

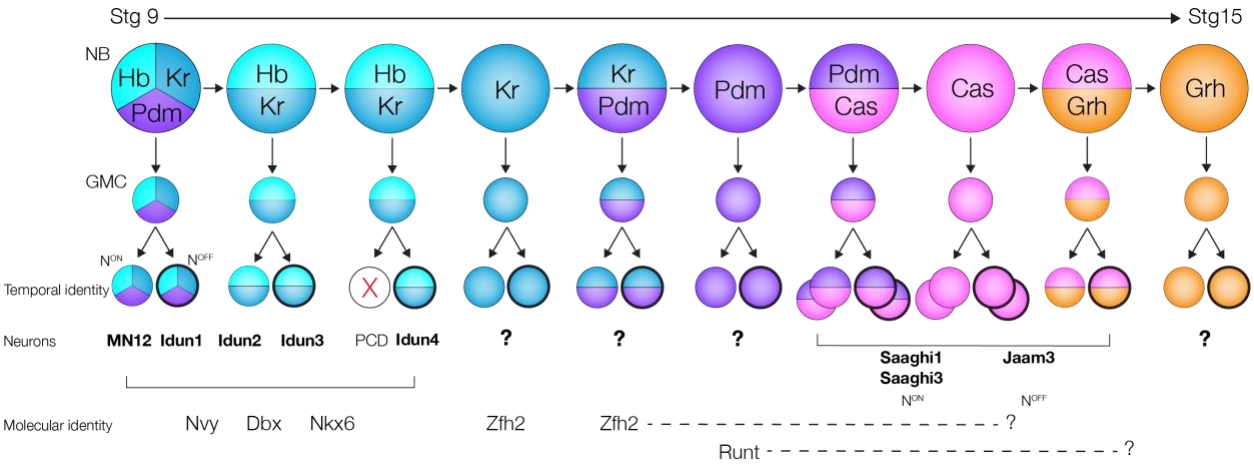

Figure 5.1. Summary of the Hunchback, Castor, and Notch hemilineage identity of NB5-2 interneurons. NB5-2 expresses the canonical TTF cascade Hunchback (Hb, cyan)> Krüppel (Kr, blue)> Pdm (purple)> Castor (Cas, pink)> Grainyhead (Grh) and produces GMCs in single and dual TTF expression windows from embryonic stage 9-15. During the Hb expression window, NB5-2 produces a single MN, MN12, and four interneurons Idun1-4 with early-born specific transcription factors (TFs) Nervy (Nvy), Dbx, and Nkx6. Later-born Cas+ interneurons, following the Hb expression window, were identified to express the late-born TFs, Zfh2 and Runt. Dashed lines indicate approximate TF expression termination; however, the precise window of late TF expression is unknown. NB5-2 generates Saagi1, Saaghi3, and Jaam3 during the Castor expression window. Dorsal/ventral neurite targeting of each neuron determines Notch$^{ON/OFF}$ ($N^{ON/OFF}$) hemilineage assignment.

Future directions investigating the role of Hunchback in interneuron identity

In Chapter II, we show that the early-born TTF, Hunchback, promotes multiple aspects of early-born NB5-2 interneuron identity including, molecular identity, distinct morphological features, and presynapse targeting. However, the downstream mechanism that subdivide and differentiate each NB5-2 Hb+ neuron remains unknown. Different levels of Hb expression have been observed in NB lineages that produce more than one GMC (Kanai et al., 2005; Mettler et al., 2006; Moris-Sanz, et al., 2014). Specifically, NB7-1 generates two Hb+ GMCs that generate the high Hb U1 and low Hb U2 motor neurons (Kanai et al., 2005). Hunchback has been shown to bind NB-specific loci in NB5-6 and NB7-4, and may function to maintain regions of open chromatin (Sen et al., 2019). Thus, it is possible that different levels of Hb expression may result in a high Hb+ NB with Hb occupying many Hb-specific loci, while a Hb in low Hb+ NB bind less Hb-specific loci, promoting the generation of different Hb+ GMCs. Combinatorial TTF expression of Kr and Pdm has also been shown to be vital for the specification of the NB7-1 VO motor neuron (Seroka et al., 2020). VO is generated during a combinatorial Kr/Pdm expression

window and transiently maintains Kr/Pdm expression (Seroka et al., 2020). NB7-1 misexpression of Pdm alone results in loss of the U3 (Kr+), normal U4 (Pdm+), and increased U5 MNs (Pdm+/Cas+) (Meng et al., 2020). In contrast, Kr/Pdm coexpression generates normal U3 MNs, increased ectopic VO MNs, and loss of U4/U5 MNs. In addition, previous work has demonstrated that differential Notch signaling of sibling neurons, generated from the same ganglion mother cell (GMC), promote differential dorsal/ventral targeting (Mark et al., 2021).

Together, I hypothesize that subdivisions during the early NB5-2 Hb window may occur through integration of TTF expression levels, TTF combinatorial expression, and differential Notch signaling (Figure 5.2). NB5-2 is observed to express a combination of Hb/Kr/Pdm in stage 9 embryos and is transiently maintained in a subset of the NB5-2 Hb+ population (Figure 2.1 and 2.2). NB5-2 Hb+ MN and interneuronal projections also show a near equal distribution in dorsal/ventral targeting, suggesting Notch signaling may promote differential fate specification from sibling neurons produced from the same GMC. Lastly, although Hb levels were not analyzed during our study, I hypothesize that the two GMCs produced during the Hb/Kr window may express different levels of Hb protein that differentiate Hb/Kr GMCs and daughter cell identity. Further, these differences in TTF and Notch signaling likely promote differential expression of downstream TFs.

Figure 5.2 (next page). Hypothesis of NB5-2 Hunchback subdivision to specify individual NB5-2 interneuron identity. I hypothesize that the NB5-2 Hb expression window is subdivided by combinatorial TTF expression of Hb (cyan)/Kr (blue)/Pdm (purple), Hb concentration, and differential Notch signaling ($N^{ON/OFF}$) between sibling neurons. These subdivisions may promote expression of interneuron specific early-born TF combinations. Previous studies have reported MN12 expresses Hb9 and the interneuron sibling expresses Dbx, likely to be Idun1 (Lacin et al., 2009). Our work shows that Idun1-3 express Nervy (Nvy) (Figure 2.6). However, the specific expression of Dbx and Nkx6 are currently unknown (grey text). In addition, we hypothesize the Idun4 sibling neuron undergoes programmed cell death (PCD), as we were only able to identify five NB5-2 Hb+ neurons. Dorsal/ventral neurite targeting of each neuron determines $Notch^{ON/OFF}$ ($N^{ON/OFF}$) hemilineage assignment.

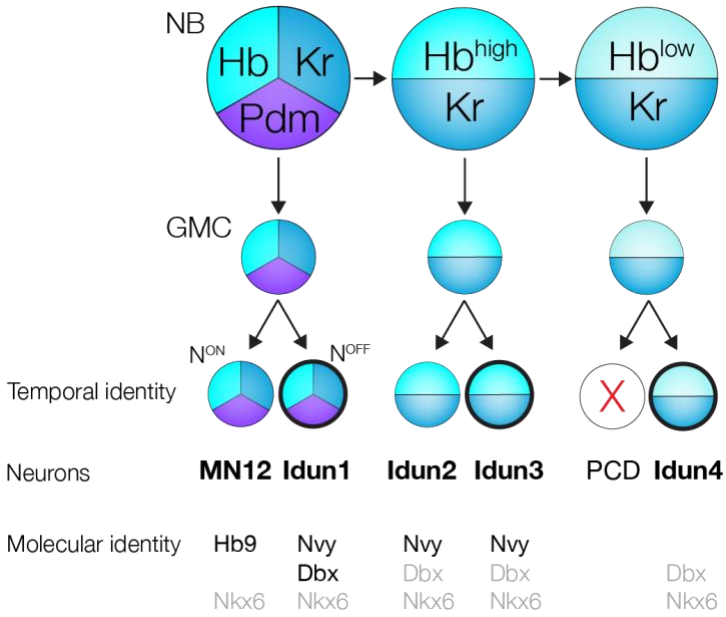

We identified that NB5-2 Hb+ neurons co-express the homeodomain TFs, Dbx and Nkx6, and Nervy (Nvy), a protein in the myeloid translocation gene family. NB5-2 Hb misexpression increases the number of NB5-2 neurons expressing each TF, suggesting that Hb promotes the expression of Dbx, Nkx6, and Nvy. However, it is currently unclear which TF combinations are expressed in each NB5-2 Hb+ neuron, as not all Hb+ neurons co-express all three TFs. In future studies, understanding the role that each of these TFs play in regulating specific aspects of NB5-2 Hb+ interneuron identity will inform our understanding of the mechanism that promote individual interneuron identity.

Previous studies have shown that Nkx6 is required for proper axonal pathfinding and muscle innervation of the VO MN (Seroka et al., 2020). NB7-1 U MNs all express the TF, Even-skipped (Eve), and all Eve+ MNs are shown to project axons along the intersegmental nerve (ISN) and innervate dorsal muscle targets (Landgraf et al., 1999; Seroka et al., 2020, Meng et al., 2020). In contrast, the VO MN diverges from the ISN and projects along the intersegmental nerve d branch (ISNd) to innervate ventral muscle targets. NB7-1 Nkx6 knockdown results in loss of ISNd projections while NB7-1 Nkx6 misexpression increases ISNd fascicle volume and innervation to ventral muscles. Combinatorial expression of Nkx6 and Hb9 promotes ventrally ISNb projecting MN fate and represses dorsal projecting MN fate (Broihier et al., 2004). Nkx6 is known to repress Eve; however, *nkx6* or *hb9* mutant embryos revealed minimal disruptions in MN Eve expression. In contrast, *nkx6*/*hb9* double mutants revealed a significant increase in Eve+

MNs indicating that Nkx6 and Hb9 expression, together, are required for the suppression of MN Eve expression (Broihier et al., 2004). Further, separate from Hb9, Nk6x plays a more predominate role in regulating axonogenesis and neurite extension by promoting expression of the adhesion molecule FasIII (Broihier et al., 2004). *nkx6* mutants display truncated MNs that remain within the CNS and decreased expression of FasIII, while Nkx6 misexpression promotes ISNb overgrowth. Thus, Nkx6 promotes axon extension in MNs and may play an important role in neurite targeting of interneurons.

Dbx is also known to specify interneuron fate and neurite guidance of the Ap/Np1p1 neuron, produced from NB5-6T (Stratmann et al., 2019). RNAseq data revealed co-misexpression of the Ap/Np1p1 specific genes, *lady bird early (lbe)* and *collier* (*col*), can downregulate Dbx expression. Interestingly, both *Dbx* mutant embryos and pan-neuronal Dbx misexpression show partial losses of Np1p1+ expressing cells and a failure of Ap/Np1p1 neurites to extend along the medial FasII longitudinal tract (Stratmann et al., 2019). The authors note that a similar outcome in Dbx manipulation experiments makes it challenging to understand the precise role of Dbx in Ap/Np1p1 fate specification of neurite guidance; however, Dbx appears to play a partial role in modulating these processes (Stratmann et al., 2019).

Within the VNC, NB Dbx expression labels progenitor cells that produce interneuron populations and Dbx expression is only observed in post-mitotic interneurons in the VNC, many of which are GABAergic (Lacin et al., 2009). Consistent with our findings, Dbx expression has been observed in two medially located NB5-2 neurons (Figure 2.5) and the single NB5-2 MN, MN12, expresses Hb9 (Lacin et al., 2009). Interestingly, pan-neuronal misexpression of Dbx in post-mitotic neurons represses Hb9 expression in the NB5-2 lineage, supporting a model that Dbx may play a role in specifying the interneuron fate of some NB5-2 neurons and repress MN fate. Further, Dbx misexpression eliminates or reduces Nkx6 expression and results in thin or broken longitudinal tracts between neuromeres and shows relative increases in the size of axonal scaffolds within segments (Lacin et al., 2009). Together, these data suggest that Dbx may function to limit CNS neurite outgrowth by repressing Nkx6 activity. Interestingly, Dbx/Hb9 cross repression may be promoted by differential Notch signaling, as *numb* mutants show increased numbers of NB5-2 Hb9+ neurons at the expense of Dbx+ neurons, while mutants for the Notch promoting factor, *sanpodo*, increases NB5-2 Dbx+ neuron number at the expense of Hb9+ neurons (Lacin et al., 2009).

Nervy also shows interactions with Notch signaling in the specification of sensory organ precursor (SOP) cells during sensory organ development (Wildonger & Mann, 2005). During imaginal disc development, proneural cluster cells express the TFs, Achaete (Ac) and Scute (Sc), which promotes expression of the Notch ligand, Delta. Increased Delta expression in a presumptive SOP increases Notch signaling in neighboring cells, inhibiting SOP differentiation (Wildonger & Mann, 2005). Ectopic Nvy expression inhibits SOP formation but does not appear to promote Delta expression. The authors hypothesize that Nvy may function to amplify Delta signaling in a presumptive SOP, therefore increasing Notch signaling in neighboring cells to inhibit SOP differentiation (Wildonger & Mann, 2005).

Interestingly, Nvy has also been observed to interact with the axon repulsive receptor, PlexinA (Terman & Kolodkin, 2004). During the process of axon/dendrite outgrowth, attractive/repulsive extracellular signaling cues direct neurite targeting and promote fasciculation/defasciculation at given choice points. The *Drosophila* Semaphorin1a (Sema1a) is expressed in extending MN axons and the developing VNC and functions as a repulsive signaling cue through the PlexA receptor to promote neurite defasciculation (Ayoob, 2004, 2006; Terman & Kolodkin, 2004; K. Yoon & Gaiano, 2005; Zlatic et al., 2009). Nervy is known to directly interact with PKA, a cAMP-depended protein kinase, to promote binding of PKA to the PlexA receptor and inhibit PlexA function (Terman & Kolodkin, 2004). In *nvy* mutant embryos, MN projections that extend along the ISN, ISNb, and segmental nerve a (SNa) tracts display defasciculation phenotypes. In the CNS, abnormal neurite defasciculation occurs within the lateral FasII longitudinal bundle (Terman & Kolodkin, 2004). In contrast, Nervy misexpression decreased MN defasciculation, inhibiting proper MN-muscle innervation and resulted in frequent fusion of the lateral and middle FasII longitudinal tracts in the VNC neuropil (Terman & Kolodkin, 2004). Thus, Nvy functions by promoting PKA-PlexA binding, consequently inhibiting PlexA response to Sema1a repulsive guidance cues. In NB5-2, Nvy is expressed in Idun1-3 (Figure 2.6) and may play an important role in neurite guidance by mediating Sema1a/PlexA signaling (see Below).

However, proper neurite guidance does not necessarily determine proper connectivity and circuit assembly. Post-synaptic dendrites follow endogenous presynapse partner neurons that have been forcibly displaced within the neuropil (Valdes-Aleman et al., 2021). In NB5-2, we show that transformed Hb+ late-born neurons target presynapses to endogenous NB5-2 Hb+

subregions (Figure 2.8); however, it remains unknown if these transformed late-born neurons form synaptic connections with early-born partner neurons. Late-born NB5-2 neurons contribute to the well characterized late-born EL proprioceptive circuit (Heckscher et al., 2015; Mark et al., 2021) and NB5-2 misexpression does disrupt proprioceptive behavior (Figure 2.9), suggesting that TTF identity is essential for proper connectivity. Yet, more direct experimental approaches are needed to address this question. This will require the identification of pre- and post-synaptic partners that exclusively connect to early NB5-2 interneurons, the development of genetic access to these partners, and analysis of partner connectivity to Hb+ transformed late-born interneurons. The potential results from this approach will yield insightful knowledge on the precise role of TTFs in interneuronal connectivity and CNS circuit establishment.

Future directions investigating the role of Castor in interneuron identity

In Chapter III, we show that the late-born pre-motor interneurons Saaghi1 (SA1) and Saahgi3 (SA3), and the late-born post-sensory interneuron Jaam3 (JA3) express the late TTF, Castor (Figure 3.1). NB5-2 Castor misexpression disrupts proprioceptive behavior (Figure 3.2), similar to NB5-2 Hb misexpression (Figure 2.9) and EL interneuron ablation (Heckscher et al., 2015). Previous studies have shown that Castor misexpression determines late-born neuron fate of neurons derived from NB5-5 and NB5-6T and truncates MN production in NB7-1 (Baumgardt, et al., 2009; Benito-Sipos et al., 2010; Meng et al., 2020). Castor is known to repress expression of Pdm and promote expression of Grh (Grosskortenhaus, 2006; Tran & Doe, 2008; Baumgardt et al., 2009). Surprisingly, we did not observed suppression of NB5-2 Pdm expression following Cas misexpression or any altering disruptions in the NB5-2 TTF cascade (Figure 3.3). Thus, there is currently a discrepancy in our results at the behavior and NB molecular levels. We are actively investigating this discrepancy and offer two possibilities that may explain our current observations.

First, our genetic transgenes may not effectively express the level of Castor required for Pdm repression, limiting our ability to conclude that NB5-2 Castor expression promotes late-born interneuron identity (Figure 5.3). Thus, in the future, we will attempt Castor misexpression using two transgenes to increase Castor protein levels during the NB5-2 Pdm expression window. If we observe repression of Pdm using two Castor transgenes, it is likely that our initial misexpression results are due to insufficient Castor levels. However, if we continue to observe

Pdm expression with two Castor transgenes, a second possibility, coupled with our behavioral data, is that the role of Castor is more prominent in the post-mitotic neurons than in the NB. Interestingly, previous studies using NB-specific drivers (*inscuteable*-Gal4 or *worniu*-Gal4) to misexpress Cas also resulted in only mild phenotypes while a pan-neuronal driver (*elav*-Gal4) show stronger phenotypes and neuron fate transformation (Benito-Sipos, et al., 2010).

In NB5-6T, the early TTF, Krüppel, is expressed early in NB5-6T divisions and then functions in the late-born Castor+ post-mitotic Apterous (Ap) expressing neurons to specify Ap/Np1p1 identity (Stratmann et al., 2016). Furthermore, the late TTF, Grh, specifies Ap/FMRFa in the NB5-6T lineage. Grh expression gradually increases during the generation of the four Ap+ neurons, but post-mitotic increase in the last Ap+ neuron, Ap/FMRFa, is required for fate specification (Baumgardt, et al., 2009). Conversely, Castor induced expression of the subtemporal gene, *nab*, in NB5-6T is necessary to promote Ap2/3 identity after Ap/Np1p1 generation (Baumgardt, et al., 2009). Nab expression must occur in the NB otherwise upregulation of Nab in the post-mitotic neurons would repress Ap/Np1p1 specification (Baumgardt, et al., 2009). Together, these studies suggest that TTFs may function at multiple levels during neurogenesis to specify individual interneuron fate. Thus, it is possible that Castor may serve an important role at the NB and post-mitotic levels in NB5-2 interneuron fate specification (Figure 5.3).

Alternatively, progressive restriction of NB competence to TTF expression versus external signaling cues may change as development progresses. In the mouse neocortex, apical progenitor (APs) cells are initially driven by intrinsic signaling mechanism to produce early-born post-mitotic neuron fates. However, APs become progressively more responsive to extrinsic signaling cues as neocortical development continues (Telley et al., 2019). During retinal development, retinal progenitors undergo progressive restriction in their ability to respond to intrinsic cues (Belliveau et al., 2000). In *Drosophila*, NB7-1 has a single competence window for responding to Hb and Kr (Cleary & Doe, 2006). Misexpression of Hb and Kr prolongs the NB7-1 competence window, resulting in an increase in the number of U1/U2 or U3 neurons, respectively. High levels of Hb or Kr present during embryonic stages when Castor is normally expressed results in production of early U MNs and a loss of U4/U5 neurons (Cleary & Doe, 2006; Grosskortenhaus et al., 2005, 2006). However, Kr misexpression results in three different phenotypes: 1) embryonic hemisegments with two ectopic U3 MNs also contain U4/U5 MNs, 2)

hemisegments with three ectopic U3 MNs typically only contain U4, and 3) hemisegments with more than three ectopic U3 MNs lacked U4 and U5. The authors state that these phenotypic differences may be due to varying decreases in Kr expression, proposing that faster decreases in prolonged NB7-1 Kr expression allows for delayed U4 and U5 production, while slower decreases in Kr expression inhibit Pdm and Castor expression past a developmental window where the NB is capable of responding to Pdm or Castor, suggesting that there is a specific window where NB7-1 is competent to respond to Pdm/Castor expression (Cleary & Doe, 2006). These data suggests that NB7-1 undergoes progressive loss of competence to respond to TTFs throughout development. In addition, NB7-1 Castor misexpression does not affect Hb or Kr expression or the generation of U1-3 MNs, indicating the early NBs are either not competent to respond to late TTFs or Cas levels are too low (Grosskortenhaus et al., 2006; Meng et al., 2020; Tran & Doe, 2008). Thus, it is possible that during the NB5-2 Castor TTF expression windows, the NB is more restrictive in its responses to intrinsic signaling cues, and genetic manipulations of Castor misexpression alone are not adequate to force changes in late TTF expression. In addition, loss of competence at one stage may allow for the reuse of the same TTF later during neurogenesis, as second expression windows of Kr and Cas have been observed during later embryonic and larval stages (Cleary & Doe, 2006; Stratmann et al., 2016). As this work progresses, it will be important to test these hypotheses so we can better understand the mechanism that specify later-born interneuron fate and promote CNS circuit assembly.

Figure 5.3. Hypothesized models of Castor function in late-born NB5-2 interneuron fate specification. NB Model: Castor expression in the NB is essential to promote aspects of late-born interneuron identity in post-mitotic progeny. Post-mitotic model: Castor plays a dual role during neurogenesis, 1) NB expression regulates expression of the TTFs, Pdm and Grh, and may promote expression of sub-temporal genes and 2) post-mitotic increase of Castor expression promotes expression of downstream TFs that specify aspects of interneuron identity.

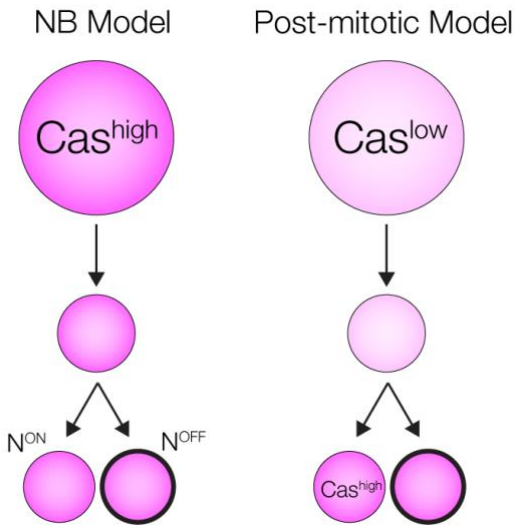

Future directions investigating Notch and Sema/Plexin signaling in hemilineage neurite targeting

In Chapter IV, we show strong evidence to conclude that Notch signaling promotes NB5-2 interneuron dorsal hemilineage targeting. Yet, the downstream mechanisms initiated by Notch to promote proper neurite targeting remain unknown. To continue this investigation, it will be important to focus on two main questions 1) Does Notch solely function to direct NB5-2 dorsal neurite targeting (through pathfinding or defasciculation) or promote additional aspects of interneuronal fate such as transcription factor expression, pre-/post-synaptic targeting, neurotransmitter expression, or electrophysiology, and 2) does NB5-2 Notch signaling inhibit Plexin expression to promote differential dorsal/ventral hemilineage neurite targeting in response to Semaphorin signaling cues? Below is a discussion highlighting what we currently know about Notch and Sema/Plexin signaling during neurogenesis to help address each of these questions.

Introduction to Notch signaling

The canonical Notch signaling pathway requires the binding of the transmembrane Notch receptor to the ligands Delta/Serrate (*Drosophila*) or Delta1-4/Delta-like1/Jagged1-2 (mammals) (Yoon & Gaiano, 2005; Zacharioudaki & Bray, 2014). Upon binding, the Notch intracellular domain (NICD) is cleaved by the γ-secretase protein complex, promoting NICD nuclear translocation. Once in the nucleus, NICD interacts with a myriad of co-activators, including Mastermind (Mam in *Drosophila*; MAML in mammals) to induce expression of basic helix-

loop-helix transcriptional regulators, Hes and Hey, well known for their role in inhibiting proneural genes to maintain progenitor cell state, but have also been shown to specify neuron fate (Udolph, 2013; Yoon & Gaiano, 2005; Zacharioudaki & Bray, 2014). Traditionally, polarization of the Notch inhibitor, Numb, during GMC cell division produces a daughter cell with active Notch signaling (N^{ON}) and another with repressed Notch signaling (N^{OFF}) (Yoon & Gaiano, 2005; Zacharioudaki & Bray, 2014).

Notch signaling specifies interneuron molecular identity

In *Drosophila*, Notch specifies neuronal fate of interneurons in the developing lamina, antennal lobe, and VNC (see Chapter IV: Introduction for more details) (Endo et al., 2007; Skeath & Doe, 1998; Xu et al., 2024). In the VNC, the neuronal identity of NB5-2 progeny following Notch misexpression (N[intra]) has not been tested. High levels of NB5-2 Notch signaling promotes dorsal neurite targeting in all NB5-2 progeny (Figure 4.1); however, this approach also induces high levels of Notch signaling in the post-mitotic progeny. Currently, it is unclear if NB5-2 Notch misexpression induces changes in cell fate, neurite trajectory, or both.

In vertebrate CNS development, Notch signaling specifies neuronal fate from many different progenitors. In the developing neural tube of mouse, chick, and zebrafish embryos, Notch signaling is required for the specification of inhibitory v2bIN interneurons derived from p2 progenitors (Peng et al., 2007). In all three organisms, Notch deficient embryos showed an increased generation of v2bINs at the expense of v2aINs. Notch signal transduction was activated by Delta4 expression of adjacent cells, promoting Notch induced expression of the v2bIN specific TF, Scl (Peng et al., 2007). In studies of the mouse cerebellum and human cerebellar organoids, Notch signaling has been shown to promote inhibitory Purkinje cell fate, derived from bi-potential embryonic cerebellar progenitors, at the expense of sibling excitatory granule cell fate (Zhang et al., 2021). In the dorsal spinal cord of chick embryos, the upregulation of Delta1 expression in dIL progenitor cells induces Notch signaling in neighboring progenitors, promoting the production of dIL_B excitatory interneurons at the expense of dIL_A inhibitory interneuron fate (Mizuguchi et al., 2006).

These studies support a model in which differential Notch signaling in VNC sibling neurons promotes a $N^{ON/OFF}$ cell fate that promotes differential downstream signaling mechanisms that include but are not limited to dorsal/ventral neurite targeting. Therefore, NB5-2

Notch misexpression may promote NB5-2 GMCs to generate sibling neurons of identical N^{ON} identity. In the future, identifying sibling specific molecular markers will help test this hypothesis. However, Notch signaling may play a more predominate role in neurite targeting, while the greater identity of a neuron is promoted more by TTF expression. Early-born NB5-2 MN12 and Idun2-3 form a uniquely early-born diagonal fascicle across the midline (Figure 3.6). MN12 and Idun2 terminate in the dorsal neuropil while Idun3 neurites terminate in the ventral domain. Interestingly, in NB5-2 N[intra] larvae, the diagonal fascicle is preserved but is lost in Notch loss of function (Figure 4.1). Idun3 is predicted to be the N^{OFF} sibling of Idun2 (N^{ON}); however, we did not observe a diagonally projecting neuron in NotchRNAi larvae. Therefore, NB5-2 Notch signaling may function more in promoting neurite guidance rather than interneuronal fate specification.

Distinguishing between these two possibilities would require a similar approach that was taken in a previous study that investigated the role of Notch in dMP2 (Odd+) and vMP2 (Odd-) interneuron fate specification, derived from the MP2 progenitor (Spana & Doe, 1996). During CNS development, dMP2 and vMP2 are pioneering neurons that form the MP fascicle and extend longitudinal axons between successive neuromeres (Goodman & Doe, 1993). Temperature sensitive Notch mutants (N^{ts1}) fail to extend axons between successive neuromeres (Giniger, 1998; Kuzina et al., 2011). However, loss of Notch signaling restricted only to the time of neuron identity choice, and then restored before axon extension (*N^{ts1}*;*elav-GAL4*;*UAS-Notch*), resulted in an increase in Odd+ cell numbers but restoration of the MP fascicle, suggesting that Notch signaling may play an essential role to promote proper interneuron neurite targeting (Giniger, 1998). Thus, in the future, identifying NB5-2 $N^{ON/OFF}$ hemilineage specific markers and preforming a similar Notch rescuing experiment may allow us to identify if Notch functions to direct dorsal neuropil targeting, separate from other aspects of interneuron identity.

Notch signaling promotes axon/dendrite guidance

Notch signaling has been shown to instruct axon/dendrite targeting in multiple contexts. In *Drosophila*, Notch signaling is required in longitudinal pioneer axons to extend neurite projections into successive VNC segments by promoting formation of growth cone filopodia (Giniger, 1998; Kuzina et al., 2011; Skeath & Doe, 1998; Spana & Doe, 1996). In the developing chick hindbrain, Notch1 is expressed in precursor cells in the ventricular zone. Weak Notch1

immunoreactivity has been observed in the cytoplasm of neurons in the mantle zone expressing the commissural cell markers, TAG1 and DCC (Shi et al., 2011). Electroporation of NICD into the rostral hindbrain showed that induced Notch signaling inhibits commissural axon outgrowth across the floor plate (Shi et al., 2011). Interestingly, electroporated commissural neurons expressing TAG1 and the commissural precursor marker, Pax7, were able to complete migration from the ventricular zone to the mantal zone, suggesting that induced Notch signaling in commissural neurons does not affect cell fate (Shi et al., 2011). NICD has also been observed in newborn hippocampal neurons and loss of Notch in hippocampal radial glia precursors results in more simplistic dendritic arborization (Breunig et al., 2007). Delta1 expression of non-neuronal cells induced Notch1 signaling in neighboring N2a neuroblastomas and increased neurite length, while induced expression of Delta1 in N2a cells reduced neurite length and primary neurite number; however, there was no effect on secondary branching (Franklin et al., 1999).

NICD and Jagged1 have been observed to colocalize at synapses in the mouse cerebral cortex and hippocampus (Alberi et al., 2011). Neuron excitation increases Notch1 somal concentration in CA3 and CA1 hippocampal regions and NICD proteolytic processing was dependent on Arc/Arg3.1 expression, known to play a role neuronal plasticity and is essential for proper actin polymerization (Alberi et al., 2011). An in vitro study using embryonic mouse cortical neurons (E16) found that NICD was located in extending neurite processes as well as growth cones (Šestan et al., 1999). Notch signaling was induced by neuronal cell-cell contact to regulate neurite outgrowth. Increased cell contacts increased Notch signaling resulting in decreased neurite outgrowth, while less cell contact resulted in less Notch signaling and continued neurite extension (Šestan et al., 1999).

Induction of Notch signaling by exposure to Jagged1 in cultured mouse primary cortical neurons increases microtubule stability and increases neurite thickness and enlarged growth cones (Ferrari-Toninelli et al., 2009). Nuclear Notch1 signaling has also been shown to inhibit dendritic outgrowth but promotes dendritic branching (Redmond et al., 2000). In contrast, Notch signaling exerts a positive effect on dendritic elongation and a negative effect on dendritic branching in cultured hippocampal neurons (Salama-Cohen et al., 2005). Further, targeted deletion of *numb* and constitutively active Notch expression in the developing mouse sensory ganglia results in decreased axon branching and reduced axon length indicating that Notch signaling inhibits axonal extension and arborization in sensory neurons (Huang et al., 2005).

Together, these studies suggest vertebrate Notch1 signaling plays an important role in neuronal morphology and emphasizes the importance of Notch signaling in a context-dependent manner.

In the VNC, NB1-2, NB5-2, and NB7-1 generate dorsal and ventral neurite projections, divided by differential Notch signaling (Mark et al., 2021). However, Notch genetic manipulations of these lineages did not assess the possibility of changes in TF expression, connectivity, or neurotransmitter expression. In addition, differential Notch signaling in NB7-4 produces N^{ON} glia and N^{OFF} interneuron hemilineages and NB3-3, a NB that undergoes Type 0 cell division to produce neurons directly from NB divisions, only produces N^{OFF} interneuron progeny (Mark et al., 2021). Collectively, these data suggest that Notch signaling may function at multiple levels during neuron differentiation to specify lineage specific neuron/glia cell type fate and promote hemilineage neurite targeting. In NB5-2, the development of individual dorsal/ventral fascicles could not be observed until embryonic stage 15, suggesting hemilineage neurites may require a signaling mechanism that requires defasciculation (Figure 4.3). However, changes in hemilineage specific TFs were not assessed in Notch[intra] and NotchRNAi embryos, restricting us from concluding if Notch induces a single pathway that promotes neurite defasciculation or additional pathways that promote specification of NB5-2 N^{ON} hemilineage fate. In future studies, investigating which aspects of interneuron identity are promoted by Notch signaling will allow us to better understand the converging or parallel pathways that differentiate individual interneurons.

Introduction to Semaphorin/Plexin signaling

Semaphorins (Sema), like Notch signaling, is a highly conserved developmental mechanism. Sema signaling is promoted by binding to a class of receptors, Plexin (Plex), to induce neurite repulsion/attraction responses. While *Drosophila* express five Semas, humans express more than 20, emphasizing the conservation and effectiveness of these guidance mechanism to promote proper development (Alto & Terman, 2018). In *Drosophila*, Sema1a, Sema2a, and Sema2b are expressed in the CNS during development and it is commonly thought that the binding pairs Sema1a/PlexA and Sema2a/PlexB elicit neurite repulsion responses and defasciculation, while binding of Sema2b/PlexB promotes an attractive response and neurite fasciculation (Alto & Terman, 2018; Ayoob, 2004, 2006; Wu et al., 2011). However, many studies in *Drosophila* alone have highlighted the complexity in Sema/Plex signaling during neurite guidance.

A potential link in Notch and Semaphorin signaling in neurite guidance

The correlation of dorsal/ventral neurite targeting, and patterned expression of the Semaphorin extrinsic guidance cues present during embryonic VNC development (Zlatic et al., 2009) may indicate that Notch signaling regulates downstream target genes that promote neurite fasciculation/defasciculation and direct neurite outgrowth in response to extrinsic guidance cues.

The cytoplasmic tyrosine kinase, D-Abl, *Drosophila* homolog of the vertebrate oncogene and tyrosine kinase, *abl*, was identified as a key factor in promoting proper axon outgrowth by Notch signaling (Giniger, 1998). *Drosophila* embryos deficient in one copy of both *Notch* and *abl* (*N/+;abl/+*) displayed breakages in the MP fascicle longitudinal tract, one of the first fascicles to form during embryo neurite extension, suggesting that pioneering axons failed to extend to adjacent segments (Giniger, 1998). In addition, *Drosophila* primary neuron cell cultures revealed that Notch protein was present in both extending axons and the growth cones (Giniger, 1998). Importantly, *N/+;abl/+* embryos displayed wildtype gross CNS and musculature morphology suggesting that Notch/Abl signaling is likely not a widely used mechanism during CNS and muscular development, but may specifically promote neurite guidance.

Abl has been shown to directly interact with the redox enzyme, Molecule interacting with CasL (MICAL), and promote axon guidance in developing motor neurons (Yoon et al., 2017). Abl and MICAL colocalize in VNC longitudinal commissural tracts and motor neurons (J. Yoon et al., 2017). *Abl+/-* or *MICAL+/-* mutants alone do not display any phenotypic changes in axon trajectory but combinatorial *Abl+/- and MICAL+/-* embryos show a loss of the ISNb tract and abnormal or absent neuron innervation to muscles 6/7 and 12/13 (Yoon et al., 2017). In the CNS, misexpression of the repulsive guidance cue receptor, PlexinA (PlexA), results in disorganization and segmental breaks of FasII longitudinal axon tracts. Co-misexpression of Abl and PlexA exacerbates axon disorganization leading to near ablation of longitudinal tracts (J. Yoon et al., 2017). In addition, biochemical assays have discovered that Abl stimulates MICAL enzymatic activity by phosphorylation to promote F-actin disassembly (Yoon et al., 2017). Collectively, these data suggest that the Notch/Abl signaling pathway may induce axonal responses to extrinsic guidance cues by activating MICAL F-actin disassembly. F-actin disassembly may then promote neurite defasciculation to properly direct neurite trajectory. Interestingly, *Drosophila*

embryonic motor neuron axon targeting requires Semaphroin1a/PlexA signaling and MICAL is required for the formation of the ISNb branch and genetically interacts of PlexA (Ayoob, 2004, 2006; Terman et al., 2002; Winberg et al., 1998; Yu et al., 1998).

Complexity and diversity of Sema/Plexin signaling in axon guidance

During the development of the *Drosophila* antennal lobe, olfactory receptor neurons (ORNs) project neurites along the dorsal and ventral periphery to form synaptic connections with partner neurons in distinct glomeruli. Notch^{ON} neurites project along the ventromedial antennal lobe and Notch^{OFF} neurites extend along the dorsolateral border. ORN axon fasciculation is promoted by Sema2b/PlexB axon-axon interneurons and requires the PlexB extracellular Sema domain (Guajardo et al., 2019; Joo et al., 2013; J. Li et al., 2018); however, axon trajectory and glomeruli targeting are predominately mediated by both extracellular and intracellular binding motifs and PlexB cleavage, which consequently regulates the strength of PlexB signaling (Guajardo et al., 2019). Although Sema2b/PlexB are most commonly thought of as an attractive signaling cue, high PlexB expression levels in dorsolateral ORN axons have been shown to function as a repulsive cue (J. Li et al., 2018). PlexB misexpression (PlexB OE) shows a predominate loss of ventromedially projecting axon in the antennal lobe and targeting to endogenously high PlexB expressing glomeruli. Complementing these finding, moderate PlexB knock down shows a loss of dorsolateral projections and incorrect targeting to terminal glomeruli. In addition, while *Sema2b+/-* pupae display wild-type axon trajectories and glomeruli targeting, ORNs of *Sema2b+/-* PlexBOE pupae phenocopy PlexBOE ORNs suggesting that high levels of PlexB suppress Sema2b activity (J. Li et al., 2018).

A combination of Sema2a and Sema2b signaling through the PlexB receptor is required in the embryo CNS to establish proper organization of the FasII intermediate longitudinal tract (Wu et al., 2011). *PlexB* null mutants show disorganized and wondering axon projections of FasII axons. Interestingly, single Sema2a or Sema2b null mutants show less severe axonal phenotypes compared to PlexB; however, Sema2a/Sema2b double mutants phenocopied axonal deviations observed in the PlexB null mutants (Wu et al., 2011). Sema2a mutants showed strong convergences of otherwise individual FasII longitudinal tracts while Sema2b mutants revealed medial/lateral defasciculated axons (Wu et al., 2011). Together, these data suggests that Sema2a

and Sema2b, signaling through the PlexB receptor, coordinate proper defasciculation (Sema2a) and fasciculation (Sema2b) to properly organize CNS longitudinal neurites.

Furthermore, axon–axon attraction by Sema1a reverse signaling has been demonstrated in the developing *Drosophila* visual system and CNS (Hernandez-Fleming et al., 2017; Hsieh et al., 2014; L. Yu et al., 2010). Semas and Plexins share the Sema domain extracellular binding motif and crystal structure analysis has revealed that CNS Semas (1a, 2a, and 2b) form homodimerized structures and that Sema2a and Sema2b can heterodimerize (Alto & Terman, 2018; Rozbesky et al., 2019). PlexA and PlexB have also been shown to physically bind and although, PlexB does not interact with MICAL directly, it has been proposed that PlexA/PlexB interactions promotes the formation of heteromultimeric complexes that allow interaction of PlexB and MICAL (Ayoob, 2006). Lastly, in the context of vertebrates, many semaphorins bind plexins complexes containing a variety of neuropilin proteins (Kruger et al., 2005), further diversifying signaling responses.

Thus, it is difficult to predict how Notch signaling may be promoting dosal/ventral neurite targeting and affect downstream Sema/Plexin signaling. Although there is a strong correlation in the localization of NB5-2 dorsal/ventral neurites and Sema dorsal/ventral expression gradients (Figure 4.2), the examples presented here emphasize that colocalization is only one component in understanding the many nuances and complex mechanisms involved in Sema/Plexin signaling. Future gain and loss of function studies will provide valuable insight into the intricate interplay between intrinsic and extrinsic cues that promote proper circuit assembly and coordinate CNS development.

Concluding Remarks

Disentangling the precise regulatory mechanisms that promote interneuron identity, downstream of Hunchback, Castor, and Notch signaling will provide a more detailed understanding of how circuits in the CNS are assembled. Untangling the mechanism that specify specific aspects of interneuron identity will progress our knowledge in the field of developmental biology to better understand the intimate coordination of mechanism required for the establishment of a functional neural circuits. This will provide valuable insights into how circuits are first established, so that

we may one day implement targeted interventions and treatments for circuits that are damaged by injury or disease.

APPENDICES

Appendix A. Chapter II supplementary figures

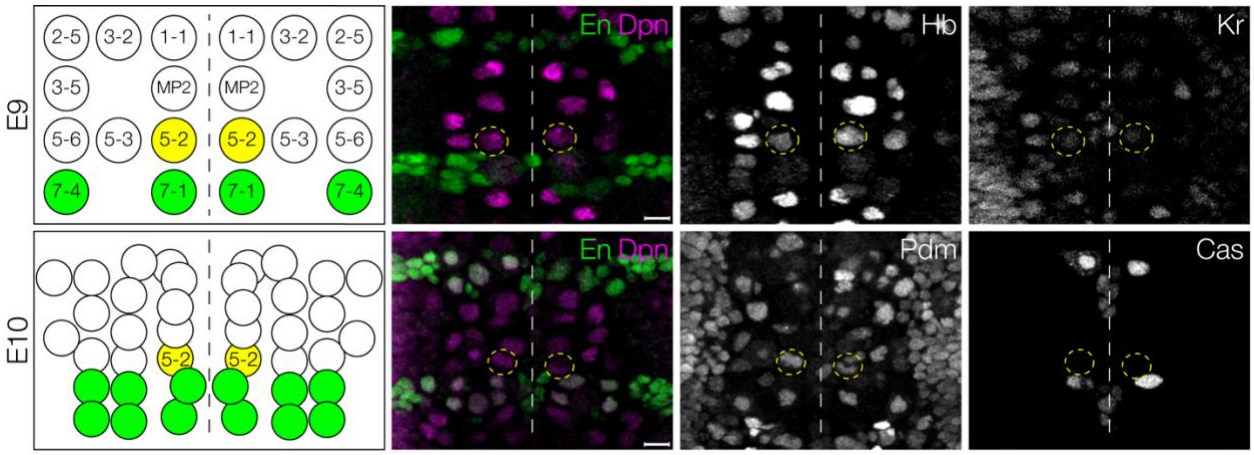

Supplemental Figure 2.1. NB5-2 can be identified by its stereotyped location in early embryos. NB5-2 (yellow in schematic) was identified using the NB marker Dpn (magenta) and the row 6/7 expressing gene, Engrailed (En; green). NB5-2 was identified as the most medial Dpn+/En-negative NB, anteriorly adjacent to the En domain. NB5-2 shows Hb/Kr expression in early stage 9 embryos (top panels) and Pdm expression by early stage10 (bottom panels). Scale bar: 5 μm.

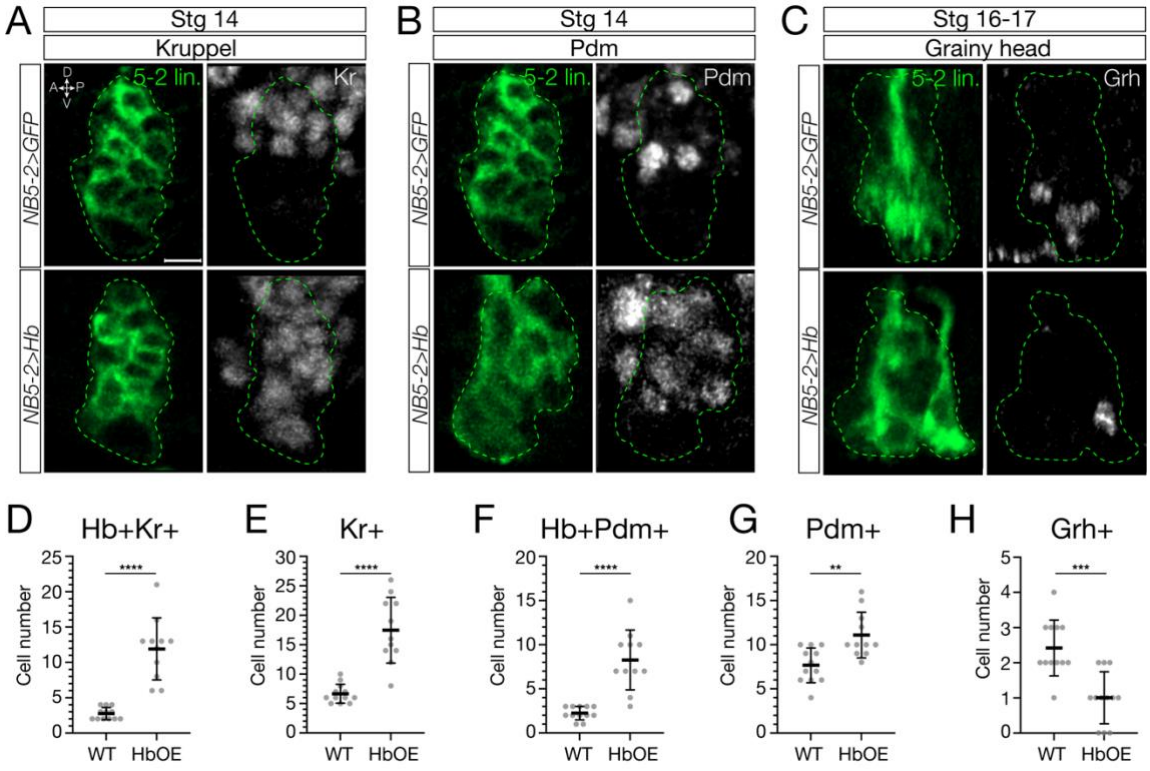

Supplemental Figure 2.2. Prolonged Hunchback expression in NB5-2 generates fewer progeny expressing late TTFs.
(A) Wildtype NB5-2>GFP (green; top panels) and NB5-2>Hb (bottom panels) progeny expressing Kr at stage 14. Anterior left, lateral view. Scale bar: 4 μm.
(B) Wildtype NB5-2>GFP (top panels) and NB5-2>Hb (bottom panels) progeny expressing Pdm at stage 14.
(C) Wildtype NB5-2>GFP (top panels) and NB5-2>Hb (bottom panels) progeny expressing Grh at stage 16-17.
(D-H) Wild type and Hb overexpression quantified for the indicated markers; quantified in a minimum of 11 hemisegments from 3 embryos. The data underlying the graph in the figure can be found in S6 Data.

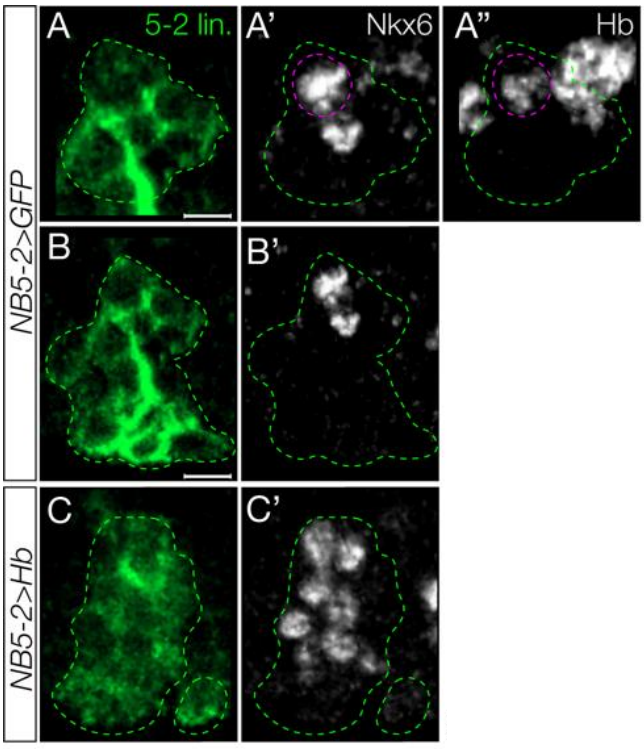

Supplemental Figure 2.3. Prolonged Hunchback expression increases the number of NB5-2 progeny that express Nkx6.
(A-B') WT NB5-2>GFP progeny (green, dotted outline) showing co-expression of Hb and the early-born marker Nkx6 at stage 17. Anterior left, lateral view. Scale bars: 4 μm.
(C-C') NB5-2>Hb progeny results in an increase in Nkx6 neurons. The data underlying the graph in the figure can be found in S2 Data.

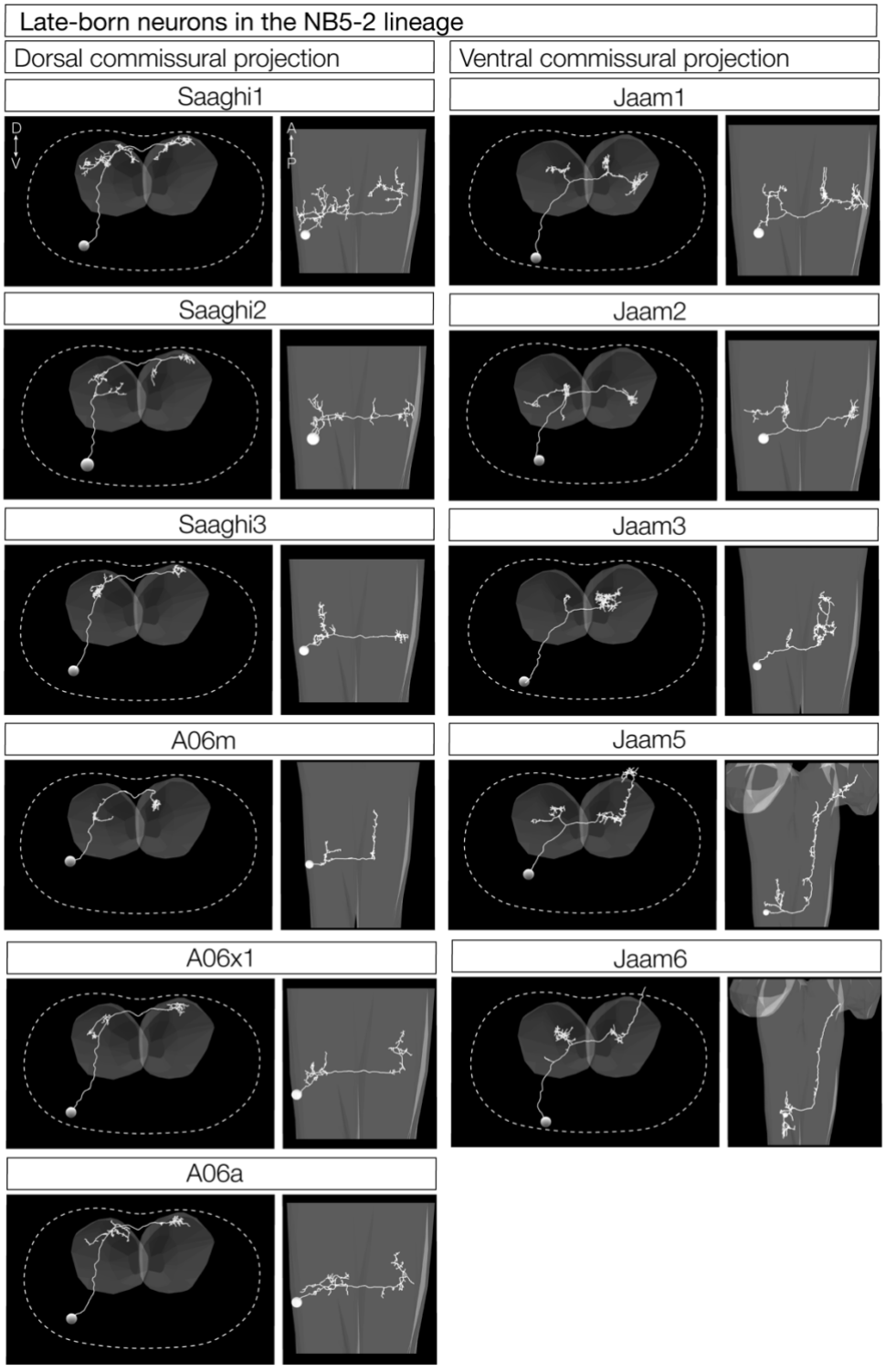

Supplemental Figure 2.4. NB5-2 late-born neurons do not possess a diagonal projecting morphology.
TEM reconstruction of wildtype NB5-2 late-born neurons organized by dorsal commissural projections (left column) and ventral commissural projections (right column). Dorsal up, posterior view (left panel); Anterior up, ventral view (right panel).

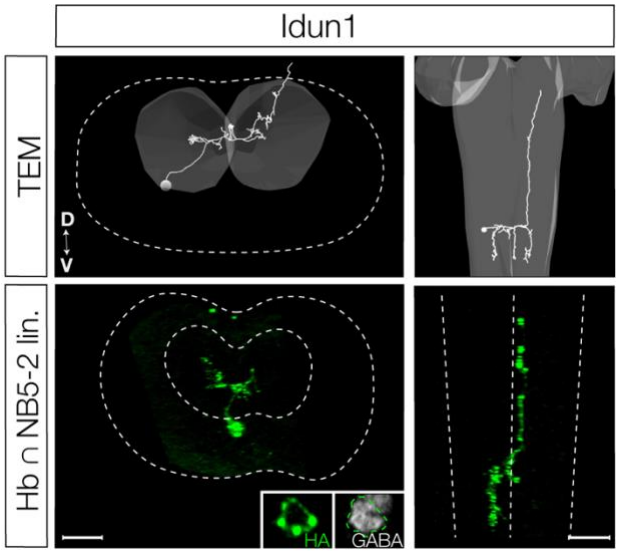

Supplemental Figure 2.5. Idun1 expresses GABA neurotransmitter. TEM reconstruction of Idun1 (upper panels) and single labeled Hb+ NB5-2 neuron genetically labeled with membrane-bound epitope tag, HA (green; bottom panels), with GABA expression (inset). Dorsal up, posterior view (left panels); Anterior up, ventral view (right panels). Scale bar: 10 μm

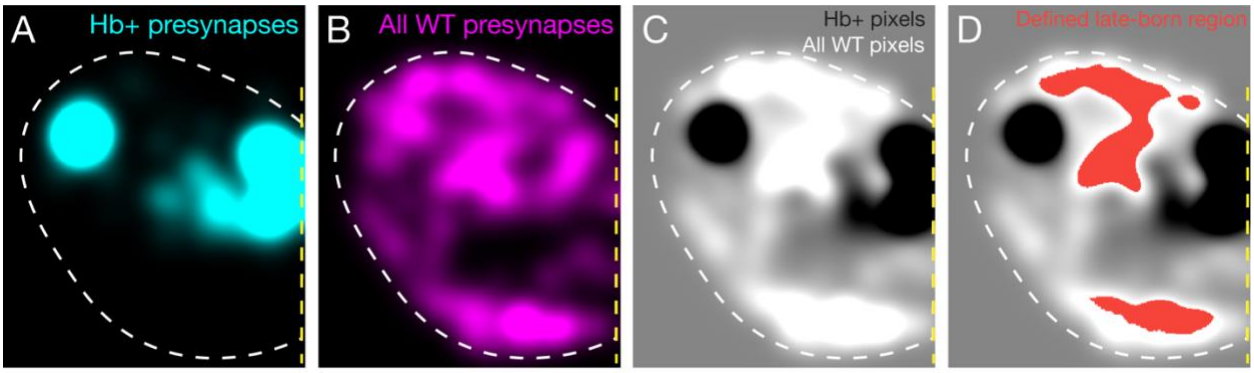

Supplemental Figure 2.6. Approach to defining late-born pre-synapse regions with computational analysis.
(A) Gaussian blur (1μm) was applied to Hb+ NB5-2 presynapses (cyan; n= 17 hemisegments, 8 animals) after aligning to a template neuropil and normalizing intensity by a factor of 10/hemisegment. A single optical slice is shown. Dorsal up, posterior view.
(B) Gaussian blur (1μm) was applied to randomly selected WT NB5-2 presynapse images (magenta; n= 4 hemisegments, 2 animals) after aligning to a template neuropil and normalizing intensity by a factor of 1/hemisegment. Differing normalization factors between

NB5-2 Hb+ and WT images were chosen to equalize intensities due to differences in presynapse number between NB5-2 Hb+ and WT images.
(C) NB5-2 Hb+ regions (black) subtracted from WT NB5-2 presynapse regions (grey) to generate an image where pixel intensity corresponds to distance from late-born presynapses.
(D) Pixels above a set threshold (red) define the late-born presynapse region. The pixel threshold was determined by setting the late-born template volume equal to the previously defined Hb+ presynapse volume.

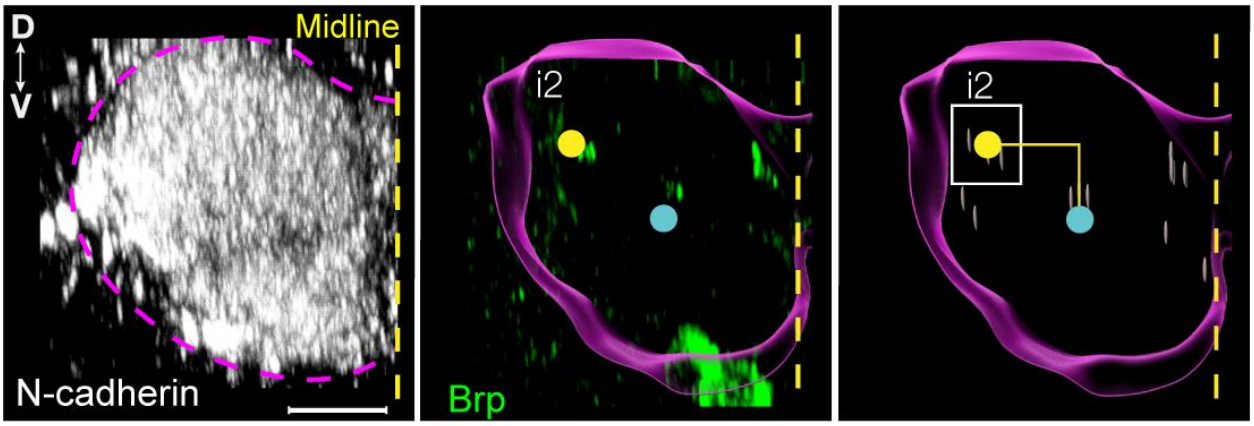

Supplemental Figure 2.7. Approach to identify NB5-2 Hb+ presynapse neuropil subregions. Neuropil labeled with N-cadherin (white) to define the neuropil border (magenta dotted line; left panel). The neuropil border (magenta) was defined using Imaris 10.0.1 surface tool to find the centroid (cyan dot) of a hemisegment and the center of Idun1-3 presynapse position labeled with Brp staining (green; middle panel). Shown is the Idun2 presynapse neuropil position (i2; yellow dot). The average i2 coordinate location was then found by measuring the dorsal-ventral and medial-lateral distance from the centroid (yellow solid line; right panel). The size of the presynapse volume (white box) was determined by the average distance from the centroid +/- 2 standard deviations. Individual presynapses were quantified using the Imaris 10.0.1 spots tool (grey dots). Dorsal up, posterior view. Scale bar: 5 µm.

Appendix B. Chapter III supplementary figures

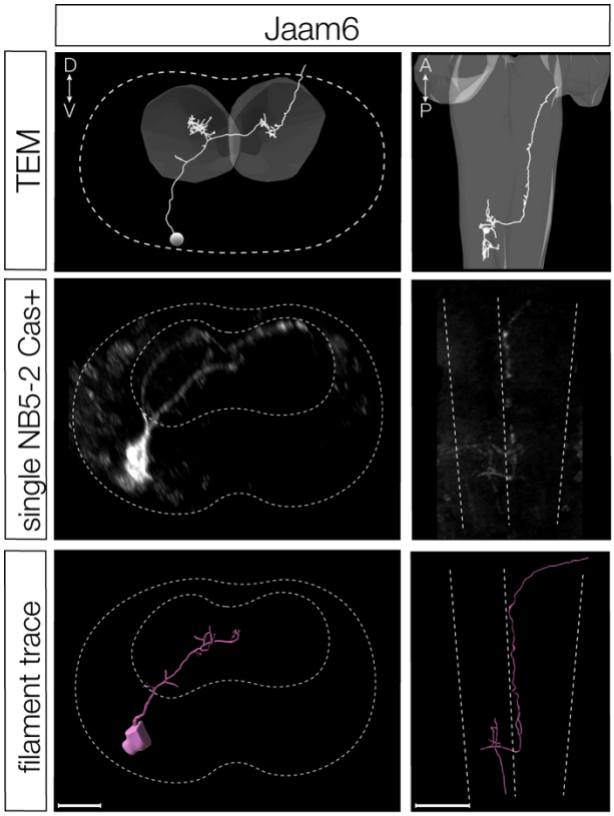

Supplementary Figure 3.1 NB5-2 Jaam6 neuron expresses Castor.

Single cell morphology of Jaam6 (n=3 animal) in L1 (0-3hr) larvae. Top panels, TEM reconstruction; left posterior view, right dorsal view. Dotted line outlines VNC border with neuropil (grey). Middle panels, Cas-filtered genetic labeling of the indicated neuron; left posterior view; right dorsal view. Dotted lines outline the VNC and neuropil borders. Bottom panels, filament tracing of Cas-filtered labeled neuron of the indicated neuron; left posterior view; right dorsal view. Dotted lines outline the VNC and neuropil borders. Scale bar: 10 μm.

Appendix C. Chapter IV supplementary figures

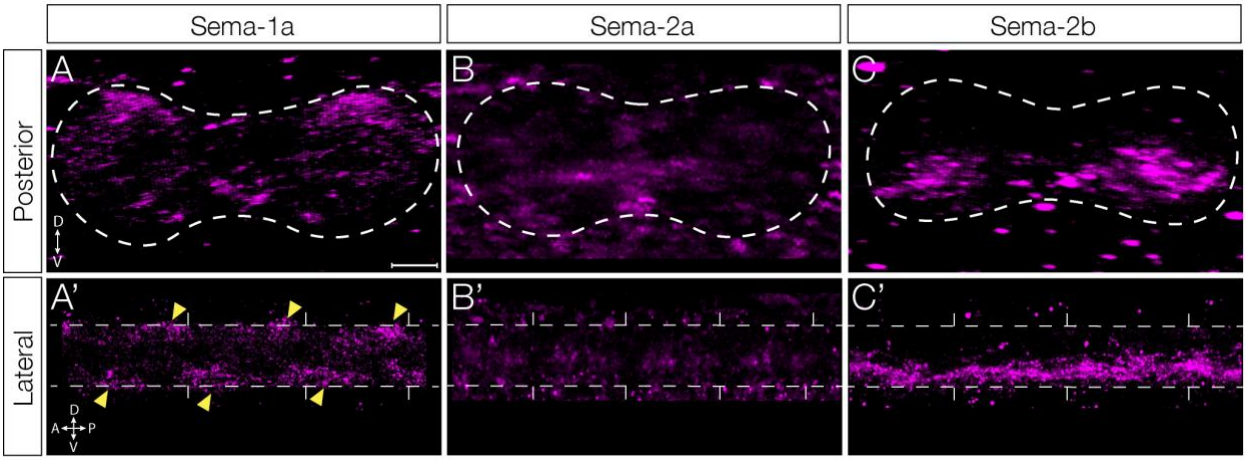

Supplementary Figure 4.1. Semaphorin 1a, 2a, and 2b expression gradients in the VNC neuropil.
(A) Sema-1a expression gradient in the A1 VNC neuropil of a stage 16/17 embryo. Dorsal up, posterior view. Lateral view shows difference in Sema1a concentration in the anterior (bottom yellow arrows) and posterior (top yellow arrows) commissures. Anterior right, lateral view (A'). Dotted lines indicate neuropil border. Vertical ticks along neuropil border indicate abdominal segments (n = 8 animals). Scale bar: 5µm.
(B) Sema-2a expression gradient in the posterior and lateral (B') views (n= 8).
(C) Sema-2b expression gradient in the posterior and lateral (C') views (n= 6).

REFERENCES

Alberi, L., Liu, S., Wang, Y., Badie, R., Smith-Hicks, C., Wu, J., Pierfelice, T. J., Abazyan, B., Mattson, M. P., Kuhl, D., Pletnikov, M., Worley, P. F., & Gaiano, N. (2011). Activity-induced Notch signaling in neurons requires Arc/Arg3.1 and is essential for synaptic plasticity in hippocampal networks. *Neuron*, *69*(3), 437–444. https://doi.org/10.1016/j.neuron.2011.01.004

Alsio, J. M., Tarchini, B., Cayouette, M., & Livesey, F. J. (2013). Ikaros promotes early-born neuronal fates in the cerebral cortex. *Proceedings of the National Academy of Sciences of the United States of America*, *110*(8), E716-25. https://doi.org/10.1073/pnas.1215707110

Alto, L. T., & Terman, J. R. (2018). *Semaphorins and their Signaling Mechanisms*. 26.

Angevine, J. B., & Sidman, R. L. (1961). Autoradiographic study of cell migration during histogenesis of cerebral cortex in the mouse. *Nature*, *192*, 766–768. https://doi.org/10.1038/192766b0

Apitz, H., & Salecker, I. (2014). A challenge of numbers and diversity: Neurogenesis in the Drosophila optic lobe. *J Neurogenet*, *28*(3–4), 233–249. https://doi.org/10.3109/01677063.2014.922558

Apitz, H., & Salecker, I. (2015). A region-specific neurogenesis mode requires migratory progenitors in the Drosophila visual system. *Nature Neuroscience*, *18*(1), 46–55. https://doi.org/10.1038/nn.3896

Apitz, H., & Salecker, I. (2018). Spatio-temporal relays control layer identity of direction-selective neuron subtypes in Drosophila. *Nature Communications*, *9*(1), 2295. https://doi.org/10.1038/s41467-018-04592-z

Averbukh, I., Lai, S.-L., Doe, C. Q., & Barkai, N. (2018). A repressor-decay timer for robust temporal patterning in embryonic Drosophila neuroblast lineages. *eLife*, *7*, e38631. https://doi.org/10.7554/eLife.38631

Ayoob, J. C. (2004). The Drosophila Receptor Guanylyl Cyclase Gyc76C Is Required for Semaphorin-1a-Plexin A-Mediated Axonal Repulsion. *Journal of Neuroscience*, *24*(30), 6639–6649. https://doi.org/10.1523/JNEUROSCI.1104-04.2004

Ayoob, J. C. (2006). Drosophila Plexin B is a Sema-2a receptor required for axon guidance. *Development*, *133*(11), 2125–2135. https://doi.org/10.1242/dev.02380

Baumgardt, M., Karlsson, D., Terriente, J., Diaz-Benjumea, F. J., & Thor, S. (2009). Neuronal subtype specification within a lineage by opposing temporal feed-forward loops. *Cell*, *139*(5), 969–982. https://doi.org/S0092-8674(09)01358-0 [pii] 10.1016/j.cell.2009.10.032

Baumgardt, M., Karlsson, D., Terriente, J., Díaz-Benjumea, F. J., & Thor, S. (2009). Neuronal Subtype Specification within a Lineage by Opposing Temporal Feed-Forward Loops. *Cell*, *139*(5), 969–982. https://doi.org/10.1016/j.cell.2009.10.032

Belliveau, M. J., Young, T. L., & Cepko, C. L. (2000). Late Retinal Progenitor Cells Show Intrinsic Limitations in the Production of Cell Types and the Kinetics of Opsin Synthesis. *The Journal of Neuroscience*, *20*(6), 2247–2254. https://doi.org/10.1523/JNEUROSCI.20-06-02247.2000

Benito-Sipos, J., Estacio-Gomez, A., Moris-Sanz, M., Baumgardt, M., Thor, S., & Diaz-Benjumea, F. J. (2010). A genetic cascade involving klumpfuss, nab and castor specifies the abdominal leucokinergic neurons in the Drosophila CNS. *Development*, *137*(19), 3327–3336. https://doi.org/137/19/3327 [pii] 10.1242/dev.052233

Bertet, C., Li, X., Erclik, T., Cavey, M., Wells, B., & Desplan, C. (2014). Temporal patterning of neuroblasts controls Notch-mediated cell survival through regulation of Hid or Reaper. *Cell*, *158*(5), 1173–1186. https://doi.org/10.1016/j.cell.2014.07.045

Bhat, K. M., Poole, S. J., & Schedl, P. (1995). The miti-mere and pdm1 genes collaborate during specification of the RP2/sib lineage in Drosophila neurogenesis. *Molecular and Cellular Biology*, *15*(8), 4052–4063. https://doi.org/10.1128/MCB.15.8.4052

Bidaye, S. S., Machacek, C., Wu, Y., & Dickson, B. J. (2014). Neuronal control of Drosophila walking direction. *Science (New York, N.Y.)*, *344*(6179), 97–101. https://doi.org/10.1126/science.1249964

Bossing, T., Udolph, G., Doe, C. Q., & Technau, G. M. (1996). The embryonic central nervous system lineages of Drosophila melanogaster. I. Neuroblast lineages derived from the ventral half of the neuroectoderm. *Dev Biol*, *179*(1), 41–64. https://doi.org/S0012-1606(96)90240-7 [pii] 10.1006/dbio.1996.0240

Breunig, J. J., Silbereis, J., Vaccarino, F. M., Sestan, N., & Rakic, P. (2007). Notch regulates cell fate and dendrite morphology of newborn neurons in the postnatal dentate gyrus. *Proceedings of the National Academy of Sciences of the United States of America*, *104*(51), 20558–20563. https://doi.org/10.1073/pnas.0710156104

Brody, T., & Odenwald, W. F. (2000). Programmed transformations in neuroblast gene expression during Drosophila CNS lineage development. *Dev Biol*, *226*(1), Article 1. https://doi.org/10.1006/dbio.2000.9829 S0012-1606(00)99829-4 [pii]

Broihier, H. T., Kuzin, A., Zhu, Y., Odenwald, W., & Skeath, J. B. (2004). Drosophila homeodomain protein Nkx6 coordinates motoneuron subtype identity and axonogenesis. *Development*, *131*(21), 5233–5242. https://doi.org/10.1242/dev.01394

Carreira-Rosario, A., Zarin, A. A., Clark, M. Q., Manning, L., Fetter, R. D., Cardona, A., & Doe, C. Q. (2018). MDN brain descending neurons coordinately activate backward and inhibit forward locomotion. *Elife*, *7*. https://doi.org/10.7554/eLife.38554

Cepko, C. (2014). Intrinsically different retinal progenitor cells produce specific types of progeny. *Nature Reviews Neuroscience*, *15*(9), 615–627. https://doi.org/10.1038/nrn3767

Cepko, C. L. (1999). The roles of intrinsic and extrinsic cues and bHLH genes in the determination of retinal cell fates. *Curr Opin Neurobiol*, *9*(1), 37–46. https://doi.org/S0959-4388(99)80005-1 [pii]

Chapman, G., Liu, L., Sahlgren, C., Dahlqvist, C., & Lendahl, U. (2006). High levels of Notch signaling down-regulate Numb and Numblike. *Journal of Cell Biology*, *175*(4), 535–540. https://doi.org/10.1083/jcb.200602009

Cheah, P. Y., Chia, W., & Yang, X. (2000). Jumeaux, a novel Drosophila winged-helix family protein, is required for generating asymmetric sibling neuronal cell fates. *Development (Cambridge, England)*, *127*(15), 3325–3335. https://doi.org/10.1242/dev.127.15.3325

Chen, G., Sima, J., Jin, M., Wang, K., Xue, X., Zheng, W., Ding, Y., & Yuan, X. (2008). Semaphorin-3A guides radial migration of cortical neurons during development. *Nature Neuroscience*, *11*(1), 36–44. https://doi.org/10.1038/nn2018

Chen, Y., Akin, O., Nern, A., Tsui, C. Y. K., Pecot, M. Y., & Zipursky, S. L. (2014). Cell-type-specific labeling of synapses in vivo through synaptic tagging with recombination. *Neuron*, *81*(2), 280–293. https://doi.org/10.1016/j.neuron.2013.12.021

Clark, B. S., Stein-O'Brien, G. L., Shiau, F., Cannon, G. H., Davis-Marcisak, E., Sherman, T., Santiago, C. P., Hoang, T. V., Rajaii, F., James-Esposito, R. E., Gronostajski, R. M., Fertig, E. J., Goff, L. A., & Blackshaw, S. (2019). Single-Cell RNA-Seq Analysis of Retinal Development Identifies NFI Factors as Regulating Mitotic Exit and Late-Born Cell Specification. *Neuron*, *102*(6), 1111-1126.e5. https://doi.org/10.1016/j.neuron.2019.04.010

Cleary, M. D., & Doe, C. Q. (2006). Regulation of neuroblast competence: Multiple temporal identity factors specify distinct neuronal fates within a single early competence window. *Genes & Development*, *20*(4), 429–434. https://doi.org/10.1101/gad.1382206

Contreras, E. G., Palominos, T., Glavic, Á., Brand, A. H., Sierralta, J., & Oliva, C. (2018). The transcription factor SoxD controls neuronal guidance in the Drosophila visual system. *Scientific Reports*, *8*(1), 13332. https://doi.org/10.1038/s41598-018-31654-5

Couturier, L., Vodovar, N., & Schweisguth, F. (2012). Endocytosis by Numb breaks Notch symmetry at cytokinesis. *Nature Cell Biology*, *14*(2), 131–139. https://doi.org/10.1038/ncb2419

Cui, X., & Doe, C. Q. (1992). Ming is expressed in neuroblast sublineages and regulates gene expression in the Drosophila central nervous system. *Development*, *116*(4), 943–952.

Deska-Gauthier, D., & Zhang, Y. (2021). The Temporal Mechanisms Guiding Interneuron Differentiation in the Spinal Cord. *International Journal of Molecular Sciences*, *22*(15), 8025. https://doi.org/10.3390/ijms22158025

Doe, C. Q. (2017). Temporal Patterning in the Drosophila CNS. *Annu. Rev. Cell Dev. Biol.*, *33*, in press.

Egger, B., Boone, J. Q., Stevens, N. R., Brand, A. H., & Doe, C. Q. (2007). Regulation of spindle orientation and neural stem cell fate in the Drosophila optic lobe. *Neural Dev*, *2*, 1. https://doi.org/1749-8104-2-1 [pii] 10.1186/1749-8104-2-1

El-Danaf, R. N., Rajesh, R., & Desplan, C. (2023). Temporal regulation of neural diversity in Drosophila and vertebrates. *Seminars in Cell & Developmental Biology*, *142*, 13–22. https://doi.org/10.1016/j.semcdb.2022.05.011

Elliott, J., Jolicoeur, C., Ramamurthy, V., & Cayouette, M. (2008). Ikaros confers early temporal competence to mouse retinal progenitor cells. *Neuron*, *60*(1), 26–39. https://doi.org/10.1016/j.neuron.2008.08.008

Endo, K., Aoki, T., Yoda, Y., Kimura, K., & Hama, C. (2007). Notch signal organizes the Drosophila olfactory circuitry by diversifying the sensory neuronal lineages. *Nature Neuroscience*, *10*(2), 153–160. https://doi.org/10.1038/nn1832

Faulkner, R. L., Low, L. K., Liu, X.-B., Coble, J., Jones, E. G., & Cheng, H.-J. (2008). Dorsal turning of motor corticospinal axons at the pyramidal decussation requires plexin signaling. *Neural Development*, *3*, 21. https://doi.org/10.1186/1749-8104-3-21

Ferrari-Toninelli, G., Bonini, S. A., Uberti, D., Napolitano, F., Stante, M., Santoro, F., Minopoli, G., Zambrano, N., Russo, T., & Memo, M. (2009). Notch activation induces neurite remodeling and functional modifications in SH-SY5Y neuronal cells. *Developmental Neurobiology*, *69*(6), 378–391. https://doi.org/10.1002/dneu.20710

Franklin, J. L., Berechid, B. E., Cutting, F. B., Presente, A., Chambers, C. B., Foltz, D. R., Ferreira, A., & Nye, J. S. (1999). Autonomous and non-autonomous regulation of mammalian neurite development by Notch1 and Delta1. *Current Biology*, *9*(24), 1448–1457. https://doi.org/10.1016/S0960-9822(00)80114-1

Giniger, E. (1998). A Role for Abl in Notch Signaling. *Neuron*, *20*(4), 667–681. https://doi.org/10.1016/S0896-6273(00)81007-7

Giniger, E. (2012). Notch signaling and neural connectivity. *Current Opinion in Genetics & Development*, *22*(4), 339–346. https://doi.org/10.1016/j.gde.2012.04.003

Goodman, C. S., & Doe, C. Q. (1993). Embryonic development of the Drosophila central nervous system. In The Development of Drosophila melanogaster. *Cold Spring Harbor, NY: Cold Spring Harbor Laboratory Press*, 1131–1206.

Grosskortenhaus, R., Pearson, B. J., Marusich, A., & Doe, C. Q. (2005). Regulation of Temporal Identity Transitions in Drosophila Neuroblasts. *Developmental Cell*, *8*(2), 193–202. https://doi.org/10.1016/j.devcel.2004.11.019

Grosskortenhaus, R., Robinson, K. J., & Doe, C. Q. (2006). Pdm and Castor specify late-born motor neuron identity in the NB7-1 lineage. *Genes Dev*, *20*(18), 2618–2627. https://doi.org/10.1101/gad.1445306

Guajardo, R., Luginbuhl, D. J., Han, S., Luo, L., & Li, J. (2019). Functional divergence of Plexin B structural motifs in distinct steps of Drosophila olfactory circuit assembly. *eLife*, *8*, e48594. https://doi.org/10.7554/eLife.48594

Hasegawa, E., Kaido, M., Takayama, R., & Sato, M. (2013). Brain-specific-homeobox is required for the specification of neuronal types in the Drosophila optic lobe. *Dev Biol*, *377*(1), 90–99. https://doi.org/10.1016/j.ydbio.2013.02.012

Hasegawa, E., Kitada, Y., Kaido, M., Takayama, R., Awasaki, T., Tabata, T., & Sato, M. (2011). Concentric zones, cell migration and neuronal circuits in the Drosophila visual center. *Development*, *138*(5), 983–993. https://doi.org/10.1242/dev.058370

Haubensak, W., Attardo, A., Denk, W., & Huttner, W. B. (2004). Neurons arise in the basal neuroepithelium of the early mammalian telencephalon: A major site of neurogenesis. *Proc Natl Acad Sci U S A*, *101*(9), 3196–3201.

Heckman, E. L., & Doe, C. Q. (2022). Presynaptic contact and activity opposingly regulate postsynaptic dendrite outgrowth. *eLife*, *11*, e82093. https://doi.org/10.7554/eLife.82093

Heckscher, E. S., Zarin, A. A., Faumont, S., Clark, M. Q., Manning, L., Fushiki, A., Schneider-Mizell, C. M., Fetter, R. D., Truman, J. W., Zwart, M. F., Landgraf, M., Cardona, A., Lockery, S. R., & Doe, C. Q. (2015). Even-Skipped(+) Interneurons Are Core Components of a Sensorimotor Circuit that Maintains Left-Right Symmetric Muscle Contraction Amplitude. *Neuron*, *88*(2), 314–329. https://doi.org/10.1016/j.neuron.2015.09.009

Hernandez-Fleming, M., Rohrbach, E. W., & Bashaw, G. J. (2017). Sema-1a Reverse Signaling Promotes Midline Crossing in Response to Secreted Semaphorins. *Cell Reports*, *18*(1), 174–184. https://doi.org/10.1016/j.celrep.2016.12.027

Hobert, O., & Kratsios, P. (2019). Neuronal identity control by terminal selectors in worms, flies, and chordates. *Current Opinion in Neurobiology*, *56*, 97–105. https://doi.org/10.1016/j.conb.2018.12.006

Hofbauer, A., & Campos-Ortega, J. A. (1990). Proliferation pattern and early differentiation of the optic lobes in Drosophila melanogaster. *Roux's Archives of Developmental Biology: The Official Organ of the EDBO*, *198*(5), 264–274. https://doi.org/10.1007/BF00377393

Holguera, I., & Desplan, C. (2018). Neuronal specification in space and time. *Science*, *362*(6411), 176–180. https://doi.org/10.1126/science.aas9435

Hsieh, H.-H., Chang, W.-T., Yu, L., & Rao, Y. (2014). Control of axon–axon attraction by Semaphorin reverse signaling. *Proceedings of the National Academy of Sciences of the United States of America*, *111*(31), 11383–11388. https://doi.org/10.1073/pnas.1321433111

Huang, E. J., Li, H., Tang, A. A., Wiggins, A. K., Neve, R. L., Zhong, W., Jan, L. Y., & Jan, Y. N. (2005). Targeted deletion of numb and numblike in sensory neurons reveals their essential functions in axon arborization. *Genes & Development*, *19*(1), 138–151. https://doi.org/10.1101/gad.1246005

Isshiki, T., Pearson, B., Holbrook, S., & Doe, C. Q. (2001). Drosophila neuroblasts sequentially express transcription factors which specify the temporal identity of their neuronal progeny. *Cell*, *106*(4), 511–521.

Javed, A., Mattar, P., Lu, S., Kruczek, K., Kloc, M., Gonzalez-Cordero, A., Bremner, R., Ali, R. R., & Cayouette, M. (2020). Pou2f1 and Pou2f2 cooperate to control the timing of cone photoreceptor production in the developing mouse retina. *Development (Cambridge, England)*, *147*(18), dev188730. https://doi.org/10.1242/dev.188730

Johnson, S. A., Zitserman, D., & Roegiers, F. (2016). Numb regulates the balance between Notch recycling and late-endosome targeting in *Drosophila* neural progenitor cells. *Molecular Biology of the Cell*, *27*(18), 2857–2866. https://doi.org/10.1091/mbc.e15-11-0751

Joo, W. J., Sweeney, L. B., Liang, L., & Luo, L. (2013). Linking Cell Fate, Trajectory Choice, and Target Selection: Genetic Analysis of Sema-2b in Olfactory Axon Targeting. *Neuron*, *78*(4), 673–686. https://doi.org/10.1016/j.neuron.2013.03.022

Kambadur, R., Koizumi, K., Stivers, C., Nagle, J., Poole, S. J., & Odenwald, W. F. (1998). Regulation of POU genes by castor and hunchback establishes layered compartments in the Drosophila CNS. *Genes Dev*, *12*(2), 246–260.

Kanai, M. I., Okabe, M., & Hiromi, Y. (2005). Seven-up Controls switching of transcription factors that specify temporal identities of Drosophila neuroblasts. *Dev Cell*, *8*(2), 203–213. https://doi.org/10.1016/j.devcel.2004.12.014

Keleman, K., & Dickson, B. J. (2001). Short- and long-range repulsion by the Drosophila Unc5 netrin receptor. *Neuron*, *32*(4), 605–617. https://doi.org/10.1016/s0896-6273(01)00505-0

Kerjan, G., Dolan, J., Haumaitre, C., Schneider-Maunoury, S., Fujisawa, H., Mitchell, K. J., & Chédotal, A. (2005). The transmembrane semaphorin Sema6A controls cerebellar granule cell migration. *Nature Neuroscience*, *8*(11), 1516–1524. https://doi.org/10.1038/nn1555

Kohwi, M., Lupton, J. R., Lai, S. L., Miller, M. R., & Doe, C. Q. (2013). Developmentally regulated subnuclear genome reorganization restricts neural progenitor competence in Drosophila. *Cell*, *152*(1–2), 97–108. https://doi.org/10.1016/j.cell.2012.11.049

Konstantinides, N., Rossi, A. M., Escobar, A., Dudragne, L., Chen, Y.-C., Tran, T., Jaimes, A. M., Özel, M. N., Simon, F., Shao, Z., Tsankova, N. M., Fullard, J. F., Walldorf, U., Roussos, P., & Desplan, C. (2021). *A comprehensive series of temporal transcription factors in the fly visual system* (p. 2021.06.13.448242). https://doi.org/10.1101/2021.06.13.448242

Kruger, R. P., Aurandt, J., & Guan, K.-L. (2005). Semaphorins command cells to move. *Nature Reviews Molecular Cell Biology*, *6*(10), 789–800. https://doi.org/10.1038/nrm1740

Kumamoto, T., & Hanashima, C. (2014). Neuronal subtype specification in establishing mammalian neocortical circuits. *Neuroscience Research*, *86*, 37–49. https://doi.org/10.1016/j.neures.2014.07.002

Kurmangaliyev, Y. Z., Yoo, J., LoCascio, S. A., & Zipursky, S. L. (2019). Modular transcriptional programs separately define axon and dendrite connectivity. *eLife*, *8*, e50822. https://doi.org/10.7554/eLife.50822

Kurmangaliyev, Y. Z., Yoo, J., Valdes-Aleman, J., Sanfilippo, P., & Zipursky, S. L. (2020). Transcriptional Programs of Circuit Assembly in the Drosophila Visual System. *Neuron*, *108*(6), 1045-1057.e6. https://doi.org/10.1016/j.neuron.2020.10.006

Kuzina, I., Song, J. K., & Giniger, E. (2011). How Notch establishes longitudinal axon connections between successive segments of the Drosophila CNS. *Development*, *138*(9), 1839–1849. https://doi.org/10.1242/dev.062471

Lacin, H., Zhu, Y., Wilson, B. A., & Skeath, J. B. (2009). Dbx mediates neuronal specification and differentiation through cross-repressive, lineage-specific interactions with eve and hb9. *Development*, *136*(19), 3257–3266. https://doi.org/10.1242/dev.037242

Landgraf, M., Bossing, T., Technau, G. M., & Bate, M. (1997). The origin, location, and projections of the embryonic abdominal motorneurons of Drosophila. *The Journal of Neuroscience: The Official Journal of the Society for Neuroscience*, *17*(24), 9642–9655.

Landgraf, M., Roy, S., Prokop, A., VijayRaghavan, K., & Bate, M. (1999). *Even-skipped* Determines the Dorsal Growth of Motor Axons in *Drosophila*. *Neuron*, *22*(1), 43–52. https://doi.org/10.1016/S0896-6273(00)80677-7

Lee, K., & Doe, C. Q. (2021). A locomotor neural circuit persists and functions similarly in larvae and adult Drosophila. *eLife*, *10*, e69767. https://doi.org/10.7554/eLife.69767

Lee, K. M., Linskens, A. M., & Doe, C. Q. (2022). Hunchback activates Bicoid in Pair1 neurons to regulate synapse number and locomotor circuit function. *Current Biology: CB*, *32*(11), 2430-2441.e3. https://doi.org/10.1016/j.cub.2022.04.025

Lee, T., & Luo, L. (1999). Mosaic analysis with a repressible cell marker for studies of gene function in neuronal morphogenesis. *Neuron*, *22*(3), 451–461.

Leighton, P. A., Mitchell, K. J., Goodrich, L. V., Lu, X., Pinson, K., Scherz, P., Skarnes, W. C., & Tessier-Lavigne, M. (2001). Defining brain wiring patterns and mechanisms through gene trapping in mice. *Nature*, *410*(6825), 174–179. https://doi.org/10.1038/35065539

Li, H., Horns, F., Wu, B., Xie, Q., Li, J., Li, T., Luginbuhl, D. J., Quake, S. R., & Luo, L. (2017). Classifying Drosophila Olfactory Projection Neuron Subtypes by Single-Cell RNA Sequencing. *Cell*, *171*(5), 1206-1220.e22. https://doi.org/10.1016/j.cell.2017.10.019

Li, J., Guajardo, R., Xu, C., Wu, B., Li, H., Li, T., Luginbuhl, D. J., Xie, X., & Luo, L. (2018). Stepwise wiring of the Drosophila olfactory map requires specific Plexin B levels. *Elife*, *7*. https://doi.org/10.7554/eLife.39088

Li, X., Erclik, T., Bertet, C., Chen, Z., Voutev, R., Venkatesh, S., Morante, J., Celik, A., & Desplan, C. (2013). Temporal patterning of Drosophila medulla neuroblasts controls neural fates. *Nature*, *498*(7455), 456–462. https://doi.org/10.1038/nature12319

Lin, S. Y., Johnson, S. M., Abraham, M., Vella, M. C., Pasquinelli, A., Gamberi, C., Gottlieb, E., & Slack, F. J. (2003). The C elegans hunchback homolog, hbl-1, controls temporal patterning and is a probable microRNA target. *Dev Cell*, *4*(5), 639–650.

Liu, S., Liu, X., Li, S., Huang, X., Qian, H., Jin, K., & Xiang, M. (2020). Foxn4 is a temporal identity factor conferring mid/late-early retinal competence and involved in retinal synaptogenesis. *Proceedings of the National Academy of Sciences of the United States of America*, *117*(9), 5016–5027. https://doi.org/10.1073/pnas.1918628117

Livesey, F. J., & Cepko, C. L. (2001). Vertebrate neural cell-fate determination: Lessons from the retina. *Nat Rev Neurosci*, *2*(2), 109–118. https://doi.org/10.1038/35053522

Luo, L. (2020). Principles of Neurobiology; Second Edition. *Boca Raton, FL: Garland Science*, *2nd edition*.

Marín, O. (2016). Developmental timing and critical windows for the treatment of psychiatric disorders. *Nature Medicine*, *22*(11), Article 11. https://doi.org/10.1038/nm.4225

Mark, B., Lai, S.-L., Zarin, A. A., Manning, L., Pollington, H. Q., Litwin-Kumar, A., Cardona, A., Truman, J. W., & Doe, C. Q. (2021). A developmental framework linking

neurogenesis and circuit formation in the Drosophila CNS. *eLife*, *10*. https://doi.org/10.7554/eLife.67510

Mattar, P., Ericson, J., Blackshaw, S., & Cayouette, M. (2015). A conserved regulatory logic controls temporal identity in mouse neural progenitors. *Neuron*, *85*(3), 497–504. https://doi.org/10.1016/j.neuron.2014.12.052

Mattar, P., Jolicoeur, C., Dang, T., Shah, S., Clark, B. S., & Cayouette, M. (2021). A Casz1-NuRD complex regulates temporal identity transitions in neural progenitors. *Scientific Reports*, *11*(1), 3858. https://doi.org/10.1038/s41598-021-83395-7

Mattar, P., Stevanovic, M., Nad, I., & Cayouette, M. (2018). Casz1 controls higher-order nuclear organization in rod photoreceptors. *Proceedings of the National Academy of Sciences of the United States of America*, *115*(34), E7987–E7996. https://doi.org/10.1073/pnas.1803069115

Meng, J. L., Marshall, Z. D., Lobb-Rabe, M., & Heckscher, E. S. (2019). How prolonged expression of Hunchback, a temporal transcription factor, re-wires locomotor circuits. *Elife*, *8*. https://doi.org/10.7554/eLife.46089

Meng, J. L., Wang, Y., Carrillo, R. A., & Heckscher, E. (2020). Temporal transcription factors determine circuit membership by permanently altering motor neuron-to-muscle synaptic partnerships. *eLife*, *9*. https://doi.org/10.7554/eLife.56898

Mettler, U., Vogler, G., & Urban, J. (2006). Timing of identity: Spatiotemporal regulation of hunchback in neuroblast lineages of Drosophila by Seven-up and Prospero. *Development*, *133*(3), 429–437. https://doi.org/dev.02229 [pii] 10.1242/dev.02229

Mizuguchi, R., Kriks, S., Cordes, R., Gossler, A., Ma, Q., & Goulding, M. (2006). Ascl1 and Gsh1/2 control inhibitory and excitatory cell fate in spinal sensory interneurons. *Nature Neuroscience*, *9*(6), 770–778. https://doi.org/10.1038/nn1706

Molyneaux, B. J., Arlotta, P., Menezes, J. R., & Macklis, J. D. (2007). Neuronal subtype specification in the cerebral cortex. *Nature Reviews. Neuroscience*, *8*(6), 427–437. https://doi.org/10.1038/nrn2151

Mora, N., Oliva, C., Fiers, M., Ejsmont, R., Soldano, A., Zhang, T.-T., Yan, J., Claeys, A., De Geest, N., & Hassan, B. A. (2018). A Temporal Transcriptional Switch Governs Stem Cell Division, Neuronal Numbers, and Maintenance of Differentiation. *Developmental Cell*, *45*(1), 53-66.e5. https://doi.org/10.1016/j.devcel.2018.02.023

Morante, J., & Desplan, C. (2008). The color-vision circuit in the medulla of Drosophila. *Current Biology: CB*, *18*(8), 553–565. https://doi.org/10.1016/j.cub.2008.02.075

Morante, J., Erclik, T., & Desplan, C. (2011). Cell migration in Drosophila optic lobe neurons is controlled by eyeless/Pax6. *Development*, *138*(4), 687–693. https://doi.org/10.1242/dev.056069

Moris-Sanz, M., Estacio-Gómez, A., Álvarez-Rivero, J., & Díaz-Benjumea, F. J. (2014). Specification of neuronal subtypes by different levels of Hunchback. *Development*, *141*(22), 4366–4374. https://doi.org/10.1242/dev.113381

Naidu, V. G., Zhang, Y., Lowe, S., Ray, A., Zhu, H., & Li, X. (2020). Temporal progression of Drosophila medulla neuroblasts generates the transcription factor combination to control T1 neuron morphogenesis. *Developmental Biology*, *464*(1), 35–44. https://doi.org/10.1016/j.ydbio.2020.05.005

Nern, A., Pfeiffer, B. D., & Rubin, G. M. (2015). Optimized tools for multicolor stochastic labeling reveal diverse stereotyped cell arrangements in the fly visual system. *Proc Natl Acad Sci U S A*, *112*(22), Article 22. https://doi.org/10.1073/pnas.1506763112

Nern, A., Pfeiffer, B. D., Svoboda, K., & Rubin, G. M. (2011). Multiple new site-specific recombinases for use in manipulating animal genomes. *Proceedings of the National Academy of Sciences of the United States of America*, *108*(34), 14198–14203. https://doi.org/10.1073/pnas.1111704108

Newstein, P. (2024). *Registration code* (Python Code doi. org/10.5281/zenodo.14510754). Zenodo. https://doi.org/doi.org/10.5281/zenodo.14510754

Novotny, T., Eiselt, R., & Urban, J. (2002). Hunchback is required for the specification of the early sublineage of neuroblast 7-3 in the Drosophila central nervous system. *Development*, *129*(4), 1027–1036.

Ohyama, T., Schneider-Mizell, C. M., Fetter, R. D., Aleman, J. V., Franconville, R., Rivera-Alba, M., Mensh, B. D., Branson, K. M., Simpson, J. H., Truman, J. W., Cardona, A., & Zlatic, M. (2015). A multilevel multimodal circuit enhances action selection in Drosophila. *Nature*, *520*(7549), Article 7549. https://doi.org/10.1038/nature14297

Oliva, C., Choi, C.-M., Nicolai, L. J. J., Mora, N., De Geest, N., & Hassan, B. A. (2014). Proper connectivity of Drosophila motion detector neurons requires Atonal function in progenitor cells. *Neural Development*, *9*, 4. https://doi.org/10.1186/1749-8104-9-4

Pearson, B. J., & Doe, C. Q. (2003). Regulation of neuroblast competence in Drosophila. *Nature*, *425*(6958), Article 6958. https://doi.org/10.1038/nature01910 nature01910 [pii]

Pearson, B. J., & Doe, C. Q. (2004). Specification of temporal identity in the developing nervous system. *Annu Rev Cell Dev Biol*, *20*, 619–647. https://doi.org/10.1146/annurev.cellbio.19.111301.115142

Peng, C.-Y., Yajima, H., Burns, C. E., Zon, L. I., Sisodia, S. S., Pfaff, S. L., & Sharma, K. (2007). Notch and MAML Signaling Drives Scl-Dependent Interneuron Diversity in the Spinal Cord. *Neuron*, *53*(6), 813–827. https://doi.org/10.1016/j.neuron.2007.02.019

Pfeiffer, B. D., Jenett, A., Hammonds, A. S., Ngo, T. T., Misra, S., Murphy, C., Scully, A., Carlson, J. W., Wan, K. H., Laverty, T. R., Mungall, C., Svirskas, R., Kadonaga, J. T., Doe, C. Q., Eisen, M. B., Celniker, S. E., & Rubin, G. M. (2008). Tools for neuroanatomy and neurogenetics in Drosophila. *Proc Natl Acad Sci U S A*, *105*(28), 9715–9720. https://doi.org/0803697105 [pii] 10.1073/pnas.0803697105

Pollington, H. Q., Seroka, A. Q., & Doe, C. Q. (2023). From temporal patterning to neuronal connectivity in Drosophila type I neuroblast lineages. *Seminars in Cell & Developmental Biology*, *142*, 4–12. https://doi.org/10.1016/j.semcdb.2022.05.022

Pollington H.Q., Doe C.Q., (2025) The Hunchback transcription factor determines interneuron molecular identity, morphology, and presynapse targeting in the *Drosophila* NB5-2 lineage. *PLOS Biology* 23(3): e3002881. doi.org/10.1371/journal.pbio.3002881

Redmond, L., Oh, S.-R., Hicks, C., Weinmaster, G., & Ghosh, A. (2000). Nuclear Notch1 signaling and the regulation of dendritic development. *Nature Neuroscience*, *3*(1), Article 1. https://doi.org/10.1038/71104

Reilly, M. B., Cros, C., Varol, E., Yemini, E., & Hobert, O. (2020). Unique homeobox codes delineate all the neuron classes of C. elegans. *Nature*, *584*(7822), 595–601. https://doi.org/10.1038/s41586-020-2618-9

Rhyu, M. S., Jan, L. Y., & Jan, Y. N. (1994). Asymmetric distribution of numb protein during division of the sensory organ precursor cell confers distinct fates to daughter cells. *Cell*, *76*(3), 477–491. https://doi.org/10.1016/0092-8674(94)90112-0

Risse, B., Thomas, S., Otto, N., Lopmeier, T., Valkov, D., Jiang, X., & Klambt, C. (2013). FIM, a novel FTIR-based imaging method for high throughput locomotion analysis. *PLoS One*, *8*(1), e53963. https://doi.org/10.1371/journal.pone.0053963

Rozbesky, D., Robinson, R. A., Jain, V., Renner, M., Malinauskas, T., Harlos, K., Siebold, C., & Jones, E. Y. (2019). Diversity of oligomerization in Drosophila semaphorins suggests a mechanism of functional fine-tuning. *Nature Communications*, *10*(1), 3691. https://doi.org/10.1038/s41467-019-11683-y

Rünker, A. E., Little, G. E., Suto, F., Fujisawa, H., & Mitchell, K. J. (2008). Semaphorin-6A controls guidance of corticospinal tract axons at multiple choice points. *Neural Development*, *3*(1), 34. https://doi.org/10.1186/1749-8104-3-34

Sagner, A., Zhang, I., Watson, T., Lazaro, J., Melchionda, M., & Briscoe, J. (2021). A shared transcriptional code orchestrates temporal patterning of the central nervous system. *PLoS Biology*, *19*(11), e3001450. https://doi.org/10.1371/journal.pbio.3001450

Salama-Cohen, P., Arévalo, M.-Á., Meier, J., Grantyn, R., & Rodríguez-Tébar, A. (2005). NGF Controls Dendrite Development in Hippocampal Neurons by Binding to p75NTR and Modulating the Cellular Targets of Notch. *Molecular Biology of the Cell*, *16*(1), 339–347. https://doi.org/10.1091/mbc.E04-05-0438

Sales, E. C., Heckman, E. L., Warren, T. L., & Doe, C. Q. (2019). Regulation of subcellular dendritic synapse specificity by axon guidance cues. *eLife*, *8*. https://doi.org/10.7554/eLife.43478

Schilling, T., Ali, A. H., Leonhardt, A., Borst, A., & Pujol-Martí, J. (2019). Transcriptional control of morphological properties of direction-selective T4/T5 neurons in Drosophila. *Development (Cambridge, England)*, *146*(2), dev169763. https://doi.org/10.1242/dev.169763

Schmid, A., Chiba, A., & Doe, C. Q. (1999). Clonal analysis of Drosophila embryonic neuroblasts: Neural cell types, axon projections and muscle targets. *Development*, *126*(21), 4653–4689.

Schmidt, H., Rickert, C., Bossing, T., Vef, O., Urban, J., & Technau, G. M. (1997). The embryonic central nervous system lineages of Drosophila melanogaster. II. Neuroblast lineages derived from the dorsal part of the neuroectoderm. *Dev Biol*, *189*(2), 186–204. https://doi.org/S0012160697986607 [pii]

Sen, S. Q., Chanchani, S., Southall, T. D., & Doe, C. Q. (2019). Neuroblast-specific open chromatin allows the temporal transcription factor, Hunchback, to bind neuroblast-specific loci. *Elife*, *8*. https://doi.org/10.7554/eLife.44036

Seroka, A. Q., & Doe, C. Q. (2019). The Hunchback temporal transcription factor determines motor neuron axon and dendrite targeting in Drosophila. *Development*, *137*. https://doi.org/10.1242/dev.175570

Seroka, A., Yazejian, R. M., Lai, S.-L., & Doe, C. Q. (2020). A novel temporal identity window generates alternating Eve+/Nkx6+ motor neuron subtypes in a single progenitor lineage. *Neural Development*, *15*(1), 9. https://doi.org/10.1186/s13064-020-00146-6

Šestan, N., Artavanis-Tsakonas, S., & Rakic, P. (1999). Contact-Dependent Inhibition of Cortical Neurite Growth Mediated by Notch Signaling. *Science*, *286*(5440), 741–746. https://doi.org/10.1126/science.286.5440.741

Shen, Q., Wang, Y., Dimos, J. T., Fasano, C. A., Phoenix, T. N., Lemischka, I. R., Ivanova, N. B., Stifani, S., Morrisey, E. E., & Temple, S. (2006). The timing of cortical neurogenesis is encoded within lineages of individual progenitor cells. *Nat Neurosci*, *9*(6), Article 6. https://doi.org/10.1038/nn1694

Shi, M., Liu, Z., Lv, Y., Zheng, M., Du, F., Zhao, G., Huang, Y., Chen, J., Han, H., & Ding, Y. (2011). Forced Notch Signaling Inhibits Commissural Axon Outgrowth in the Developing Chick Central Nerve System. *PLOS ONE*, *6*(1), e14570. https://doi.org/10.1371/journal.pone.0014570

Simpson, J. H., Bland, K. S., Fetter, R. D., & Goodman, C. S. (2000). Short-range and long-range guidance by Slit and its Robo receptors: A combinatorial code of Robo receptors controls lateral position. *Cell*, *103*(7), 1019–1032. https://doi.org/10.1016/s0092-8674(00)00206-3

Skeath, J. B., & Doe, C. Q. (1998). *Sanpodo and Notch act in opposition to Numb to distinguish sibling neuron fates in the Drosophila CNS*. 9.

Skeath, J. B., & Thor, S. (2003). Genetic control of Drosophila nerve cord development. *Curr Opin Neurobiol*, *13*(1), 8–15. https://doi.org/S0959438803000072 [pii]

Spana, E. P., & Doe, C. Q. (1996). Numb Antagonizes Notch Signaling to Specify Sibling Neuron Cell Fates. *Neuron*, *17*(1), 21–26. https://doi.org/10.1016/S0896-6273(00)80277-9

Stratmann, J., Ekman, H., & Thor, S. (2019). A branching gene regulatory network dictating different aspects of a neuronal cell identity. *Development*, *146*(6), dev174300. https://doi.org/10.1242/dev.174300

Stratmann, J., Gabilondo, H., Benito-Sipos, J., & Thor, S. (2016). Neuronal cell fate diversification controlled by sub-temporal action of Kruppel. *Elife*, *5*, e19311. https://doi.org/10.7554/eLife.19311.001

Struhl, G., & Greenwald, I. (2001). Presenilin-mediated transmembrane cleavage is required for Notch signal transduction in Drosophila. *Proceedings of the National Academy of Sciences of the United States of America*, *98*(1), 229–234.

Sullivan, L. F., Warren, T. L., & Doe, C. Q. (2019). Temporal identity establishes columnar neuron morphology, connectivity, and function in a Drosophila navigation circuit. *eLife*, *8*. https://doi.org/10.7554/eLife.43482

Suzuki, T., Kaido, M., Takayama, R., & Sato, M. (2013). A temporal mechanism that produces neuronal diversity in the Drosophila visual center. *Dev Biol*, *380*(1), 12–24. https://doi.org/10.1016/j.ydbio.2013.05.002

Sweeney, L. B., Couto, A., Chou, Y.-H., Berdnik, D., Dickson, B. J., Luo, L., & Komiyama, T. (2007). Temporal Target Restriction of Olfactory Receptor Neurons by Semaphorin-1a/PlexinA-Mediated Axon-Axon Interactions. *Neuron*, *53*(2), 185–200. https://doi.org/10.1016/j.neuron.2006.12.022

Telley, L., Agirman, G., Prados, J., Amberg, N., Fièvre, S., Oberst, P., Bartolini, G., Vitali, I., Cadilhac, C., Hippenmeyer, S., Nguyen, L., Dayer, A., & Jabaudon, D. (2019). Temporal patterning of apical progenitors and their daughter neurons in the developing neocortex. *Science (New York, N.Y.)*, *364*(6440), eaav2522. https://doi.org/10.1126/science.aav2522

Terman, J. R., & Kolodkin, A. L. (2004). *Nervy Links Protein Kinase A to Plexin-Mediated Semaphorin Repulsion | Science*. https://www.science.org/doi/10.1126/science.1092121?url_ver=Z39.88-2003&rfr_id=ori:rid:crossref.org&rfr_dat=cr_pub%20%200pubmed

Terman, J. R., Mao, T., Pasterkamp, R. J., Yu, H.-H., & Kolodkin, A. L. (2002). MICALs, a Family of Conserved Flavoprotein Oxidoreductases, Function in Plexin-Mediated Axonal Repulsion. *Cell*, *109*(7), 887–900. https://doi.org/10.1016/S0092-8674(02)00794-8

Tran, K. D., & Doe, C. Q. (2008). Pdm and Castor close successive temporal identity windows in the NB3-1 lineage. *Development*, *135*(21), 3491–3499. https://doi.org/10.1242/dev.024349

Tran, K. D., Miller, M. R., & Doe, C. Q. (2010). Recombineering Hunchback identifies two conserved domains required to maintain neuroblast competence and specify early-born neuronal identity. *Development*, *137*(9), 1421–1430. https://doi.org/10.1242/dev.048678

Udolph, G. (2013). NOTCH SIGNALING AND THE GENERATION OF CELL DIVERSITY IN DROSOPHILA NEUROBLAST LINEAGES. In *Madame Curie Bioscience Database [Internet]*. Landes Bioscience. https://www.ncbi.nlm.nih.gov/books/NBK47089/

Urban, J., & Mettler, U. (2006). Connecting temporal identity to mitosis: The regulation of Hunchback in Drosophila neuroblast lineages. *Cell Cycle*, *5*(9), 950–952. https://doi.org/2727 [pii]

Valdes-Aleman, J., Fetter, R. D., Sales, E. C., Heckman, E. L., Venkatasubramanian, L., Doe, C. Q., Landgraf, M., Cardona, A., & Zlatic, M. (2021). Comparative Connectomics Reveals How Partner Identity, Location, and Activity Specify Synaptic Connectivity in Drosophila. *Neuron*, *109*(1), 105-122.e7. https://doi.org/10.1016/j.neuron.2020.10.004

Wildonger, J., & Mann, R. S. (2005). Evidence that *nervy*, the *Drosophila* homolog of ETO/MTG8, promotes mechanosensory organ development by enhancing Notch signaling. *Developmental Biology*, *286*(2), 507–520. https://doi.org/10.1016/j.ydbio.2005.08.026

Winberg, M. L., Noordermeer, J. N., Tamagnone, L., Comoglio, P. M., Spriggs, M. K., Tessier-Lavigne, M., & Goodman, C. S. (1998). Plexin A Is a Neuronal Semaphorin Receptor that Controls Axon Guidance. *Cell*, *95*(7), 903–916. https://doi.org/10.1016/S0092-8674(00)81715-8

Wreden, C. C., Meng, J. L., Feng, W., Chi, W., Marshall, Z. D., & Heckscher, E. S. (2017). Temporal Cohorts of Lineage-Related Neurons Perform Analogous Functions in Distinct Sensorimotor Circuits. *Current Biology*, *27*(10), 1521-1528.e4. https://doi.org/10.1016/j.cub.2017.04.024

Wu, Z., Sweeney, L. B., Ayoob, J. C., Chak, K., Andreone, B. J., Ohyama, T., Kerr, R., Luo, L., Zlatic, M., & Kolodkin, A. L. (2011). A Combinatorial Semaphorin Code Instructs the Initial Steps of Sensory Circuit Assembly in the Drosophila CNS. *Neuron*, *70*(2), 281–298. https://doi.org/10.1016/j.neuron.2011.02.050

Xu, C., Ramos, T. B., Marshall, O. J., & Doe, C. Q. (2024). Notch signaling and Bsh homeodomain activity are integrated to diversify Drosophila lamina neuron types. *eLife*, *12*, RP90136. https://doi.org/10.7554/eLife.90136

Xu, C., Theisen, E., Maloney, R., Peng, J., Santiago, I., Yapp, C., Werkhoven, Z., Rumbaut, E., Shum, B., Tarnogorska, D., Borycz, J., Tan, L., Courgeon, M., Griffin, T., Levin, R., Meinertzhagen, I. A., de Bivort, B., Drugowitsch, J., & Pecot, M. Y. (2019). Control of Synaptic Specificity by Establishing a Relative Preference for Synaptic Partners. *Neuron*, *103*(5), 865-877.e7. https://doi.org/10.1016/j.neuron.2019.06.006

Yasugi, T., Umetsu, D., Murakami, S., Sato, M., & Tabata, T. (2008). Drosophila optic lobe neuroblasts triggered by a wave of proneural gene expression that is negatively regulated by JAK/STAT. *Development*, *135*(8), 1471–1480. https://doi.org/10.1242/dev.019117

Yoon, J., Kim, S. B., Ahmed, G., Shay, J. W., & Terman, J. R. (2017). Amplification of F-Actin Disassembly and Cellular Repulsion by Growth Factor Signaling. *Developmental Cell*, *42*(2), 117-129.e8. https://doi.org/10.1016/j.devcel.2017.06.007

Yoon, K., & Gaiano, N. (2005). Notch signaling in the mammalian central nervous system: Insights from mouse mutants. *Nature Neuroscience*, *8*(6), 709–715. https://doi.org/10.1038/nn1475

Yu, H.-H., Araj, H. H., Ralls, S. A., & Kolodkin, A. L. (1998). The Transmembrane Semaphorin Sema I Is Required in Drosophila for Embryonic Motor and CNS Axon Guidance. *Neuron*, *20*(2), 207–220. https://doi.org/10.1016/S0896-6273(00)80450-X

Yu, L., Zhou, Y., Cheng, S., & Rao, Y. (2010). Plexin A-Semaphorin-1a Reverse Signaling Regulates Photoreceptor Axon Guidance in Drosophila. *Journal of Neuroscience*, *30*(36), 12151–12156. https://doi.org/10.1523/JNEUROSCI.1494-10.2010

Yu, Y.-C., Bultje, R. S., Wang, X., & Shi, S.-H. (2009). Specific synapses develop preferentially among sister excitatory neurons in the neocortex. *Nature*, *458*(7237), Article 7237. https://doi.org/10.1038/nature07722

Zacharioudaki, E., & Bray, S. J. (2014). Tools and methods for studying Notch signaling in *Drosophila melanogaster*. *Methods*, *68*(1), 173–182. https://doi.org/10.1016/j.ymeth.2014.03.029

Zhang, T., Liu, T., Mora, N., Guegan, J., Bertrand, M., Contreras, X., Hansen, A. H., Streicher, C., Anderle, M., Danda, N., Tiberi, L., Hippenmeyer, S., & Hassan, B. A. (2021). Generation of excitatory and inhibitory neurons from common progenitors via Notch signaling in the cerebellum. *Cell Reports*, *35*(10). https://doi.org/10.1016/j.celrep.2021.109208

Zhu, H., Zhao, S. D., Ray, A., Zhang, Y., & Li, X. (2022). A comprehensive temporal patterning gene network in Drosophila medulla neuroblasts revealed by single-cell RNA sequencing. *Nature Communications*, *13*(1), 1247. https://doi.org/10.1038/s41467-022-28915-3

Zlatic, M., Li, F., Strigini, M., Grueber, W., & Bate, M. (2009). Positional cues in the Drosophila nerve cord: Semaphorins pattern the dorso-ventral axis. *PLOS Biology*, *7*(6), e1000135. https://doi.org/10.1371/journal.pbio.1000135

Zou, Y., Stoeckli, E., Chen, H., & Tessier-Lavigne, M. (2000). Squeezing Axons Out of the Gray Matter: A Role for Slit and Semaphorin Proteins from Midline and Ventral Spinal Cord. *Cell*, *102*(3), 363–375. https://doi.org/10.1016/S0092-8674(00)00041-6